Fall 1999

A Fluid Inclusion and Structural Analysis of the West Chance Vein System, Sunshine Mine, Kellogg, Idaho

David S. (David Scott) Boyer
Western Washington University, dsboyergeo@gmail.com

A FLUID INCLUSION AND STRUCTURAL ANALYSIS OF THE WEST CHANCE VEIN SYSTEM, SUNSHINE MINE, KELLOGG, IDAHO

BY
DAVID S. BOYER

Accepted in Partial Completion
of the Requirements for the Degree
Master of Science

Moheb A. Ghali, Dean of Graduate School

ADVISORY COMMITTEE

Co-chair, Dr. Antoni Wodzicki

Co-chair, Dr. Elizabeth R. Schermer

Dr. Michael E. Ratchford

MASTER'S THESIS

In presenting this thesis in partial fulfillment of the requirements for a master's degree at Western Washington University, I agree that the Library shall make its copies freely available for inspection. I further agree that extensive copying of this thesis is allowable only for scholarly purposes. It is understood, however, that any copying or publication of this thesis for commercial purposes, or for financial gain, shall not be allowed without my written permission.

Signature _____

Date 12/17/99

MASTER'S THESIS

In presenting this thesis in partial fulfillment of the requirements for a master's degree at Western Washington University, I grant to Western Washington University the non-exclusive royalty-free right to archive, reproduce, distribute, and display the thesis in any and all forms, including electronic format, via any digital library mechanisms maintained by WWU.

I represent and warrant this is my original work, and does not infringe or violate any rights of others. I warrant that I have obtained written permissions from the owner of any third party copyrighted material included in these files.

I acknowledge that I retain ownership rights to the copyright of this work, including but not limited to the right to use all or part of this work in future works, such as articles or books.

Library users are granted permission for individual, research and non-commercial reproduction of this work for educational purposes only. Any further digital posting of this document requires specific permission from the author.

Any copying or publication of this thesis for commercial purposes, or for financial gain, is not allowed without my written permission.

David Boyer
February 28, 2018

A FLUID INCLUSION AND STRUCTURAL ANALYSIS OF THE WEST CHANCE VEIN SYSTEM, SUNSHINE MINE, KELLOGG, IDAHO

A Thesis
Presented to the Faculty of
Western Washington University

In Partial Fulfillment
of the Requirements for the Degree
Master of Science

---

by
David S. Boyer
December, 1999

ABSTRACT

The Sunshine mine, near Kellogg ID, is a mesothermal Ag-Pb vein deposit in the Coeur d'Alene mining district. Proterozoic siliciclastic rocks of the Ravalli Group, Belt Supergroup, host the ore bodies. The recently discovered West Chance ore body has been under development for the past five years. This tabular ore body strikes west and dips steeply to the south, has 300m (~1000 ft) strike length and extends approximately 914m (~3000 ft) down dip. Ore is located where the WNW-striking Chance fault changes to a predominately west-striking structure. This study consists of a fluid inclusion and structural analysis of the West Chance ore body to determine pressure, temperature, and composition parameters of mineralization, and to evaluate possible structural controls on ore deposition.

Fluid inclusion analysis of over 60 primary inclusions from quartz veins within the West Chance ore body show the dominant type of fluid inclusion to be liquid-rich inclusions composed of H_2O-NaCl. Homogenization temperatures, T(h), range from 190.6°C to 325.8 °C, with a mean value of 270.9°C. There is no systematic variation of $T_{(h)}$ with respect to depth and no evidence of boiling. Salinities increase with depth through the vein system; thus range from 0.5 wt.% NaCl in the upper portions to 12.2 wt. % NaCl lower in the ore body. Increasing salinity with depth suggests that ore deposition in the West Chance is a result of mixing of two fluids of similar temperature but varying salinities or that boiling occurred higher in the system yielding the observed salinity contrast. A constructed P-V-T diagram suggests that the West Chance ore body formed at pressures in the range of 0.5-2 kbars, corresponding to depths of 1.75-7 km for fluid pressure under lithostatic load.

Structural analysis consisted of mapping, petrofabric analysis, and compilation of existing data and showed that the mineralized fault system consists of an anastomosing series of smaller faults that strike WSW to WNW. Megascopic features and petrographic textures indicate that the fault has been reactivated over time. Ore shoots plunge steeply to the west with a 60-70° rake. Previous work on structural control of ore fluids has suggested mineralization took place during left-lateral or reverse motion. The present study of the West Chance ore body shows there is evidence for both types of motion and supports left-lateral, reverse, and right-lateral as a sequence of fault motions, with right lateral motion occurring after ore deposition. However, there are no constraints on the absolute timing of faulting.

ACKNOWLEDGMENTS

There have been many people who have helped me with this project and I am very thankful for all their help.

Professor Antoni "Jontek" Wodzicki was the first person who got me interested in a thesis on this subject, and it was on a fieldtrip to Sunshine mine where it all started. His continued support, insight, and open mindedness are inspirational. I wish him the best with the challenge he has in front of him. I'm sure he will approach this challenge the way he did with all of his life – with honor and optimism*.

Professor Elizabeth "Liz" Schermer has given never-ending support and advice to a project that many times seemed overwhelming. Her patience in explaining difficult concepts and her critical evaluations of the project was very appreciated, as was her friendship.

Dr. Michael "Ed" Ratchford provided very important guidance while working at the mine. His meticulous expertise with structural and Sunshine mine geology was greatly appreciated and greatly aided this project. His willingness to put in extra time after hours and during underground excursions was invaluable.

Sunshine Mining and Refinery Inc. was generous in partially funding this project and in employing me during summers and interim periods. All the Sunshine geologists provided insight into this project. I would like to thank Rod Cleland for discussing his knowledge of closed sections of the mine and in helping out in accessing some of these areas. Jeff Moe was critical in aiding with the computer work. I would have spent at least twice as much time without his help. I thank Cole Carter for his support and for

allowing me to work and visit the mine. All the mine geologists were especially important in giving critical feedback when I suggested new ideas.

I would also like to thank the entire Geology faculty for their support over the course of the entire project. Vicki Critchlow and Chris Sutton were extremely helpful in advising on all the logistics of being in graduate school, and I'd like to thank George Mustoe in helping out with technical advice, especially the countless hours George put in while I was revamping the fluid inclusion apparatus. Many graduate students also lent their support and lengthy discussions.

Finally, I would like to thank my family for their unconditional support. They have been there all along and are very much a part of this project.

*Antoni "Jontek" Wodzicki passed away on November 30, 1999. It was with great regret he could not witness the end of this project. I will always remember him for his wisdom, honor, and optimism.

TABLE OF CONTENTS

LIST OF FIGURES

LIST OF TABLES

INTRODUCTION

The Sunshine mine is located in the Coeur d'Alene mining district, Shoshone County, Idaho, section 15 T48N R3E. (figure 1). This world class silver-base metal district has produced over 1 billion ounces of silver, 500,000 ounces of gold, 8 million tons of lead, and 3 million tons of zinc (Springer, 1993). Sunshine mine, which has been in production for over a hundred years, accounts for a third of the district's silver production, making it one of the world's primary silver producers.

Proterozoic fine-grained siliciclastic rocks of the Belt Supergroup host the ore veins. Metamorphism has caused the host rocks to reach greenschist facies and a long and complex structural history has caused several stages of deformation. The Lewis and Clark line, a major zone of WNW-trending faults and WNW and NS-trending folds transects the district. To the South lies the Idaho batholith, a Cretaceous plutonic body ranging in composition from a granodiorite in the center to a tonalite on the eastern edge. The Wallowa terrane, an early Permian to late Jurassic, intra-oceanic volcanic arc sequence (White et al., 1992) lies to the southwest. Within the Coeur d'Alene district is a zone of anonymously rich silver veins known as the silver belt. The Sunshine mine is found on the western margin of the silver belt.

Despite a prolific production history and the work of numerous geologists, many questions with respect to age, origin, mineralization, and deformation sequence are unanswered. The age of mineralization is considered to be Proterozoic (Leach et al., 1988), Cretaceous (Eaton et al., 1995), or a combination of both (Leach et al., 1998). Basin dewatering during Belt metamorphism (Sorensen, 1968; Ramalingaswamy and Cheney, 1982) or hydrothermal solutions generated from the Idaho batholith or the Gem

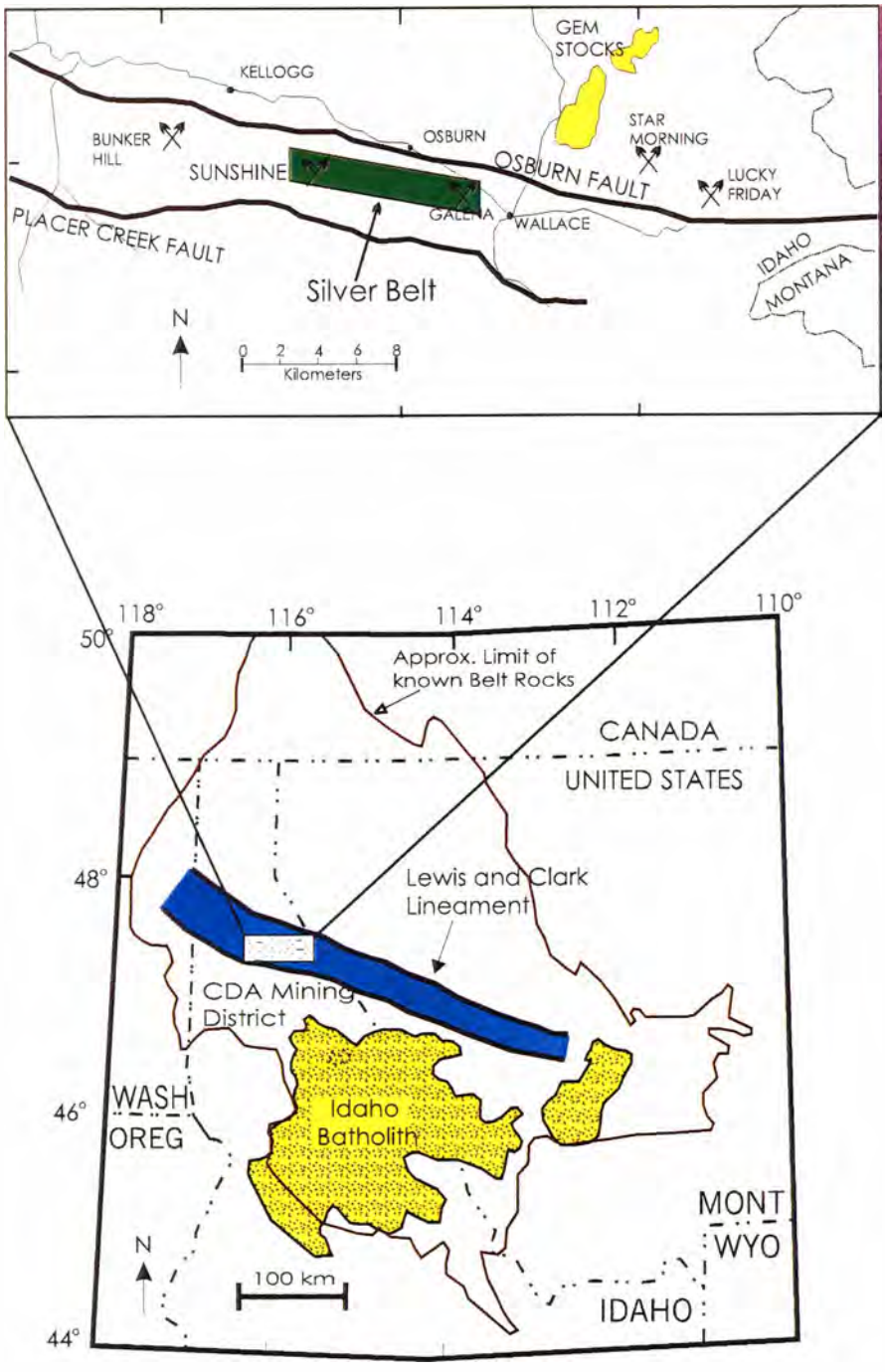

Figure 1. Location of the Couer d'Alene Mining District and geologic features associated with the district. Modified after Wavra et al. (1994) and Gott and Cathrall (1980).

batholith or the Gem stocks (Ransome and Calkins, 1908; Umpleby and Jones, 1923; Anderson, 1949; and Hobbs and Fryklund, 1968) have been suggested as possible mechanisms associated with ore deposition.

This study focuses on the West Chance vein system in the Sunshine mine. Specifically, it examines conditions during mineralization by studying fluid inclusions, and determining pressure, temperature, and composition of these inclusions. Additionally, by combining existing structural data together with detailed mapping and thin section analysis, the structural controls of mineralization in the West Chance vein system are examined.

Previous Work

Because the Coeur d'Alene district has been in production since the late 1800's, published literature is extensive. Fryklund (1964) and Hobbs et al, (1965) provided the original framework of ideas. As additional studies have been conducted and data collected, new concepts of district geology have evolved. This section provides a brief summary of pertinent details regarding geological work and the evolution of geological ideas with respect to stratigraphy, structure, mineralology, alteration, age, and origin of the Coeur d'Alene mining district.

Stratigraphic units of the Belt rocks present locally are the Prichard through Wallace Formations (figure 2). Those units which are most important to ore deposition are the lower Belt rocks of the Prichard Formation and the units of the Ravalli Group consisting of the Burke, Revett, and St. Regis Formations. These fine-grained siliciclastic rocks include thick- to thin-bedded argillite and quartzose argillite of the Prichard Formation, thick-bedded quartzite and siltite of the Revett Formation, and

STRATIGRAPHIC SECTION FOR COEUR d'ALENE DISTRICT

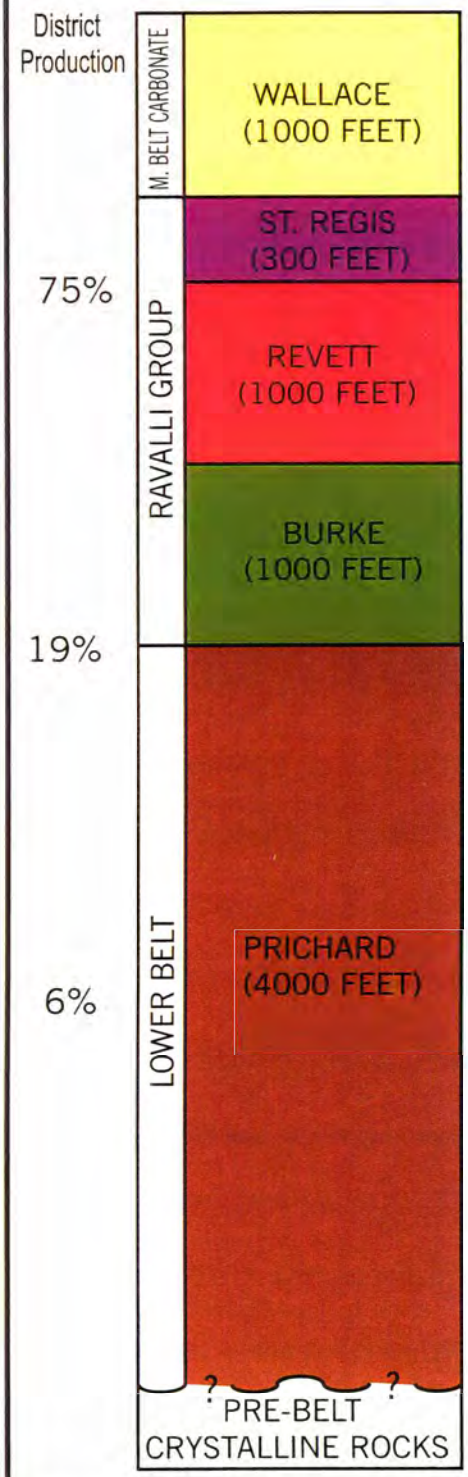

Wallace: silty, tan to brown dolomite interbedded with clean gray dolomite with local beds of non-calcareous siltite and argillite.

St. Regis: dark grey to purple siltites and quartzites; very fine sand and silt layers forming parallel-laminated to slightly wavy, continuous fining upward sequences.

Revett: dark grey to light grey pure and impure quartzites; flat laminated sands and cross-bedded sands interstratified with intervals of discontinuous, wavy and climbing ripple fine sand, silt, and clay.

Burke: dark blue-grey beds of siltite interlayered with argillite and locally thin, tabular interbeds of quartzite Tabular quartzite beds gradually become thicker as the Burke grades into Revett.

Prichard: dark grey to black, thinly laminated argillite and siltite turbidites and cross-bedded quartzites in lower section. Planar laminated black and grey siltites and argillites to cross-bedded siltites and quartzites in upper section.

UNCONFORMITY

Archean crystalline basement rocks of the North American craton

Figure 2. Stratigraphic section of Belt strata in the CDA Mining District, and production % at stratigraphic horizons (modified after Crosby, 1984; Winston, 1986; and White, 1998)

reddish purple, interbedded argillite and impure quartzite of the St. Regis Formation. Subordinate carbonate bearing units are also present throughout the district. Deposition of the Belt rocks occurred from ~1500-1250 Ma and perhaps to 900 Ma (Winston, 1986). Ore veins in the district tend to occur at contacts between lithologic formations (Crosby, 1984). Seventy five percent of the production in the district lies in the St. Regis-Revett transition, 19% in the Burke-Prichard transition zone, and 6% in the middle quartzites of the Prichard Formation (figure 2; Crosby, 1984).

The Coeur d'Alene mining district, including the silver belt, lies within the Lewis and Clark lineament (figure 3). This is a complex structural discontinuity that extends over 400 km from Helena, Montana, to Coeur d'Alene, Idaho, and contains WNW striking faults and WNW and N-trending folds (Sprenke et al., 1991). The Lewis and Clark lineament has been geologically active since middle Proterozoic time and experienced several tens of kilometers of right lateral slip during Late Cretaceous time (Wallace et al., 1990). A dominant structure in the Lewis and Clark lineament, within the Coeur dAlene is the Osburn fault, a deep crustal feature thought to be active since the Late Proterozoic (Bennett, 1982). The Osburn fault presently exhibits 26 km (16.2 miles) of right-lateral offset.

A major structure within the Silver belt, associated with mineralization, is the Big Creek anticline, an asymmetric fold regionally overturned to the north (figure 4; Wavra et al, 1994). The axis of the anticline is approximately horizontal and trends WNW. The south limb of the anticline is internally unstrained, homoclinal, shallowly dipping, and unmineralized. The north limb is upright on the surface, but at depth, is overturned,

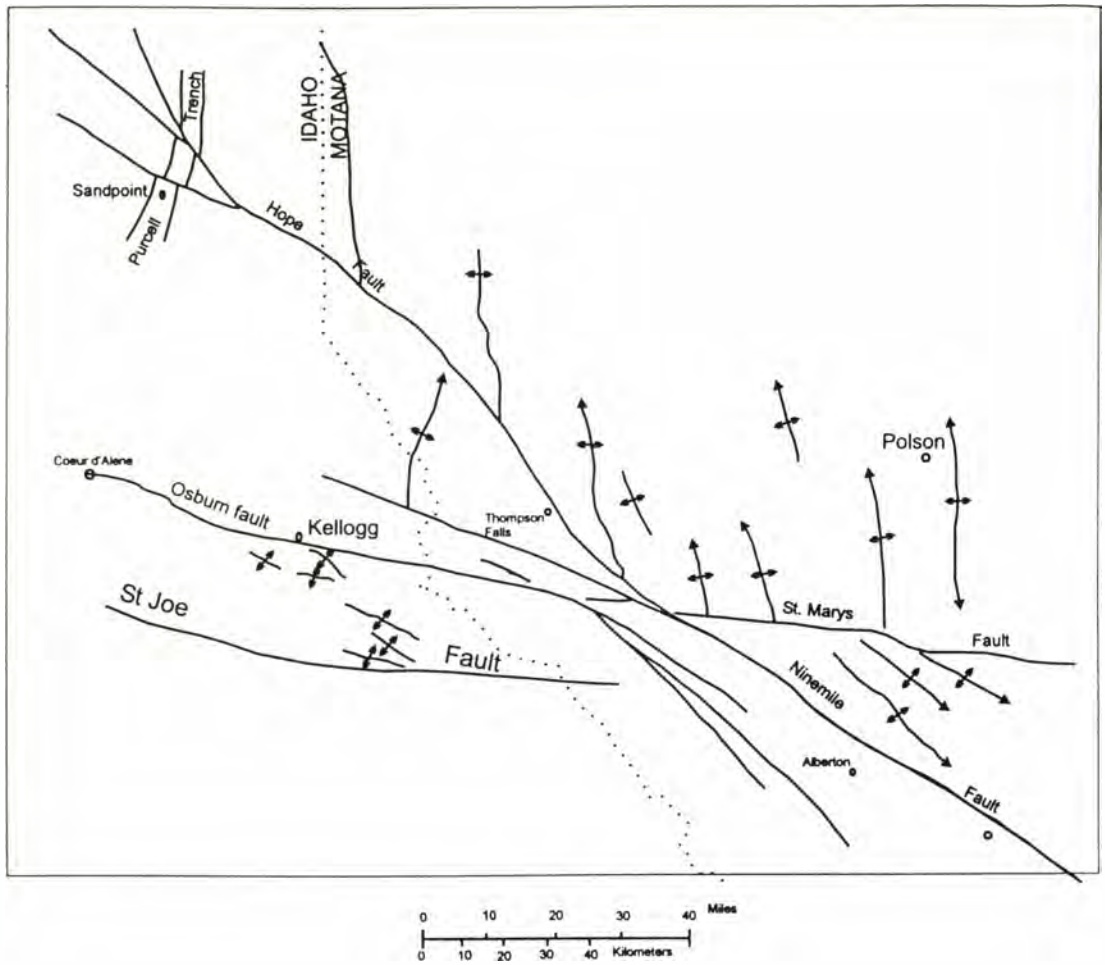

Figure 3. Map of the Lewis and Clark lineament showing north-south-trending folds north of the Osburn fault and west-trending folds south of the Osburn fault (modified after Harrison et al., 1974).

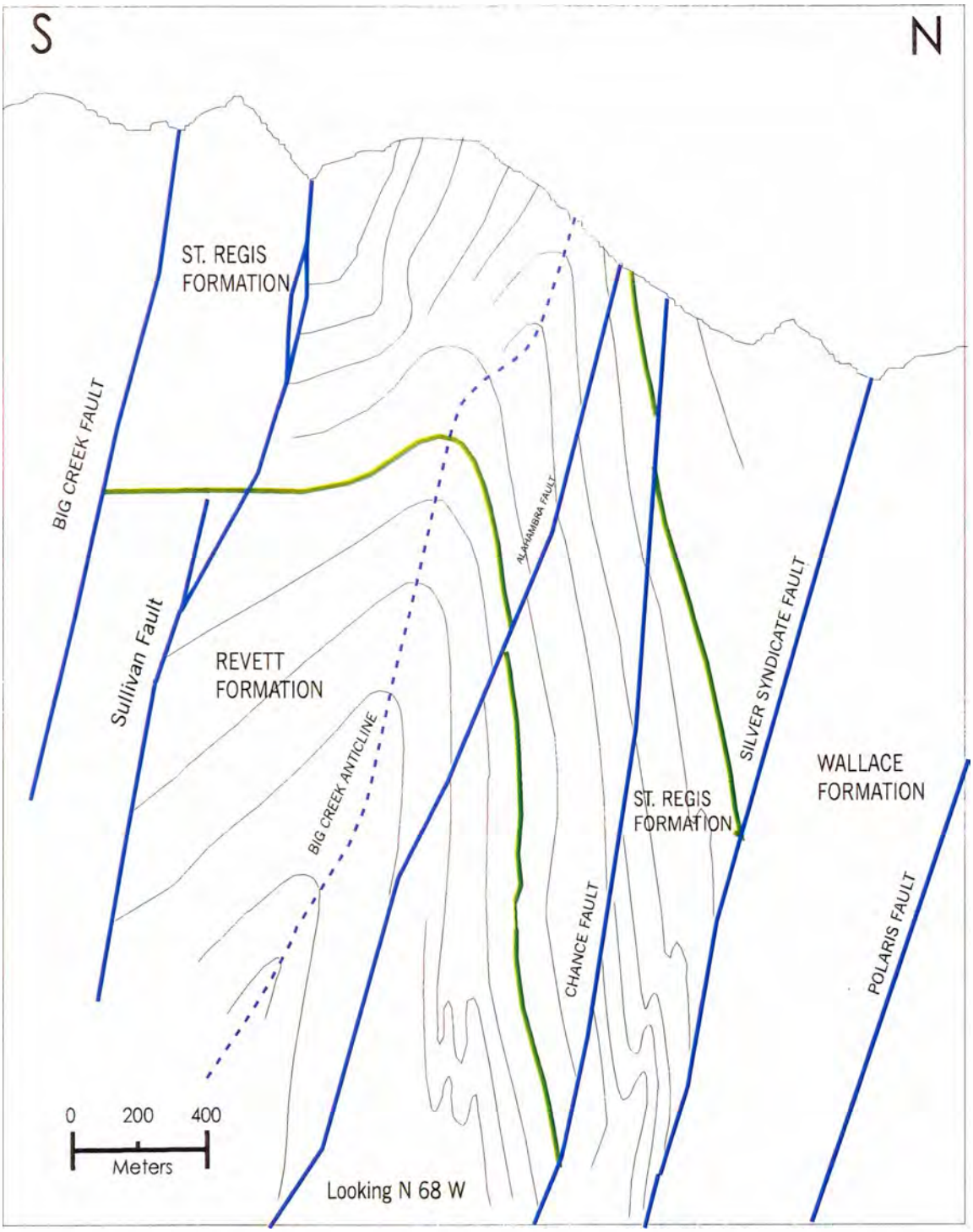

Figure 4. Cross-sectional view of the Big Creek Anticline, looking west. Green lines indicate formation boundaries, blue lines indicate faults, dashed blue lines indicate axial plane trace. Modified from Wavra et al. (1994)

highly strained, contains an abundance of parasitic folds and is strongly mineralized. The north limb is cut by major reverse and normal faults. The age of the anticline is unknown and may be Proterozoic, Cretaceous or both (Wavra et al, 1994).

Hobbs et al. (1965) first noticed the obvious patterns formed on geologic maps by tight, large scale folds (figure 3). This pattern revealed that north of the Osburn fault, folds trend north, whereas south of the Osburn fault, folds trend northwesterly. This difference in fold pattern was interpreted by Hobbs et al. (1965) to be a result of left lateral transcurrent movement along the Osburn fault. Hobbs suggested that folds were originally north trending and formed during the same compressional event. Transcurrent movement along the Osburn fault then caused folds to the south to rotate to a westerly trend. Subsequent studies (Juras, 1982, and White, 1989) suggest that the two fold sets represent two different episodes of folding.

Hobbs et al. (1965) also made the interpretation that veining within the district was a product of left-lateral movement along WNW faults. This interpretation was based primarily on geometric relationships between faults and veins as seen in figure 5. More recently, Wavra et al., (1994) have interpreted the mineralization to be related to reverse movement along faults. Evidence supporting this interpretation includes the identification of a weak but pervasive shearing lineation in wall rocks and kinematic indicators in veins which show reverse motion has occurred along faults in the mine. These kinematic indicators and lineations parallel ore shoots and led Wavra et al. (1994) to suggest reverse motion was synchronous with mineral deposition.

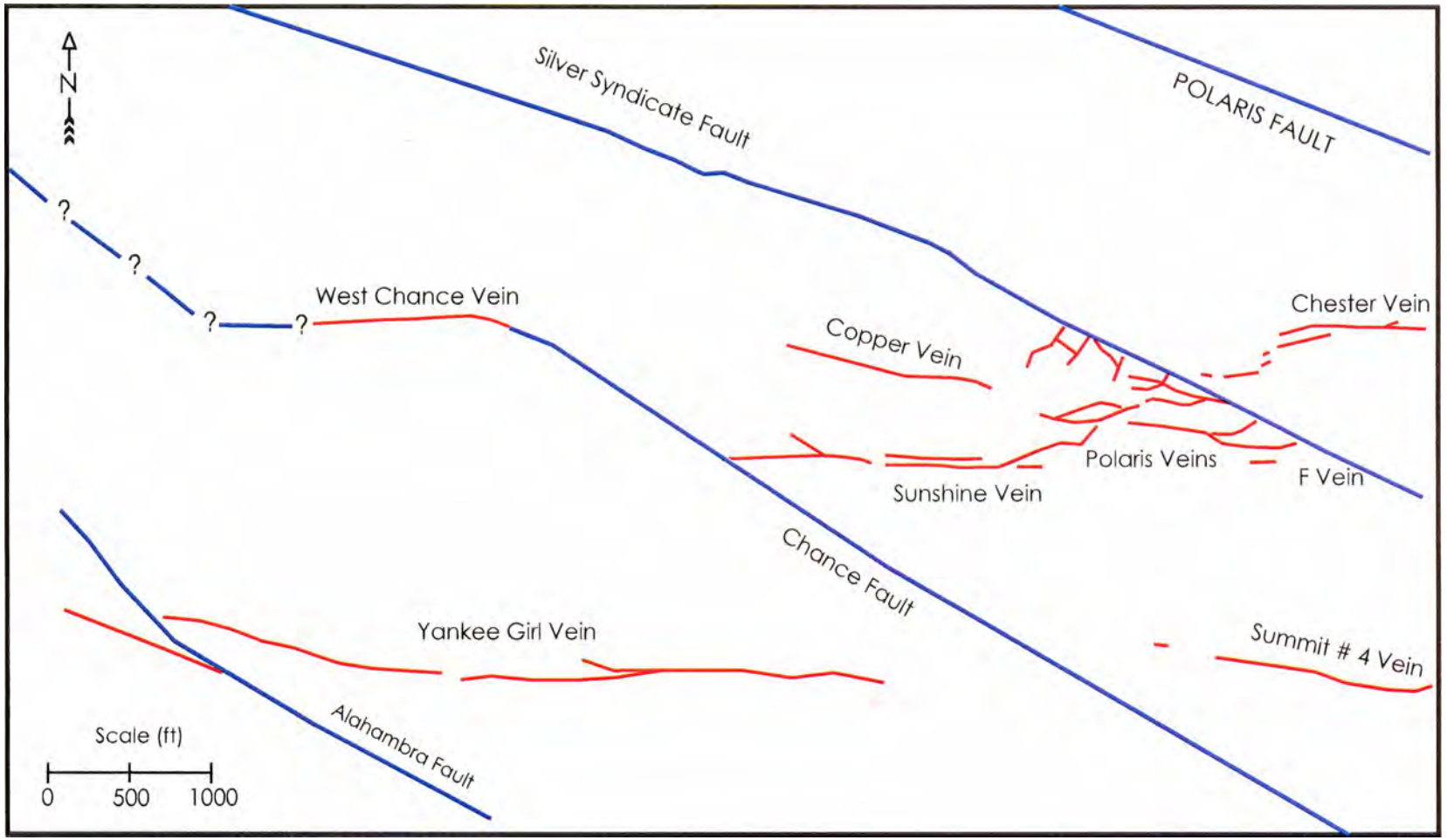

Figure 5. Plan view, 3700 level showing fault-vein geometric relationships. Sunshine Mine, ID. Modified from 3700 geologic level maps (unpublished).

The main silver-bearing mineral in the district is tetrahedrite, $Cu_{12}Sb_4S_{13}$, a sulfosalt, with Ag substituting into the divalent Cu sites. Other sulfide minerals include freibergite, galena, bournonite, arsenopyrite, pyrite, chalcopyrite, and pyrargyrite. Siderite and quartz comprise the gangue minerals. Several types of wall rock alteration exist in the Coeur d'Alene district. Hydrothermal bleaching was first recognized at the Sunshine mine by Rasor (1934). Although this type of alteration does not exist everywhere, where it does exist, bleaching typically extends 10 to 30m outward form the ore bodies, and a 0.5m wide zone of coarse, euhedral pyrite occurs at the edge of this zone (Sunshine mine geologists, pers. comm., 1996). Carbonate zoning in wall rocks adjacent to silver-bearing veins also occurs in the district. A zone of disseminated siderite (10-100m wide) next to the vein is flanked by an intermediate zone of siderite and ankerite (1-30m wide), bordered by a distal zone of ankerite and calcite (many tens of meters wide; White, 1998). Sulfide zoning within the district is also present. According to White (1998), most of the vein systems become more lead-rich as one progresses from depth to the surface.

The age and origin of the ore deposits within the district have been controversial since the early 1900's. Early field studies by Ransome and Calkins (1908), Umpleby and Jones (1923), and Fryklund (1964) suggested that the veins are related to Cretaceous magmatism and compression, including the intrusion of the Idaho batholith and the Gem stocks (figure 1). Subsequent U-Pb determination on uraninite (Kerr and Kulp, 1952) and Pb-Pb model ages on galena (Zartman and Stacey, 1971) have suggested highly variable Precambrian ages ranging from 750 to 1500 Ma. More recent oxygen and carbon isotopic studies (Eaton, 1995) indicate that the veins were deposited in a dynamic,

nonequilibrium system from ascending, highly evolved fluids that acquired their isotopic character from meta-sedimentary rocks, probably during Cretaceous or early Tertiary time. Eaton (1995) also found low $^{87}Rb/^{86}Sr$ and high $^{87}Sr/^{86}Sr$ ratios in mine siderites, and concluded that the radiogenic Sr component was inherited from adjacent wall rocks of the Belt Supergroup. This conclusion lead to the interpretation that mineralization could not have been Precambrian because insufficient time would have elasped for high Rb/Sr wall rocks to become sufficiently radiogenic. Eaton also argued that Precambrian vein formation followed by the injection of radiogenic Sr would require complete recrystallization and destroy discrete oxygen and carbon signatures found in vein siderites. Recent $^{40}Ar/^{39}Ar$ on sericite and additional lead isotope work by Leach et al. (1998) suggest that two major vein-forming events are responsible for the mineralization in the Coeur d'Alene mining district. This idea is derived from the fact that two distinctly different lead ages, Proterozoic and Cretaceous, are found in the district. For example, galena from silver-rich veins in the Sunshine mine yielded a Cretaceous age and galena from lead-rich veins yielded a Precambrian age. $^{40}Ar/^{39}Ar$ data on sericite from the same study suggests a Late Cretaceous age. Supporters of a Precambrian age suggest that the precious-metal veins of the Coeur d'Alene district are the product of deformation coupled with regional metamorphism of the Belt basin around 850 Ma. Supporters of a Cretaceous age suggest mineralization is related to hydrothermal fluids associated with the emplacement of the Idaho batholith during the Laramide orogeny.

Four previous fluid inclusion studies have been completed in the district (Yates and Ripley, 1985; Leach et al., 1988; Constantopolus, 1989; Trachte, 1993). These studies found homogenization temperatures ranging from 180 to 430 °C. Leach et al.

(1988) concluded that the mineralizing solutions were complex CO_2-CH_4-C_nH_m-N_2.H_2 O-NaCl solutions and ore deposition occurred between approximately 250 to 350 °C and at pressures in excess of 1 kb. The inclusions were of three types: 1) H_2O dominant inclusions 2) gas dominant inclusions, and 3) inclusions with salinities of less than 1 equivalent wt.% NaCl. Leach et al. (1988) proposed that these fluids changed in composition with time during at least two major periods of deformation. The systematic shift from CH_4.C_nH_m rich fluids in older zinc-rich veins to CO_2 rich fluids in the younger silver-rich veins records the evolution of the metamorphic fluids to higher fO_2 conditions. Although the mechanism by which the metamorphic fluids attained high fO_2 values is not clear, this change in fluid composition has been documented in many other metamorphic terranes (Crawford, 1981).

Sunshine Mine Geology

Several major vein systems have been exploited during the history of the mine, namely the Chester, Sunshine, and Copper vein systems (figure 6). These vein systems have been studied through a variety of analysis by mine geologists, consultants, and graduate students. As a result, the mineralization sequence and basic structure of these areas are established and discussed below. The study of the vein systems has contributed to the understanding of district geology, discussed in the previous section.

The major vein systems shown in figure 6 have several defining characteristics. In general, they have a westerly trend and occur as link veins between WNW trending faults. Within these major systems, individual veins may strike east, northeast, and west-northwest. The recently discovered West Chance ore body is distinct from most vein systems in the mine. Ore in the West Chance is associated with a major fault

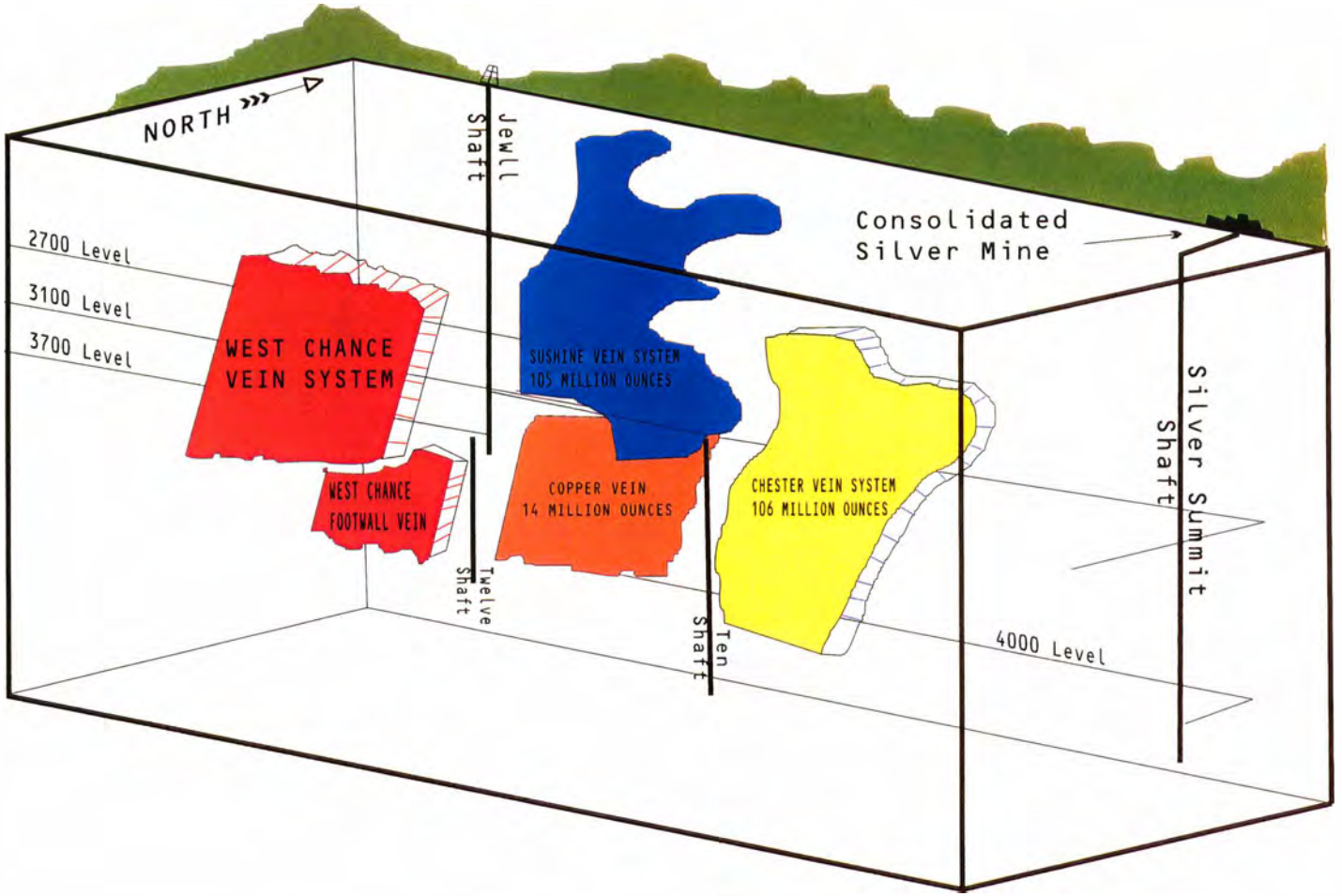

Figure 6. Vein systems of the Sunshine Mine.
(Compiled by Sunshine Geologists from unpublished mine data)

system. More specifically ore is found on a westerly bend within a northwest trending fault system, not as a link vein. Mineralization is discontinuous along the West Chance ore body due to its spatial association with a major fault system.

The chronology of mineralizing events was first documented by Umpleby and Jones (1923), and has been supported by observations by mine geologists throughout the district. Cross-cutting relationships show that the quartz-carbonate veins were deposited first, followed by sulfide mineralization (tetrahedrite, pyrite, pyrargyrite, bournonite, chalcopyrite), with galena being deposited in the last stage. Figure 7 shows a paragenetic sequence for the Sunshine mine, based on these cross-cutting relationships and observations from this study. Tetrahedrite is typically found as fracture-fill material in siderite, but can also occur in concentrated veinlets. Tetrahedrite defines ore shoots within the vein systems at the Sunshine mine. These ore shoots are distinct mineralogically from the host siderite-quartz veins, and have elongate to pipe-like forms (Bond et al., 1992). Regardless of the strike of the siderite-quartz veins (west, northeast, and west-northwest), the major ore shoots plunge steeply to the southwest (Bond et al., 1992). Microprobe and geochemical analysis suggest that different Cu:Ag ratios exist within the vein systems. Mine geologist Rod Cleland (pers. communication) has observed 100:1 veins cutting 60:1 veins which cut 40:1 veins, suggesting the highest ratio is the youngest. Lead zoning is present in the Sunshine mine. As a general rule, most ore bodies become lead rich towards the top of the vein system, similar to other parts of the district.

The deformational history at the Sunshine mine has been subdivided into 5 stages by Wavra et al. (1994) as follows: stage 1: development of the Big Creek anticline; stage

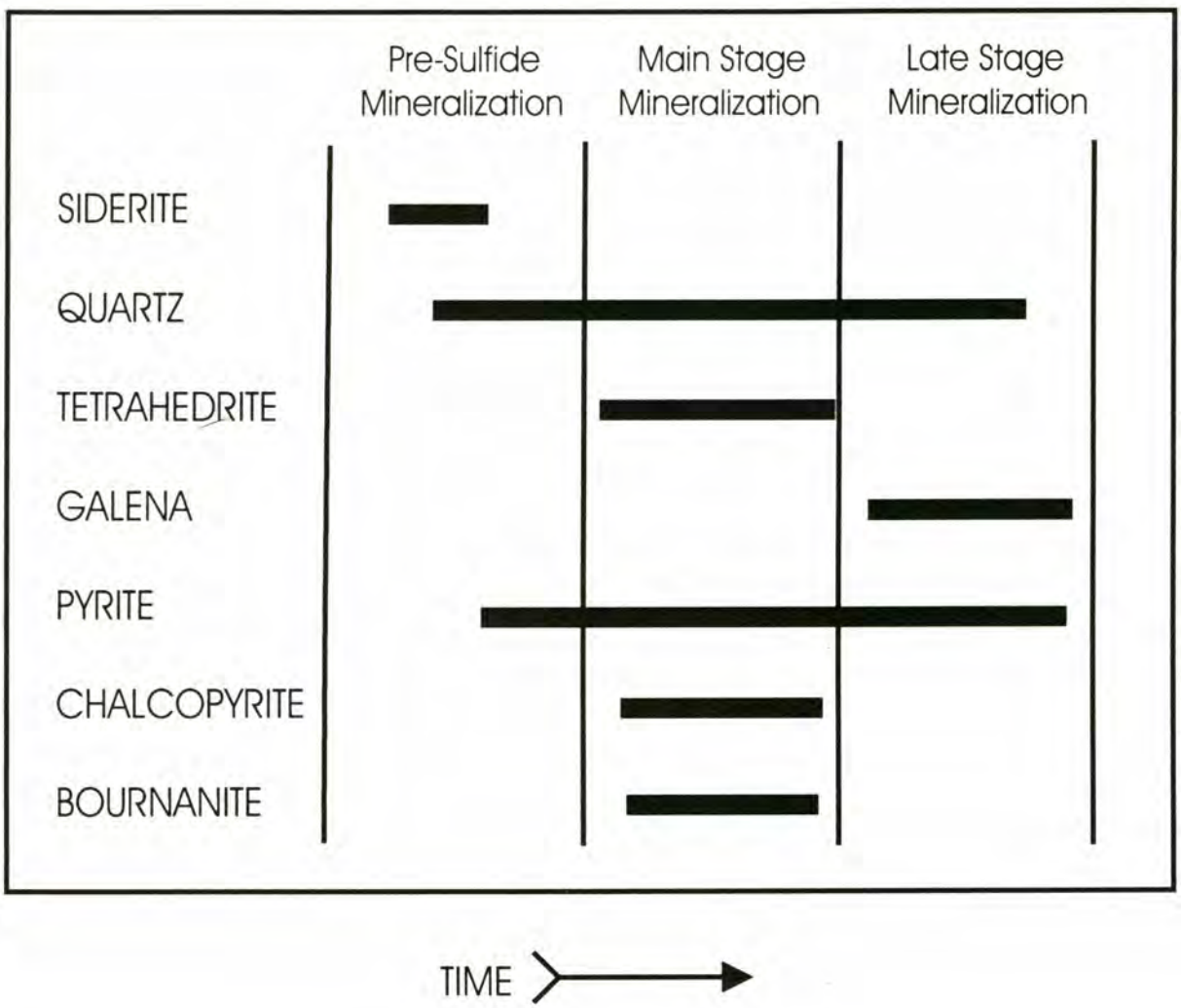

Figure 7. Paragenetic sequence for ore and gangue mineralization, Sunshine Mine, ID (Hobbs and Fryklund, 1968)

2: development of transectional cleavage and greenschist metamorphism; stage 3: reactivation of cleavage and the formation of siderite-quartz veins along high angle reverse and normal fractures, also associated with this stage is late vein deformation and the generation of steeply west-plunging ore shoots; stage 4: late extensional event which produced normal faults and kink bands. The normal faults commonly offset veins and ore shoots and possibly could be related to the Polaris fault (a normal fault within Sunshine mine northeast of the West Chance ore body see figure 5); stage 5: minor, brittle strike-slip faulting related to the Osburn fault. Horizontal slickenlines, typically found in lead rich veins, have been observed to overprint steeper slickenlines, and are thought to be associated with this event.

The causes of ore deposition are not known. A small decrease in temperature and pressure of the fluid is expected over the vertical extent of the fracture-vein system, and that could have resulted in mineral deposition. The presence of immiscible fluids trapped in some inclusions suggests that pressure fluctuations occurred. Pressure fluctuations could have resulted from tectonic activity or from periods of hydrofracturing (Leach et al., 1988). Ore deposition may also have resulted from mixing of vein fluids with fluids of contrasting composition in adjacent wall rocks.

Previous work in the Sunshine mine and other mines in the Coeur d'Alene district has provided insight on the geology of this region, however many questions remain unanswered. Isotopic data suggest that the origin and age of mineralization is related to pluton emplacment during the Cretaceous (Ransome and Calkins, 1908; Umpleby and Jones, 1923; Anderson, 1949; and Hobbs and Fryklund, 1968) or basin dewatering during the Precambrian (Sorensen, 1968; Ramalingaswamy and Cheney, 1982). Mineralization

has been suggested to be associated with strike-slip or dip-slip movement and precipitation mechanisms are thought to be the result of fluid mixing or pressure fluctuations. Each individual debate has supporting and contradictory evidence, and it is currently undecided which of these arguments are correct.

Mine development of the West Chance vein system began in 1991. Consequently, the structural and stratigraphic controls and genetic origin for this ore body have not been studied extensively. This vein system will be the main focus of this study and provides additional insight into these questions.

Objectives

The purpose of the present study is as follows:

1. To understand the structural control of the West Chance ore body and its relation to other veins in the Sunshine mine.
2. On the basis of fluid inclusion analysis determine (a) the pressure, temperature, and composition of hydrothermal fluids responsible for the West Chance vein system (b) how these parameters vary as a function of depth and (c) how the West Chance system compares with other vein systems in the mine.
3. To use the information obtained above together with previous work and construct a structural and ore depositional model for the West Chance vein system.

This study will help to define transport and precipitation mechanisms in the West Chance area and may be useful in exploration for extensions of ore bodies and/or discovery of unknown ore bodies at the Sunshine mine.

CHAPTER 2: FLUID INCLUSIONS

Fluid inclusion analyses have provided some of the most useful information for determining the physical and chemical environments of mineral formation. This study focuses on fluid inclusions found in quartz veins in the West Chance vein system. Compositions of fluid inclusions were determined from temperatures of phase changes during microthermometric analysis of selected samples. This study indicates that homogenization temperatures were constant and that salinity varied with depth. Two models are proposed to explain these observations. Additionally, this data is used to constrain formation conditions during mineral deposition by comparing it to experimentally determined pressure-volume-temperature-composition (PVTX) data for the H_2O-NaCl system.

Sample Collection

Fluid inclusion samples were collected during the 1996 field season and during subsequent visits and short-term employment periods. Samples from the 4400 level were collected from 44CF-4, a stope located in the footwall of the main West Chance ore body. Samples from the 4200 level were collected from the back (or ceiling) of the main drift during a visit to this now closed area of the mine. All other samples were collected from working stopes during routine sampling and mapping. Locations (figure 8) and general characteristics of fluid inclusion samples from the West Chance area were recorded during sample collection.

Classification of Fluid Inclusions

This study focused on primary inclusions found in longitudinal and ladder quartz veins of the West Chance vein system. In other vein systems within the mine, quartz

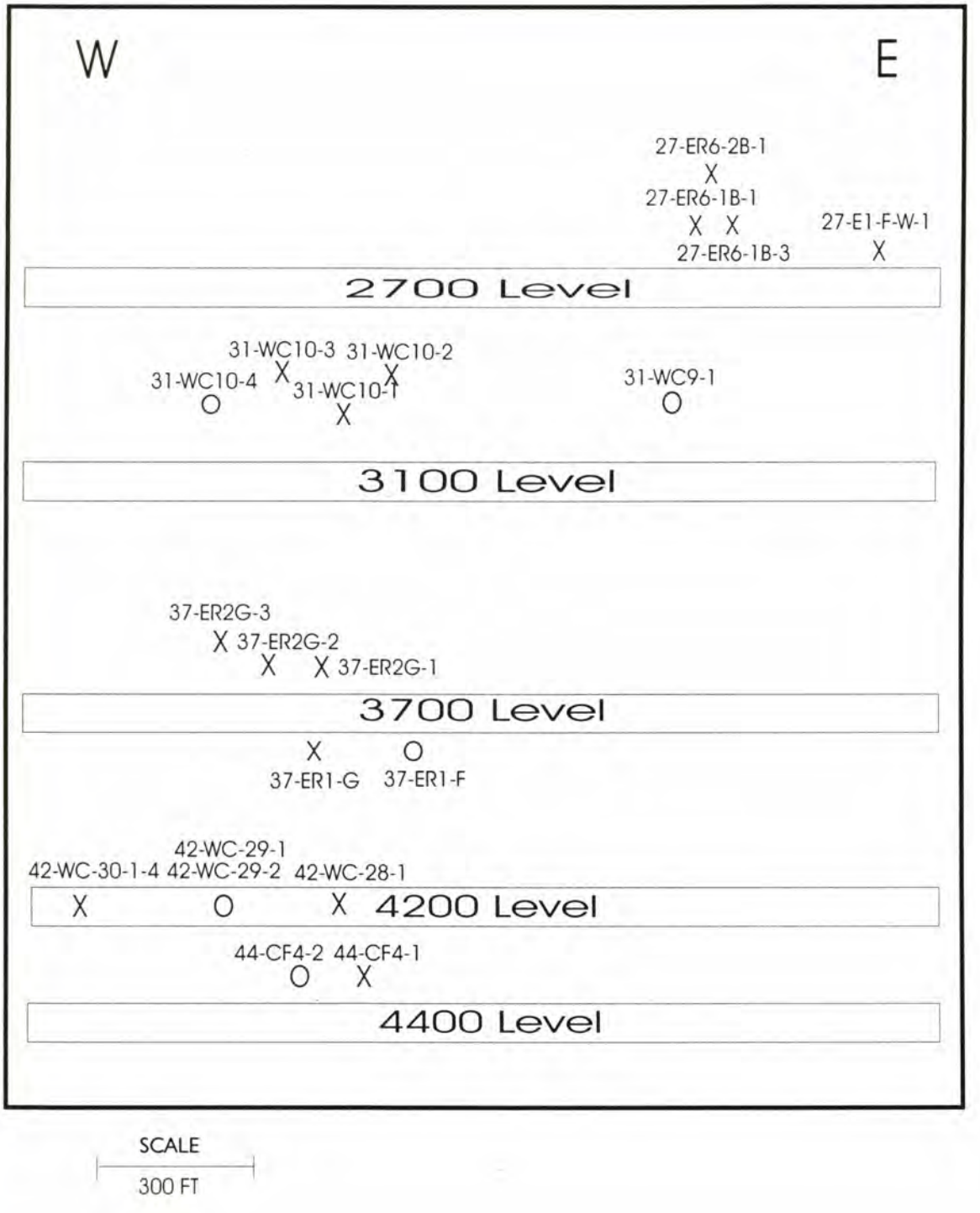

Figure 8. Sample locations plotted on a longitudinal section of the West Chance vein system, looking north. X: longitudinal quartz veins; O: ladder quartz veins

veins have been previously categorized by mine geologist Craig Wavra (Trachte, 1993) as (from oldest to youngest) sigmoidal, longitudinal, ladder, and later vein set. Generally, the same types of quartz veins were present in the West Chance. Cross-cutting relationships show the same relative ages of these quartz veins. Samples collected from the sigmoidal and later vein types did not contain inclusions adequate for analysis due to their small size and secondary nature, therefore all fluid inclusions used in this study were collected from longitudinal and ladder veins. It was initially determined that temperatures and pressures gathered from these data sets would be accurate in representing conditions present during mineralized vein formation, since the described quartz veins were formed after the deposition of siderite, but before and/or during the deposition of Ag and Pb.

The general characteristics of the two vein types used in this study are presented in Table 1. Figures 9a and 9b shows photographs of the two types of quartz veins from stope faces. Samples from the two different types of quartz appear similar in hand specimen. Typically, quartz in the observed samples is massive and milky. When observed with the petrographic microscope in thin section, ladder veins exhibited a fracture filling texture and more often are deformed. As a result, these samples did not preserve primary inclusions as well as longitudinal quartz veins.

The vein sets not used in this study (later and sigmoidal) generally had a northeast to northwest strike and dip to the south. Both vein sets were barren, 10-15 cm thick (3.9-5.9 inches) and cut mineralized veins.

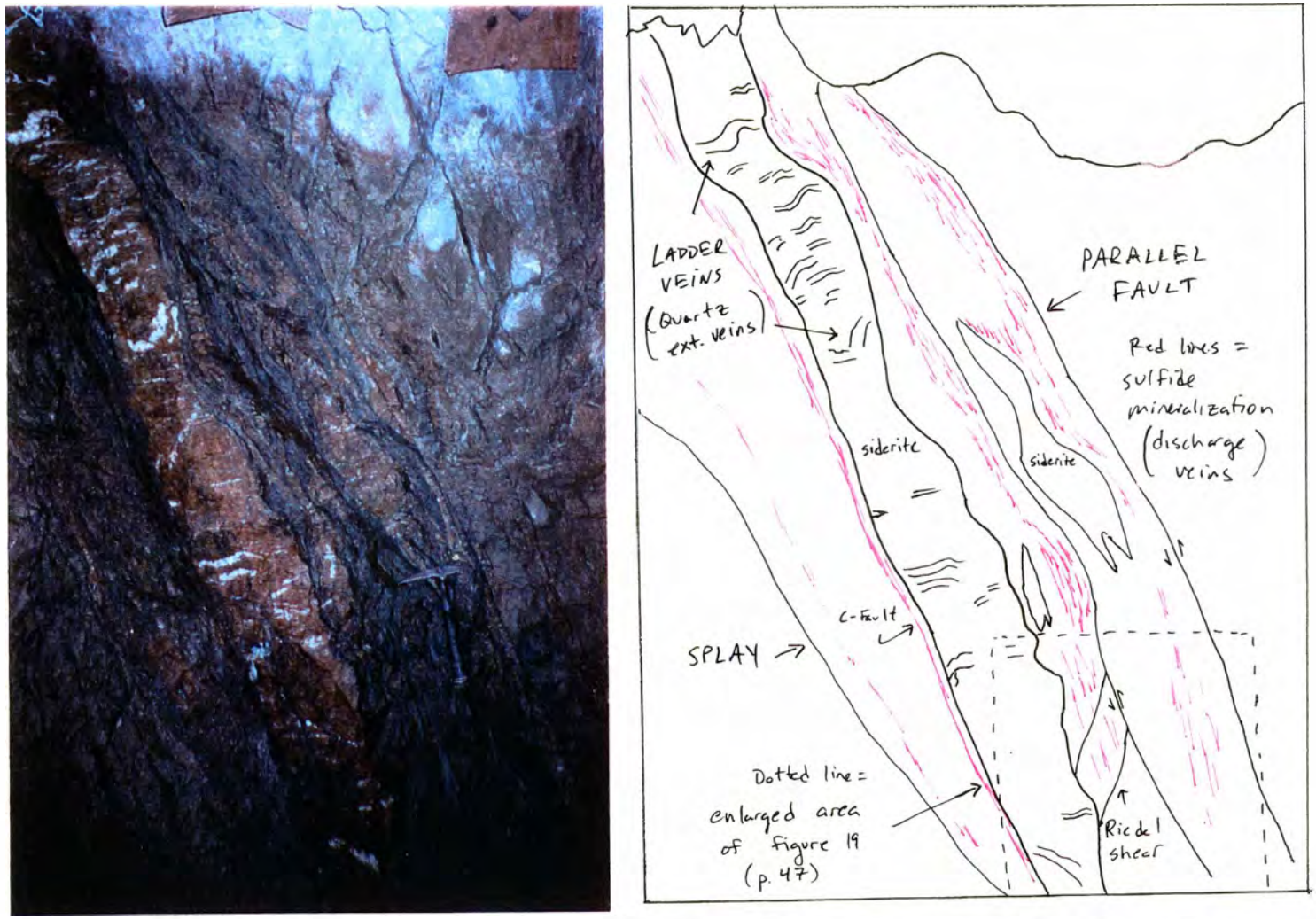

Figure 9a. Face photo from 3700 ER2B E showing several features of the West Chance vein system as referred in text. Quartz ladder veins in siderite veins, anastomosing nature of shears, fractures, and veins; comparison of splays and Riedel shears; and cross-cutting relationships between extension veins and discharge veins.

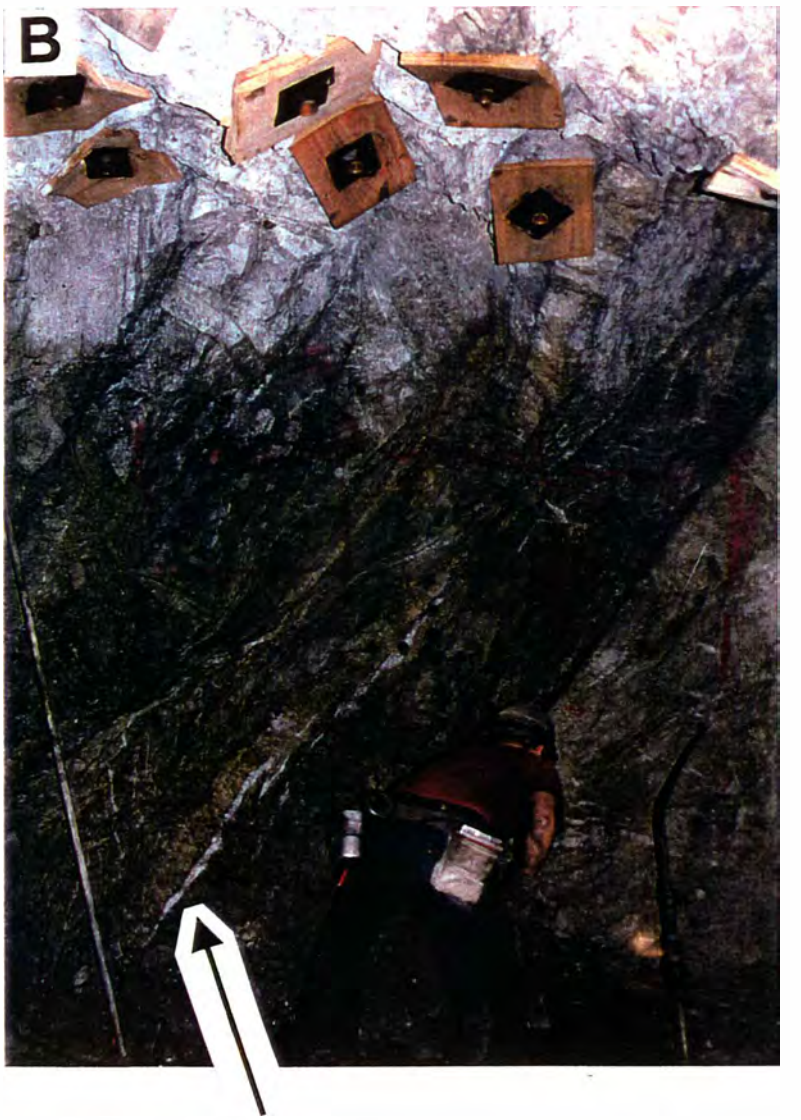

Figure 9b. Photo from 2700 ER2B W showing example of longitudinal quartz veins used in fluid inclusion analysis.

TABLE 1 – GENERAL CHARACTERISTICS OF QUARTZ USED IN FLUID INCLUSION ANALYSIS	
TYPE	**FEATURE**
Longitudinal	- parallels mineralized veins (strike E, dip steeply S) - 5 to 15 cm thick - occasionally contains clasts of siderite - massive and milky - equigranular texture - better preservation of primary inclusions
Ladder	- strike northeast to northwest, shallow dip north - 1 to 15 cm thick - bounded by vein-wall rock interface - appear as ladder rungs in cross section (in stope face) - massive and milky - exhibit microscopic fracture-filling texture

Quartz crystals used for fluid inclusion analysis are subhedral to anhedral and 1-5 mm long. All of the samples showed some degree of strain characterized, in order of abundance, by undulatory extinction, serrated grain boundaries, deformation bands, elongate subgrains surrounded by small domains of recrystallized quartz, and sutured boundaries. The frequency of occurrence and intensity of these deformational features vary among samples. In general, these deformational features were more prevalent in the ladder veins and less abundant in longitudinal veins.

Qualitative observations on the inclusions are presented below with respect to the following classification: size, genetic classification, descriptive classification, and shape.

Size: Most inclusions were less than 5 microns (1.9×10^{-5} inches) in diameter, a few were between 5 and 10 microns, and very few were greater than 10 microns (3.9×10^{-6} inches). No systematic variation in homogenization temperature, T_h, was observed

between different sizes of inclusions. The small size of the inclusions was a limiting factor in the type and certainty of observations that could be made. In general, inclusions less than 5 microns yielded homogenization temperature data only. Inclusions in the 5 to 10 micron range and above, were adequate to obtain temperatures of last melt (and therefore salinity).

Genetic classification: Textural features of fluid inclusions can be used to distinguish between the primary, psuedosecondary, and secondary nature of the inclusions (Roedder, 1984). The criteria used in genetic classification is detailed below.

Primary and pseudosecondary inclusions: The distinction between these two genetic classifications of fluid inclusions is problematic for hydrothermal veins. By definition, primary inclusions are formed when a crystal growing in a fluid medium traps some of the fluid as a result of a growth irregularity in the crystal; pseudosecondary inclusions are the result of the healing of fractures formed during crystal growth (Roedder, 1984). No pseudosecondary inclusions were observed. Four criteria that can be used to define primary origin for inclusions are as follows: 1) occurrence parallel to growth zones, 2) three-dimensional random distribution, 3) isolation and 4) large size. Only criteria 2 and 3 could be applied in this study and emphasis was put on isolation in the selection of "primary" inclusions for microthermometry measurements. Figure 10 shows a photomicrograph of primary inclusions used in this study. The criteria of random distribution and isolation can be seen. The recognition of growth zones in the samples from the West Chance area was not possible.

Secondary inclusions were abundant in all samples. Secondary inclusions are those that form by any process after the crystallization of the host mineral is essentially

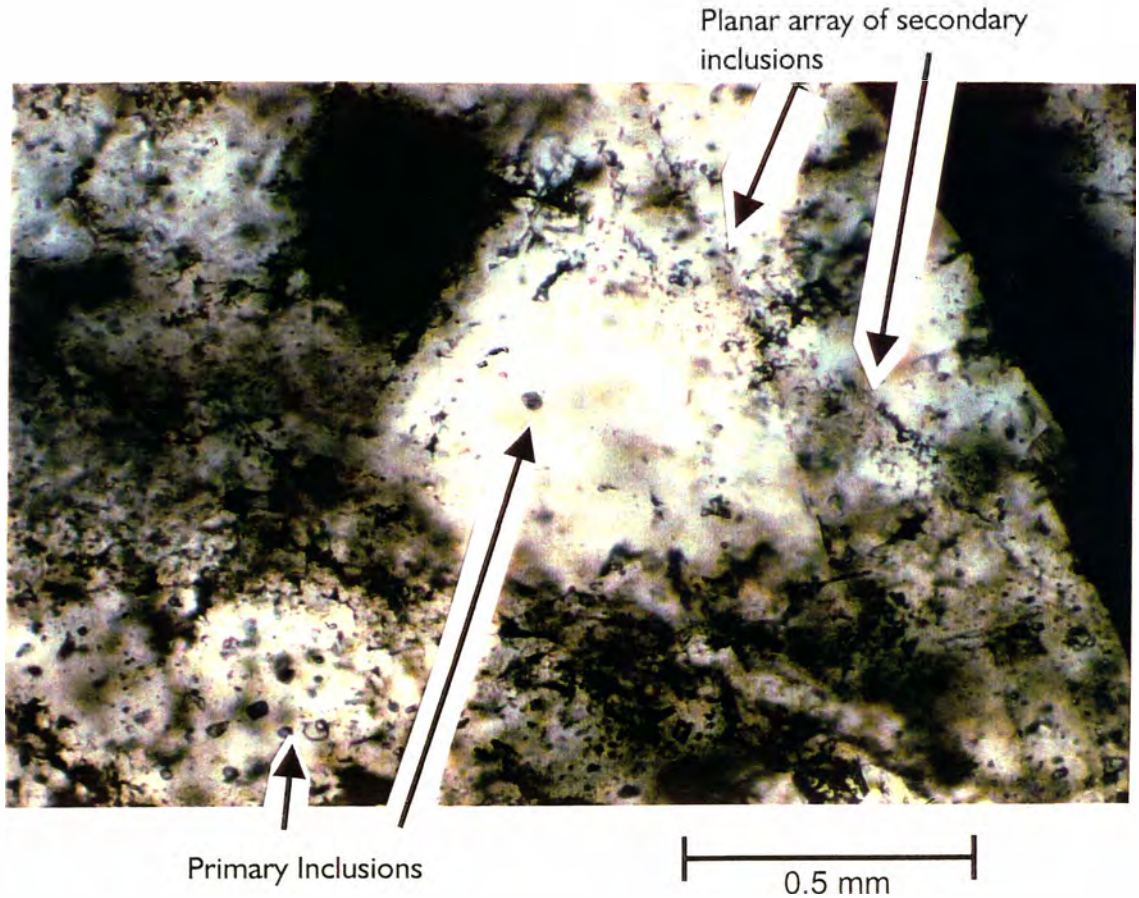

Figure 10. Photomicrograph of primary fluid inclusions from the West Chance vein system. Primary inclusions in this photo show distinguishing criteria for primary inclusions - random distribution and isolation. Photo also shows planar array of secondary inclusions. Sample 31-WC10-3-1.

complete (Roedder, 1984). Mode of occurrence and geometry of secondary inclusion arrays vary considerably. The arrays of secondary inclusions are planar to curved and can be closely spaced, although the orientation of planes containing secondary inclusions varies widely. These inclusions are interpreted to fill healed fractures in the quartz.

Descriptive Classification: The nomenclature used for delineating fluid inclusion types is specific to this study. Two types of primary fluid inclusions were observed in samples collected from the West Chance vein system. Type I inclusions, those with small vapor bubbles (<<40% by volume) and relatively low salinity (<20 wt.% equivalent NaCl), were abundant and could be positively identified by the movement of their bubbles. Type II inclusions, those in which CO_2 is present, were not as common. A double meniscus was not observed in the type II inclusions, but the presence of CO_2 was identified by the presence of a clathrate melt. Liquid CO_2 was also not identified in type II inclusions. Inclusions were either too small to identify a double meniscus, or the critical concentration of CO_2 was not reached in this hydrothermal system to allow formation of an immisicible liquid CO_2 phase.

Shape: The shape of the inclusions varied from to spherical to oblong to irregular to angular. Of all the different morphologies, the oblong and irregular were best suited for study because the bubble remained visible during microthermometry measurements.

An outline of experimental procedures for microthermometry measurements, which includes sample preparation and equipment, can be found in Appendix A.

Homogenization Data

Most fluid inclusions consist of H_2O-NaCl solutions with a few inclusions consisting of a H_2O-CO_2-NaCl solution. All inclusions homogenized to liquid with the

vapor bubble decreasing in size until final disappearance at the homogenization temperature, $T(h)_{liquid}$. Homogenization data are shown in table 2. The longitudinal set of quartz veins represents the majority of data (78%) recorded. Figure 11 shows a histogram of the two data sets. The longitudinal quartz data set had a mean homogenization temperature of 268.7 °C with a standard deviation of 21.8 °C, and the ladder quartz data set had a mean homogenization temperature at 275.8 °C with a standard deviation of 25.0 °C. There is no significant variation of homogenization temperatures between the two types of quartz veins, and henceforth they will be referred to as one data set.

Data from the Silver Line, a small ore body northeast of the West Chance vein system are also shown in table 2. Temperatures from this ore block range from 269.0-302.9 °C. Only 5 inclusions were analyzed from this suite of rocks due to a lack of primary inclusions in collected samples. It was concluded that these 5 samples did not constitute a representative sample population and therefore the data from these inclusions were not used in further analysis.

The distribution of homogenization temperatures for the West Chance vein system show a Gaussian distribution. Homogenizing temperatures range from 190.6 to 325.8 °C, with a mean temperature of 270.9 °C and a standard deviation of 22.5 °C. Figure 12 shows temperature fluctuations with respect to level and table 3 records the mean homogenization temperature for each level. Although the highest mean temperatures occur on the 3700 level, the data indicates no systematic variation of temperature with respect to level.

TABLE 2. Fluid inclusion data for the West Chance and Silverline ore bodies.

SAMPLE LOCATION *	TYPE	$T(h)_{liquid}$ °C	$T_{(m)}$ °C	salinity (wt. %)	theta (0 - f.p.)	
27-ER6-2B-W-1-1	longitundinal	225.7	-0.3	0.5	0.3	1
27-ER6-2B-W-2-1	longitundinal	282.5	-1.1	1.9	1.1	1
27-E1-F-W-1-1	longitundinal	294.8	-0.7	1.2	0.7	1
27-E1-F-W-1-2	longitundinal	264.3				1
27-ER6-1B-1-1	longitundinal	270.3	-2.5	4.2	2.5	1
27-ER6-1B-3-1	longitundinal	294.6				1
31-WC10-1-1	longitundinal	257.5	-5.2	8.1	5.2	1
31-WC10-1-2	longitundinal	279.7	-3.6	5.8	3.6	1
31-WC10-1-3	longitundinal	270.8	-8.4	12.2	8.4	1
31-WC10-1-4	longitundinal	264.1	-2.4	4.0	2.4	1
31-WC10-2-1	longitundinal	190.6	-1.3	2.2	1.3	1
31-WC10-2-2	longitundinal	272.4	-5.6	8.7	5.6	1
31-WC10-2-3	longitundinal	275.3	-2.6	4.3	2.6	1
31-WC10-3-1	longitundinal	260	-2.8	4.6	2.8	1
31-WC10-4-1	ladder	278.7	-1.4	2.4	1.4	2
31-WC10-4-2	ladder	263.4	-4.4	7.0	4.4	2
31-WC10-4-3	ladder	224.2	-5.2	8.1	5.2	2
31-WC9-1-1	ladder	315.1	-4.2	6.7	4.2	2
31-WC9-1-2	ladder	283.6				2
37-ER2G-1-1	longitundinal	259.7				1
37-ER2G-1-2	longitundinal	278.8	-2.1	3.5	2.1	1
37-ER2G-2-1	longitundinal	283.5				1
37-ER2G-2-2	longitundinal	285.7				1
37-ER2G-2-3	longitundinal	278.6				1
37-ER2G-3-1	longitundinal	290.3	-2.5	4.2	2.5	1
37-ER1F-1-1	ladder	312.6				2
37-ER1F-1-2	ladder	275.3				2
37-ER1G-1-1	longitundinal	286.5				1
37-ER1G-1-2	longitundinal	267.5				1
42-WC-28-1-1	longitundinal	246.3				1
42-WC-28-1-2	longitundinal	275.6	-1.2	2.1	1.2	1
42-WC-29-1-1	ladder	272.3	-4.2	6.7	4.2	2
42-WC-29-1-2	ladder	264.5				2
42-WC-29-2-1	ladder	259.3	-5.6	8.7	5.6	2
42-WC-30-1-1	longitundinal	287.5				1
42-WC-30-1-2	longitundinal	263.7	-5.3	8.3	5.3	1
42-WC-30-1-3	longitundinal	295.6				1
42-WC-30-2-1	longitundinal	325.8				1
42-WC-30-2-2	longitundinal	260.2	-3.9	6.3	3.9	1
42-WC-30-2-3	longitundinal	268.2				1
42-WC-30-2-4	longitundinal	257.3				1
42-WC-30-3-1	longitundinal	258.8				1
42-WC-30-3-2	longitundinal	272.4				1
42-WC-30-3-3	longitundinal	235.9				1
42-WC-30-3-4	longitundinal	260.2				1
42-WC-30-4-1	longitundinal	253.4				1
44-CF4-1-1	longitundinal	282.3	-7.6	11.2	7.6	1
44-CF4-1-2	longitundinal	275.6	-5.5	8.5	5.5	1
44-CF4-1-3	longitundinal	264.2				1
44-CF4-1-4	longitundinal	274.3	-5.3	8.3	5.3	1
44-CF4-1-5	longitundinal	265.8				1
44-CF4-2-1	ladder	254.3				2
44-CF4-2-2	ladder	296.5	-4.2	6.7	4.2	2
44-CF4-2-3	ladder	271.3				2
44-CF4-2-4	ladder	279.4	-5.3	8.3	5.3	2
44-CF4-2-5	ladder	225.1				2
37-SL-1	longitundinal	280.2	-7.2	10.7	7.2	1
37-SL-2	longitundinal	269.0	-8.6	12.4	8.6	1
37-SL-3	longitundinal	302.9	-12.8	16.8	12.8	1
37-SL-4	longitundinal	301.0	-8.3	12.1	8.3	1
37-SL-5	longitundinal	292.0	-2.1	3.5	2.1	1

*Sample Notation = level-stope-chip# - inclusion #

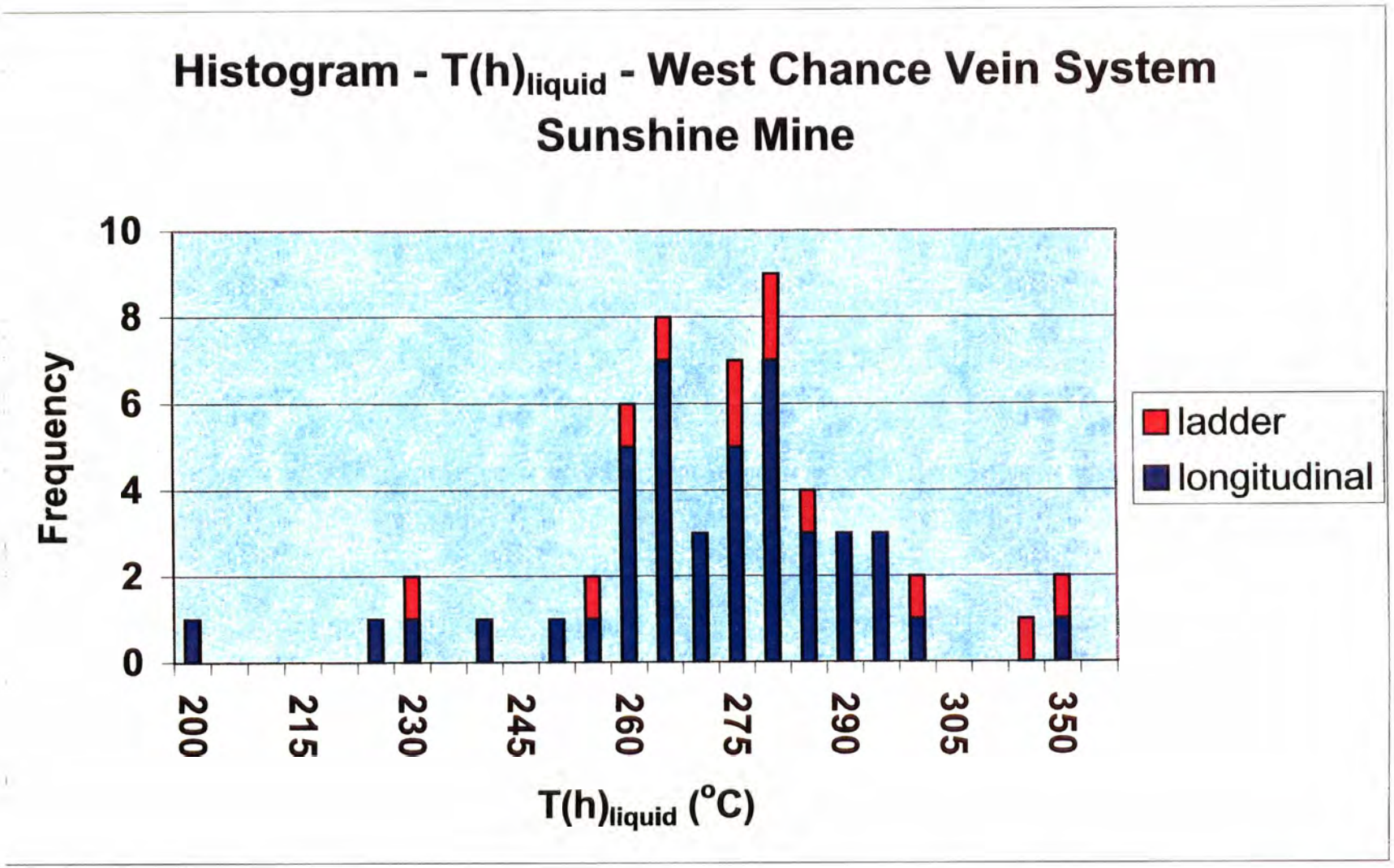

Figure 11. Comparison and distribution of $T(h)_{liquid}$ for fluid inclusions in longitudinal and ladder veins in the West Chance Vein System

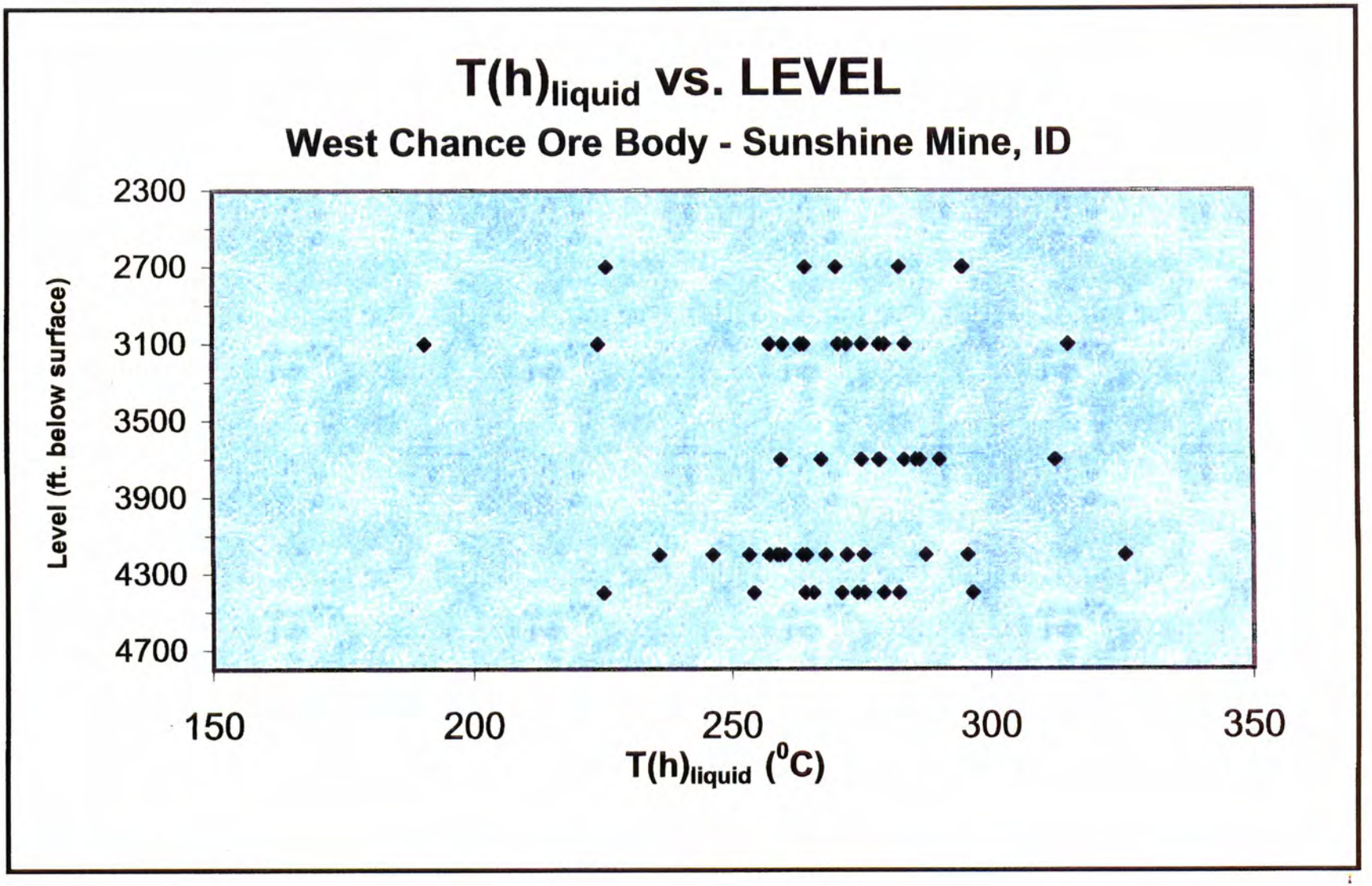

Figure 12. Homogenization temperature fluctuation with respect to depth, showing T(h) does not vary as a function of depth.

TABLE 3 – MEAN HOMOGENIZATION TEMERATURES FOR LADDER AND LONGITUDINAL VEIN SETS		
LEVEL	TEMPERATURE (°C)	SALINITY (wt. % NaCl)
2700	272.0 +/- 22.5	1.9 +/- 3.0
3100	264.0 +/- 22.5	6.2 +/- 3.0
3700	281.9 +/- 22.5	3.8 +/- 3.0
4200	268.1 +/- 22.5	6.4 +/- 3.0
4400	268.9 +/- 22.5	8.6 +/- 3.0

Freezing Data

Due to the overall small size of the fluid inclusions found in this study, only half of the inclusions were adequate to obtain final melt temperatures. Freezing data are also presented in table 2. Temperatures of final melt range from –8.4 to – 0.3 °C. This range of values yield a range of salinities of 0.5 to 12.2 weight percent NaCl, with a mean value of 5.9 +/- 3.0 weight percent NaCl. Figure 13 shows a plot of salinity and homogenization temperature for the West Chance Vein system. The graph shows a narrow range of homogenization temperatures, but a wider range of salinities. Figure 14 is a plot of salinity vs. level and indicates a slight increase in salinity with depth. Salinities were calculated as described in appendix A.

Discussion and Interpretation of Fluid Inclusion Data

The following discussion will focus on how fluid inclusion data from the West Chance vein system pertains to the genetic development of this ore body. Homogenization temperatures and salinities are compared to similar parameters of other vein systems in the mine and the district.

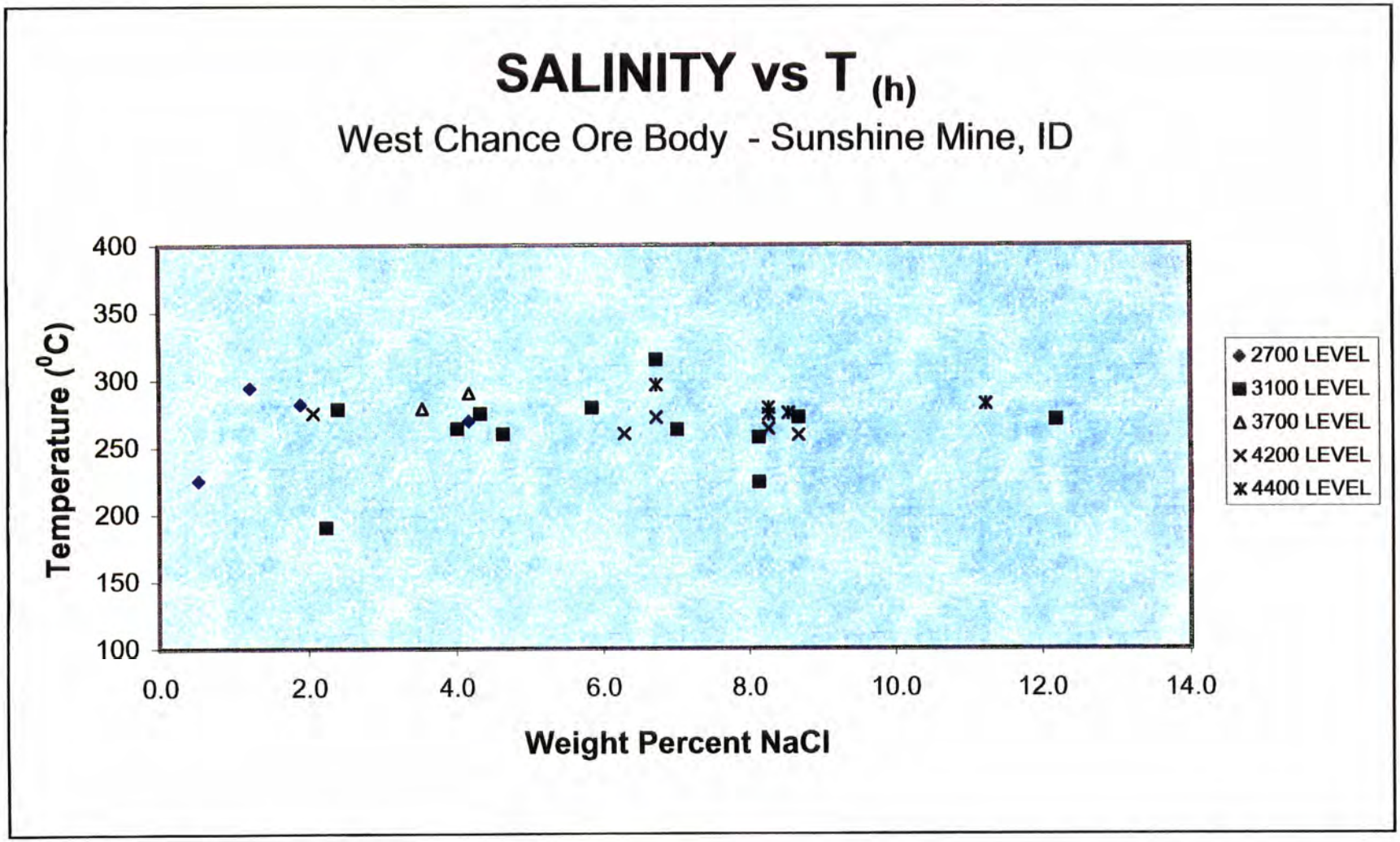

Figure 13. Chart showing the variation of homogenization temperature as a function of salinity, indicating temperature is relatively constant and salinity varies.

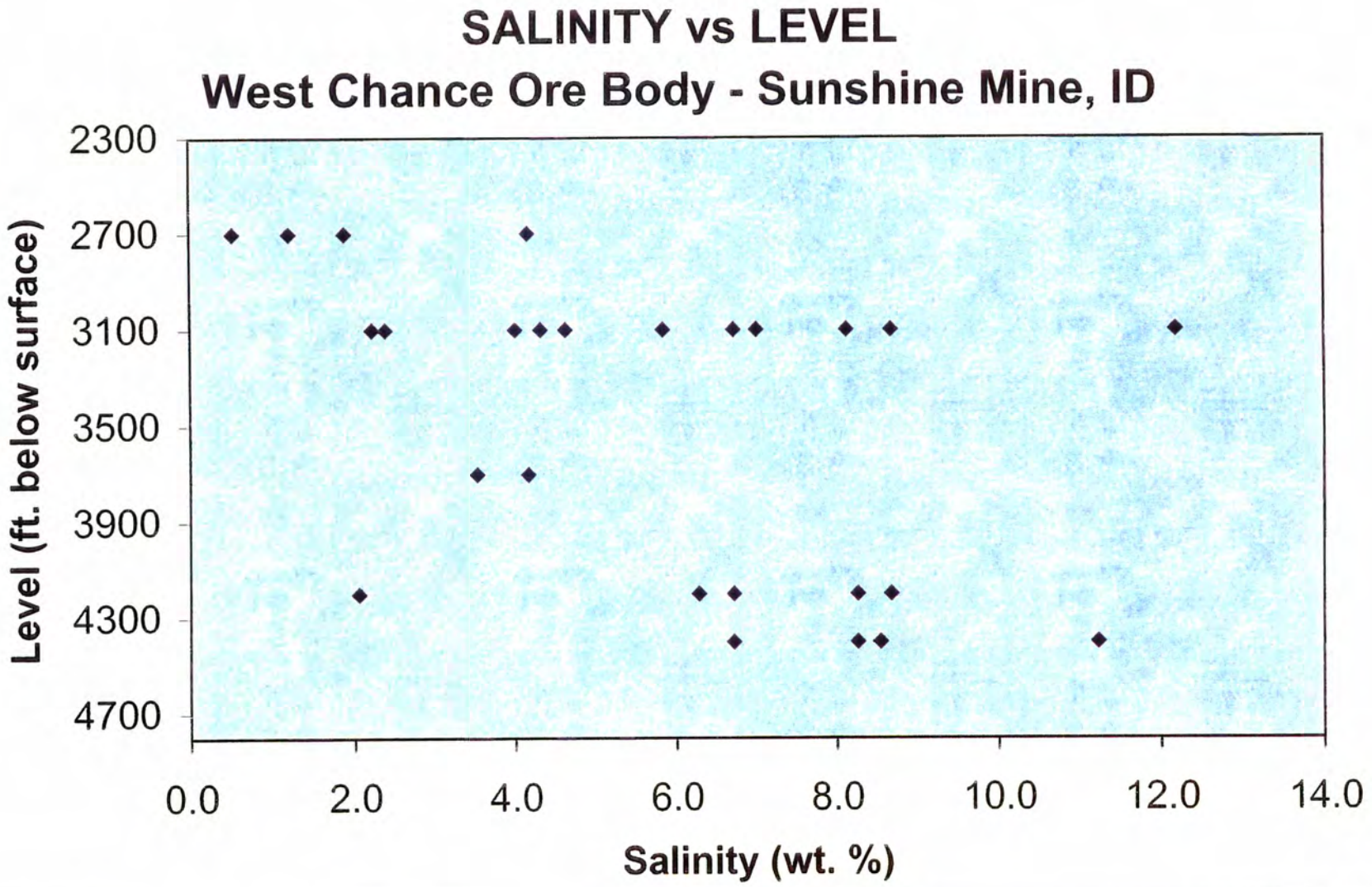

Figure 14. Plot of salinity vs. level for quartz veins in the West Chance vein system.

Temperatures of homogenization do not vary widely within the West Chance system. This study indicates that homogenization temperatures for the West Chance fall within the previously determined range of 250 to 350° C for quartz veins in the Coeur d'Alene mining district (Yates and Ripley, 1985; Leach et al., 1988; Constantopolus, 1989). The homogenization temperatures for the West Chance system show a narrower range and lower mean temperatures than other mineralized vein systems in the Sunshine mine. Trachte (1993) studied over 400 inclusions from various vein sets from the Copper vein. Homogenization temperatures ranged from 180-430 °C. The differences in data sets could result from different characteristics of the two vein systems. The Copper vein is situated much deeper and does not occur along a major fault system. Trachte 1993 used all four quartz vein sets (ladder, longitudinal, sigmoidal, and later), whereas the later and sigmoidal quartz vein sets were not used in this study due to a lack of primary inclusion and small size.

It was also shown that salinity increases with depth in the West Chance system. Other fluid inclusion studies (Leach, 1988 and Trachte, 1993) did not reach this same conclusion. Leach (1988) collected samples from a number of different mines and made no reference to a correlation between depth and salinity. Trachte, (1993), had little success with obtaining final melt temperatures from collected samples, and also made no correlation between salinity and depth. There is insufficient data to determine whether the observed salinity contrast is specific to the West Chance system or is indeed a district-wide phenomenon.

A PVTX diagram can be helpful in fluid inclusion studies to define or narrow a range of trapping temperatures, T(t), and pressures, P(t). Salinities of fluid inclusions

represented by the H_2O-NaCl system were determined from temperature of phase changes during microthermometric analysis (see Appendix A). The liquid-vapor curve and critical point were then calculated using the mean salinity of 5.9 weight percent NaCl and are shown on figure 15. The isochores (lines of equal volume) representing the mean T(h), +/- one standard deviation are also shown and the slopes of these isochores were calculated using the mean salinity. Although salinity was found to vary with depth in the West Chance vein system, the mean salinity was accurate in delineating the PVTX conditions since the variation in salinity produces an insignificant change in the slopes of the isochores. Slopes of the isochores were calculated based on techniques from Bodnar and Vityk, (1994). Normally, an independent geothermometer, determined from leachate analysis or stable isotope studies, would give a trapping temperature and be plotted on the PVTX diagram. The intersection of the independent temperature with isochores from this study would then indicate trapping pressures. To date, an independent geothermometer has not been calculated for the Coeur d'Alene mining district. Historically, a temperature of 325 °C has been quoted as the average trapping temperature for the district. This temperature, used in oxygen isotope studies of Eaton et al. (1994) and Constantopolus (1994), represents the average homogenization temperature determined from 3 different fluid inclusion studies – Leach et al. (1988), Constantopolus (1989), and Trachte (1993), and suggests only a minimum trapping temperature. Due to a lack of an independent geothermometer, the biotite isograd was used to further constrain trapping conditions. Biotite is not found in the Coeur d'Alene mining district although the bulk composition of wall rocks would allow biotite formation. Given these constraints, figure 15 suggests a T(t) range of 250-435°C and P(t) of 0.2-2.6 kbar. The

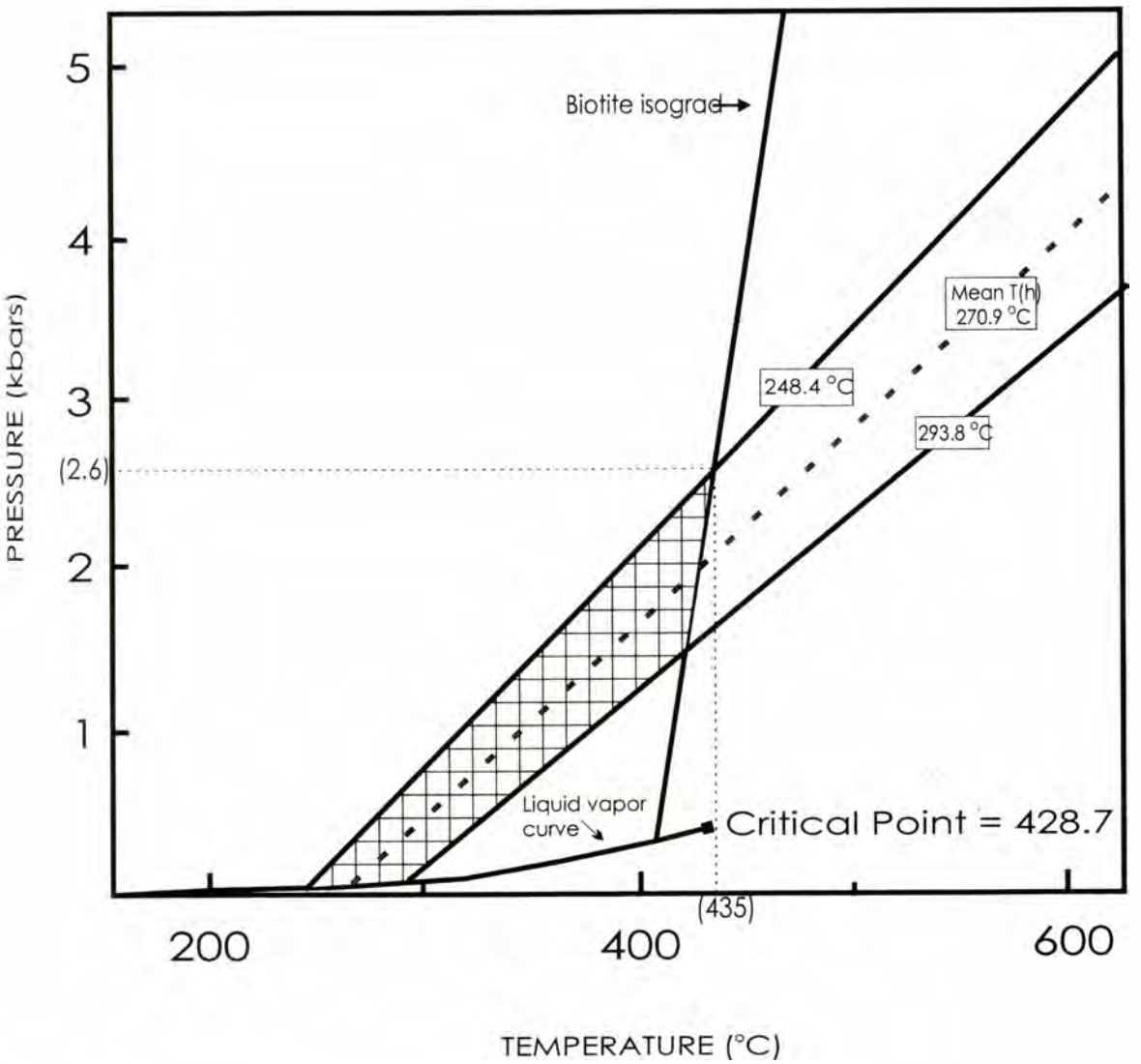

Figure 15. PVTX diagram showing probable range of trapping conditions for fluid inclusions from the West Chance ore body. Liquid-vapor curve, critical point and slope of NaCl isochores calculated using average salinity of 5.9 wt. % NaCl. Isochores represent mean T(h) (red dotted line) +/- 1 standard deviation (black lines). Biotite isograd determined from Yardley, 1989. This figure suggests Tt range of 250-435 °C and Pt of 0.2-2.6 kbar.

P(t) range corresponds to depths of burial of 0.7 to 9.1 km for fluid under normal lithostatic load. Exploration diamond drill holes and mined-out portions of the West Chance ore body shows the present day extent of the vein system is from approximately 820-1335m (2700 to 4400 feet).

Two models– mixing and boiling – are proposed to explain increasing salinity with depth and are shown in figure 16. In a mixing model, shown in figure 16a, a less saline fluid A, mixes with a denser, more saline, fluid B. Stable isotope studies conducted by Eaton et al., (1995) suggests that mixing of fluids did occur at other veins in the Sunshine mine; however, the two fluids were determined to be meteoric and hydrothermal in origin. Fluid inclusions from this study showed consistent temperature of homogenization, which would not be expected if mineralization in the West Chance was a result of the mixing of meteoric and hydrothermal fluids. Geological processes that could cause mixing of fluids in the Belt basin have occurred. The observed salinity contrast could be a result from the slow mixing of fluids of varying salinities during basin dewatering. The depositional environment for the Belt basin has been suggested to be a warm shallow sea (Winston, 1986). Variations in salinity in this shallow sea would cause fluids trapped during lithification to have varying salinities. Presumably then these fluids would mix during metamorphism. A pulsing hydrothermal system derived from a plutonic body could also provide a salinity contrast. Two fluids of varying salinity could be injected in the ore body over a geologically short period of time resulting in a mixed solution. In a steam driven system, fluid A is injected into the ore body. Subsequent fluids which are injected into the ore body (fluid B), are more saline as more water leaves the system.

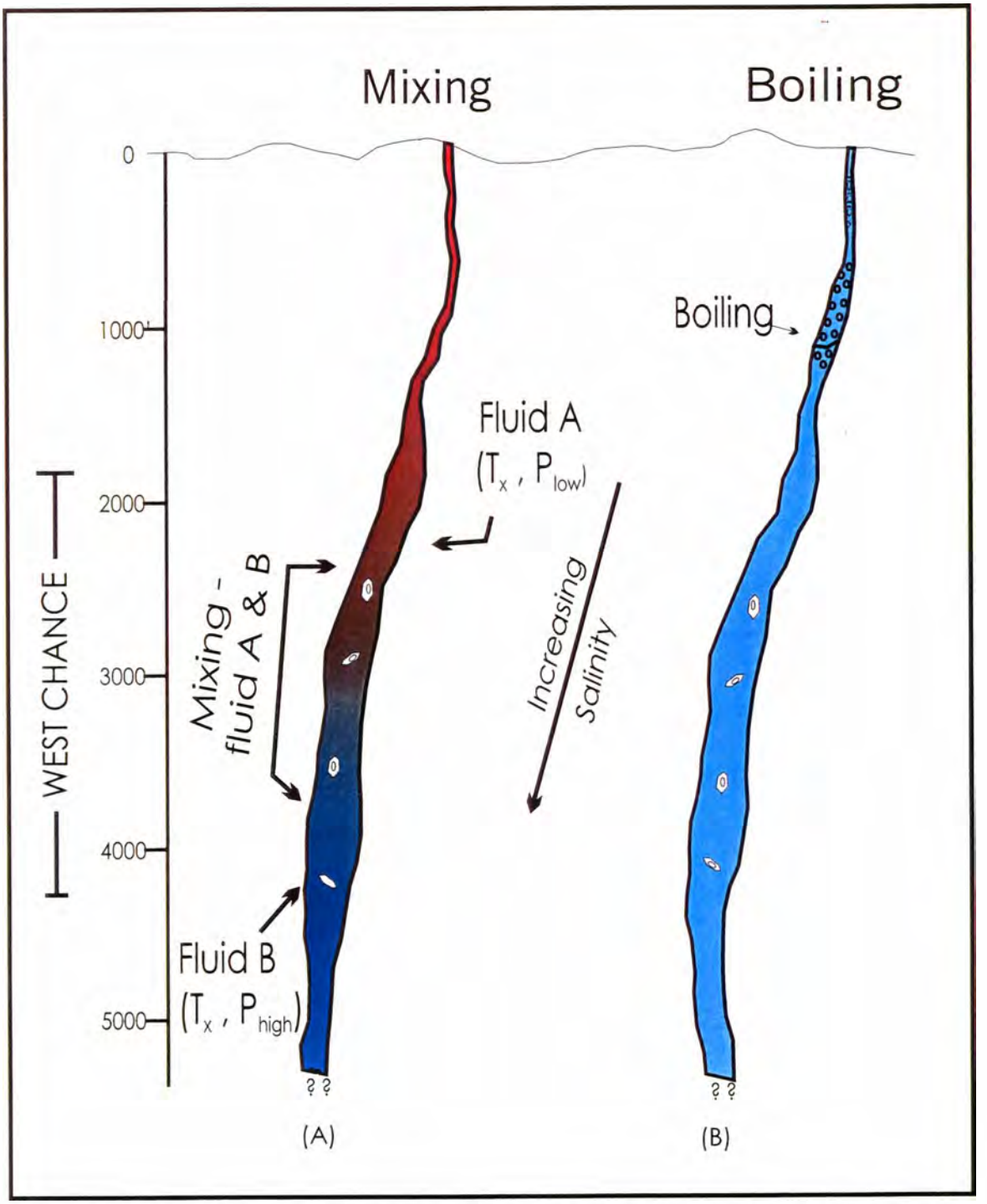

Figure 16. Schematic diagram,looking west, showing two possible explanations for increasing salinity with depth. (A) shows the mixing of two fluids of different salinity but similar temperatures. (B) shows a vein system where boiling occurs above the West Chance ore body. Boiling causes fluids to become more saline and dense with depth. No evidence for boiling is found at the Sunshine Mine, but is found locally at shallow levels in other parts of the district (see text). The vertical extent of the West Chance ore body is shown on the left.

A second model, shown in figure 16b, suggests the West Chance vein system to be a result of boiling above the mineralized section of the vein system. Before further discussing this model, it is important to discuss how boiling conditions can be determined from fluid inclusions. Evidence such as a series of inclusions that have trapped different proportions of liquid and vapor indicate boiling (Roedder, 1984). Another clue to boiling conditions would be inclusions homogenizing to different phases – liquid or gas. Pure vapor inclusions will contain very little liquid and a very large bubble at room temperature. On heating they will homogenize in the vapor phase by evaporation of the liquid, ideally at the same temperature as that at which the liquid inclusions homogenize.

In this study, fluid inclusions from the West Chance, in general, did not show varying proportions of liquid and vapor. In addition, no vapor rich inclusions were observed and all inclusions homogenized to liquid. These three pieces of evidence strongly suggest boiling did not occur within the West Chance vein system; however, it is possible that the observed salinity contrast may be a result of boiling above the vein system.

In the model shown in 15b, boiling causes inclusions to become more saline and dense, settling over time. Although rare in the district, coevally trapped gas-dominant and H_2O-dominant fluid inclusions have been observed in samples from the Gold Hunter mine (located close to the Lucky Friday mine; Leach, 1988). Boiling conditions at shallow levels in the Gold Hunter mine suggest the boiling model could explain the salinity contrast.

With homogenization temperatures well above the boiling point, why is there no evidence of boiling in the West Chance vein system and why are boiling conditions rare in the Coeur d'Alene mining district? Explanations include the following: trapping

pressures could have been at the upper end (~3-7kbar) of the proposed range. Over time, uplift of material would cause evidence for boiling to be eroded away. The coexistence of liquid-rich and vapor-rich inclusions is the single, most often cited evidence in support of entrapment from boiling fluids (Bodnar et al., 1985). However, conditions could have existed whereby all fluid phases were not recorded by fluid inclusions. For example, the vapor phase resulting from near surface boiling may not be trapped in the precipitating minerals, but may simply escape through the system plumbing. Additionally, a common assumption that is made in obtaining salinity is that the depression of the freezing point is due solely to dissolved solids, mainly chlorides of sodium, potassium, and calcium. However, some inclusions from the epithermal environment may also contain small amounts of gases that are not usually detectable by normal petrographic, microthermometric, or crushing studies, and these gases also contribute to the freezing point depression (Bodnar, 1985, p94). Samples from the West Chance vein system did indicate small amounts of CO_2. Consequently, conditions could have existed where formation of the deposit developed in a slightly boiling or effervescing system, as might occur when a fluid moves down a pressure gradient and slowly exsolves small amounts of vapor.

Deposition of metals in epithermal systems can occur under boiling conditions, or when there is a change in temperature, pH, or salinity. Changes in temperature, pH or salinity are documented by observing variation of these parameters with distance (depth). Changes in pH were not analyzed, however this study did show that fluid inclusion temperatures do not vary with depth and salinity increases slightly with depth. It is was suggested above that the observed salinity contrast is a result of boiling above the West

Chance ore body. This model is favored over a fluid mixing model because there is limited evidence that suggests boiling occurred at shallow levels in the mineralized vein system of the Coeur d'Alene district and no evidence for mixing. It is the author's interpretation that mineral deposition in the West Chance vein system is in part a result of the observed salinity contrast. The interplay of fault movement, fluids, and mineral deposition will be discussed in the next section.

CHAPTER 3: STRUCTURE

The structural geology of the Sunshine mine has a reputation for being complex and challenging. Understanding the relationship between structure and mineralization has long been recognized as a key to defining and developing new ore bodies. Despite knowing the importance of this relationship, key questions regarding the structural geology in the mine persist – namely, what is the style and timing of deformation in the mine? This section uses newly acquired structural data and observations from mapping, petrofabric analysis, and sampling in the West Chance vein system. Compilation and analysis of existing data from other areas of the mine was also done to further the understanding of the structure and the structural control of ore at the Sunshine mine.

Summary of Fieldwork

Observations and measurements of structural features were completed during the 1996 field season and on subsequent short visits to the mine. During the summer of 1996, development of the West Chance vein system was focused primarily on the 3100 level, in the E9 and E10 stopes. Data from other sections of the vein system were collected during subsequent mine visits and short term employment periods. Typically, observations and measurements were made in active stopes on daily routine visits and from stope and drift level mapping.

Fault Characteristics within the West Chance Vein System

The Chance fault is one of several WNW-trending faults in the Sunshine mine (figure 5). Economic grade ore is located in veins where the fault makes a bend to the west. This west trending portion of the fault is referred to as the West Chance fault. The term West Chance fault or "C" fault as it is often referred to , can be ambiguous.

Typically, C-fault refers to the prominent fault plane in a stope, which was mineralized, and being mined, or the main fault plane that was in close proximity to a mineralized vein. However, mineralized splays or veins often deviate from this initial orientation and may or may not still be referred to as C-fault by mine geologists. Upon closer inspection of exposed portions of the fault, the fault-vein system consists of a 1.5 to 4.6 meter (5 to 15 foot) wide zone of anastomosing veins, shears, and fractures. For the purposes of this study, the West Chance vein system, or simply West Chance, refers to this zone of anastomosing features and C-fault refers to a single planar feature identified in each stope within this vein system.

Characteristics of the West Chance vein system can best be described with several equal area stereographic plots and photographs. Figure 17 shows a plot of poles to measured mineralized shear planes, or C-fault, in the study area of the West Chance. The figure shows a variation in strike from 065° to 120° azimuth, and relatively little variation in dip. The average attitude of C-fault is 093°, 64SW. This average was compiled from a database with measurements taken by all mine geologists. A stereographic plot of splays and Riedel shears in the mineralized section of the West Chance vein system is shown in figure 18. Although the terms splays and Riedel shears are often used interchangeably, for the purposes of this study, splays will refer to larger scale features which are still part of the anastamosing shear zone, and Riedel shears are smaller scale features on the scale of 1-2 feet in length along dip. Criteria often used in this study to additionally define a Riedel shear was that the shear was bounded on both sides by a larger shear. The described difference is exemplified in figures 9a and 19. The face photograph (figure 9a) from 3700 ER2B- E shows a splay splitting from C-fault. Riedel shears are shown in

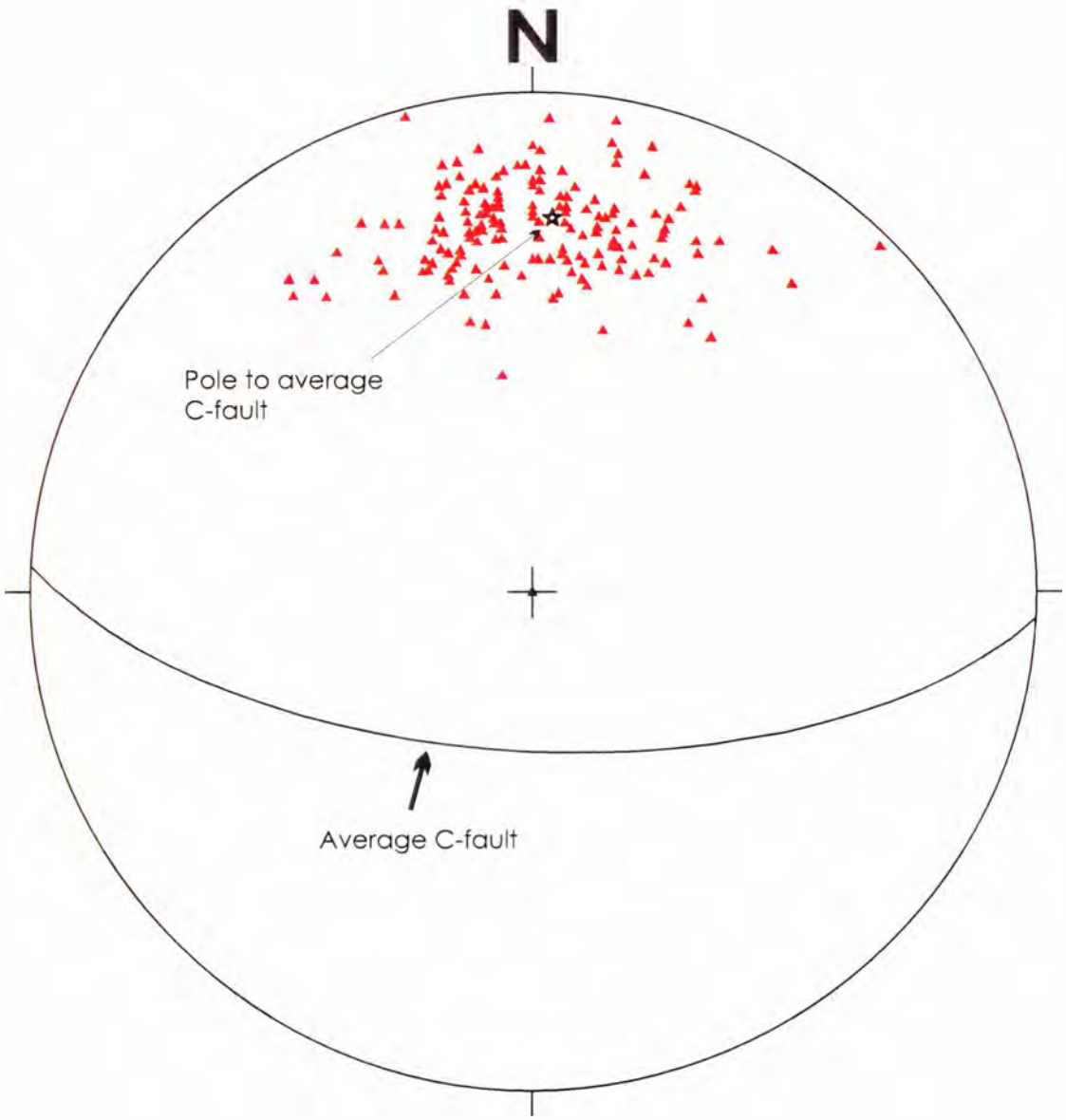

Figure 17. Equal area steroegraphic plot of poles to mineralized shear planes in the West Chance vein system. The shear planes represent faults identified (see text) as "C" fault and faults parallel to these shears. Average value plotted for C-fault = 093, 64SW. Star denotes pole to average C-fault value. N=181.

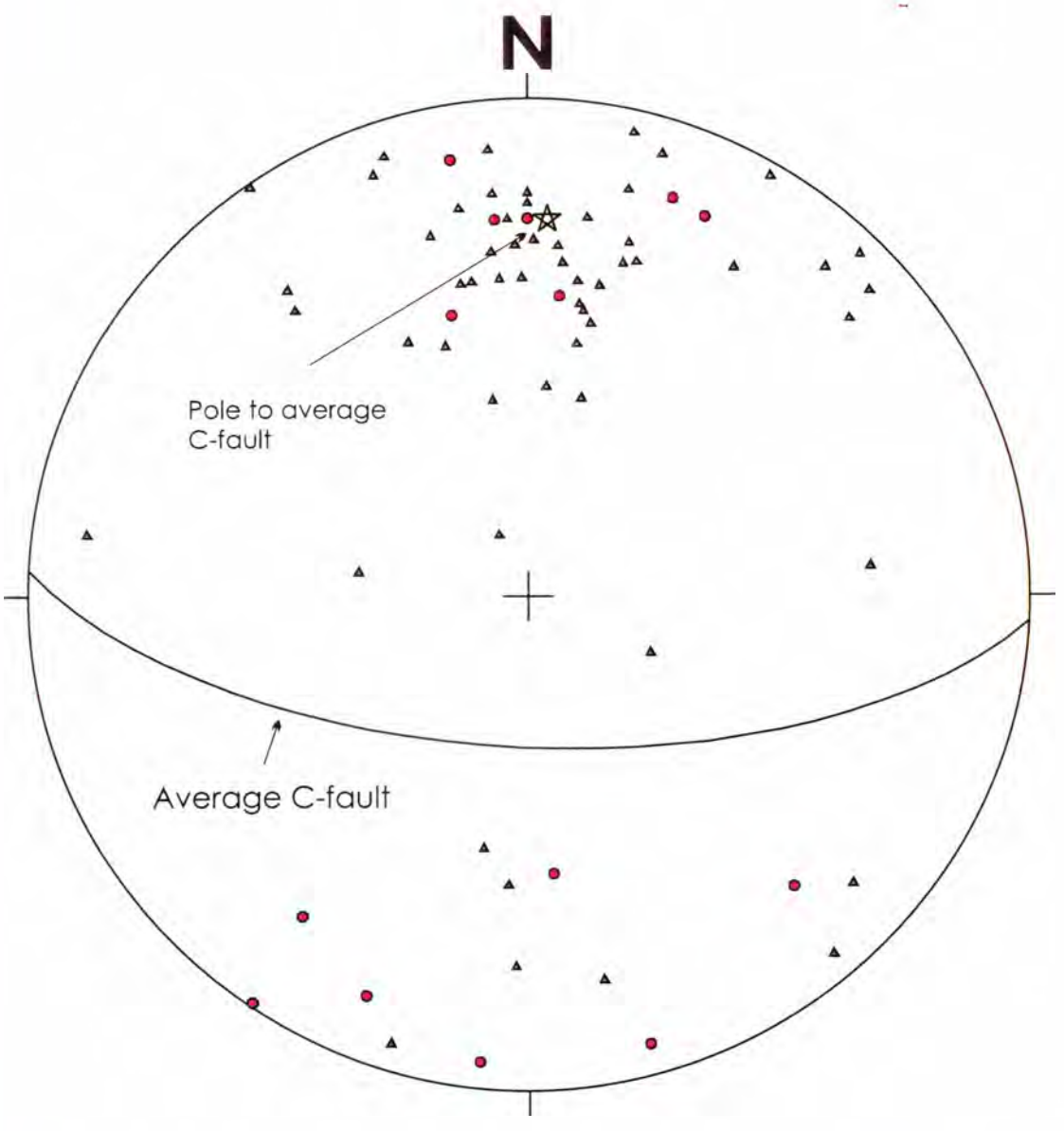

Figure 18. Equal area stereographic plot of poles to splays (blue triangles,n=58) and Riedel shears (red circles, n=14). Planes represented in this diagram were typically unmineralized. Star denotes pole to average C-fault value.

Figure 19. Photograph from 3700 ER2B-W exemplifying characteristics of Riedel shears. This photo is an enlarged area of figure 9a.

the enlarged photo in figure 19. The splays represented in figure 9a are typically unmineralized in contrast to C-fault. Based on the orientations shown in the stereographic plots shown in figure 17 and 18, the geometry of the West Chance fault-fracture system, is an anastomosing E-W zone of shears, splays and Riedel shears. This geometry is particularly well documented in figure 9a.

Lineations

Several types of lineations were found in the West Chance vein system. The orientation and slip direction of these lineations are shown in the two slip linear plots of figure 20. A slip linear plot is a stereographic technique used to show the orientation and direction of slip of a fault plane together on one stereogram. A line, representing the direction of slip, is plotted on the symbol representing the pole to the fault (Marshak and Mitra, 1988). If a directional indicator is observed on the lineation, an arrow is placed on this line. The reference frame is a hanging wall-fixed frame, or more specifically, the arrow indicates the sense of motion of the footwall across a fixed hanging wall. Figure 20a shows slickenline lineations found on fine-grained sulfide veins in the West Chance and represents post-ore movement. Most of lineations in this plot indicate strike-slip movement; 6 lineations show dip-slip movement with a plunge E of S, and 4 lineations show dip-slip movement with a plunge W of S. Often strike-slip and dip-slip to oblique motion would be observed in the same plane. Although not observed by this author, Wavra et al., (1994) observed that horizontal slickenlines overprinted vertical slickenlines. The author did observe one set of vertical slickenlines that overprinted horizontal slickenlines in 3100 E9E floor 22. Figure 20b is a plot of chlorite mineral lineations and ridge and groove lineations found in wallrocks adjacent to the West

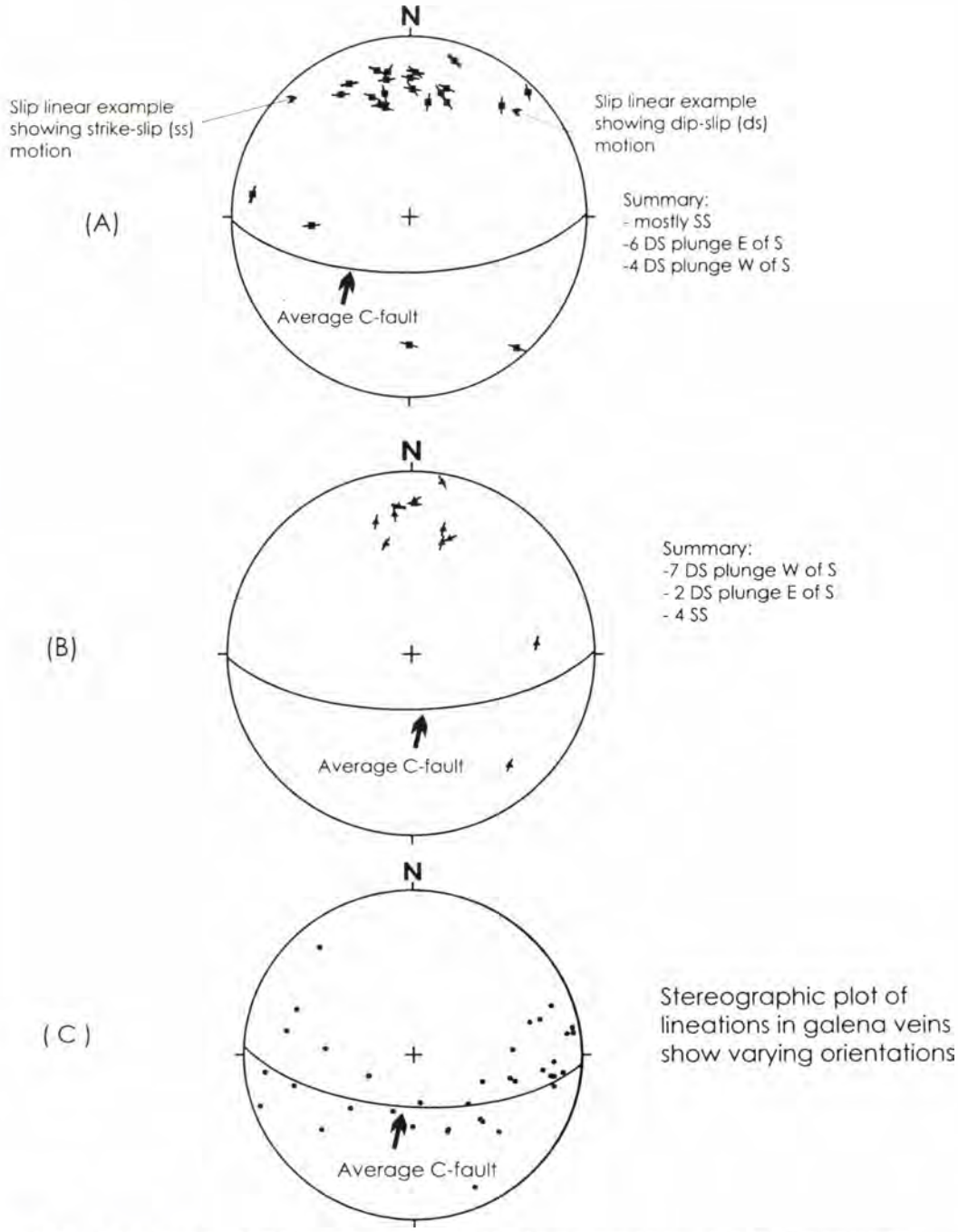

Figure 20. Slip linear (a&b) and normal (c) stereographic plot for lineations measured in the West Chance. Data includes both C-fault and splays of C-fault. (A) shows slickenlines measured on galena veins.(B) shows chlorite lineations and ridge and groove lineations found in wall rocks adjacent to the Chance fault. (C)shows normal stereographic plot lineations in galena veins. In general two populations of fault movement are indicated: dip-slip and strike-slip; however, most wall rock slip linears are dip-slip and most galena vein slip linears are strike-slip.

Chance fault zone which could be pre-, syn-, or post-ore. In this figure, 7 lineations show dip-slip movement with a plunge W of S, 2 show dip-slip with a plunge E of S, and 4 show strike-slip movement.

Broadly speaking, figures 20a and b show evidence for multiple stages of movement along the West Chance fault. However, closer inspection reveals that lineations associated with lead veins vary from lineations associated with wall rocks. Most of the lead vein lineations show strike-slip motion, with a smaller population showing dip-slip motion, whereas most wall rock lineations show dip-slip motion, with a small population showing strike-slip motion.

Several interpretations are given to explain the variation in lineations found in wall rocks and Pb-veins. Both wall rock and lead vein data could all represent post-ore movement, and that an episode of dip-slip movement was followed by strike-slip movement. This interpretation assumes that pre-ore wall rock lineations were not preserved or that no pre-ore or syn-ore movement occurred. A second interpretation suggests that a shift in fault movement from reverse motion to strike slip occurred during mineralization, and the population of steep wall rock lineations represents early pre-mineralization fault movement. This motion was ongoing into the late stages of mineral deposition and is represented by the smaller population of steep lineations in Pb-veins. At some point during mineralization the stress field changed, causing strike-slip motion to occur. Finally, the lineation data could represent more than two episodes of faulting, suggesting that a highly varying stress field was operative throughout the kinematic history of the West Chance vein system. This is consistent with observations that dip slip

lineations are cut by and cut strike slip lineations. Evidence of kinematics of dip slip and strike slip motion will be discussed below.

Fault/Fracture Characteristics Outside of the Main West Chance Vein System

Orientations of faults outside of the main fault zone were compiled from drift and attack ramp maps. Faults were typically 0.63 to 2.54 cm (¼" to 1.0 inches) wide and contained small amounts of gouge. Some faults showed minor displacement. Results of this compilation are shown in the stereographic projection, histogram, and block diagram of figure 21 (right hand rule (RHR) convention is used in this study). Figures 21a and b show that there are several populations of faults contained in the West Chance fault zone. The majority of faults are parallel to the trend of the WNW-trending Chance fault; however, some of these faults dip north and some dip south. Smaller populations of faults strike ENE, dip steeply SE; strike SSE, dip SW; or strike S, dip steeply W. Cross-cutting relationships were rare - only 5 relationships were recorded on the West Chance maps. Where present, cross-cutting relationships showed that ENE striking faults were cut by faults which were WNW striking, and that the S and SSE striking faults cut faults which paralleled WNW-trending Chance fault. It was also determined that the small population of SSE faults cut ENE faults.

Fault Displacement

Mapping on the 2700 West Chance drift by mine geologists located a green marker bed near the base of the St. Regis Formation. This marker bed is interpreted to be a partially reworked ash layer. Exposed sections of the marker bed are located in both the hanging wall and footwall of the WNW trending section of the Chance fault, although the actual bedding-fault contact is not exposed in the drift. Linear features indicating

(A)

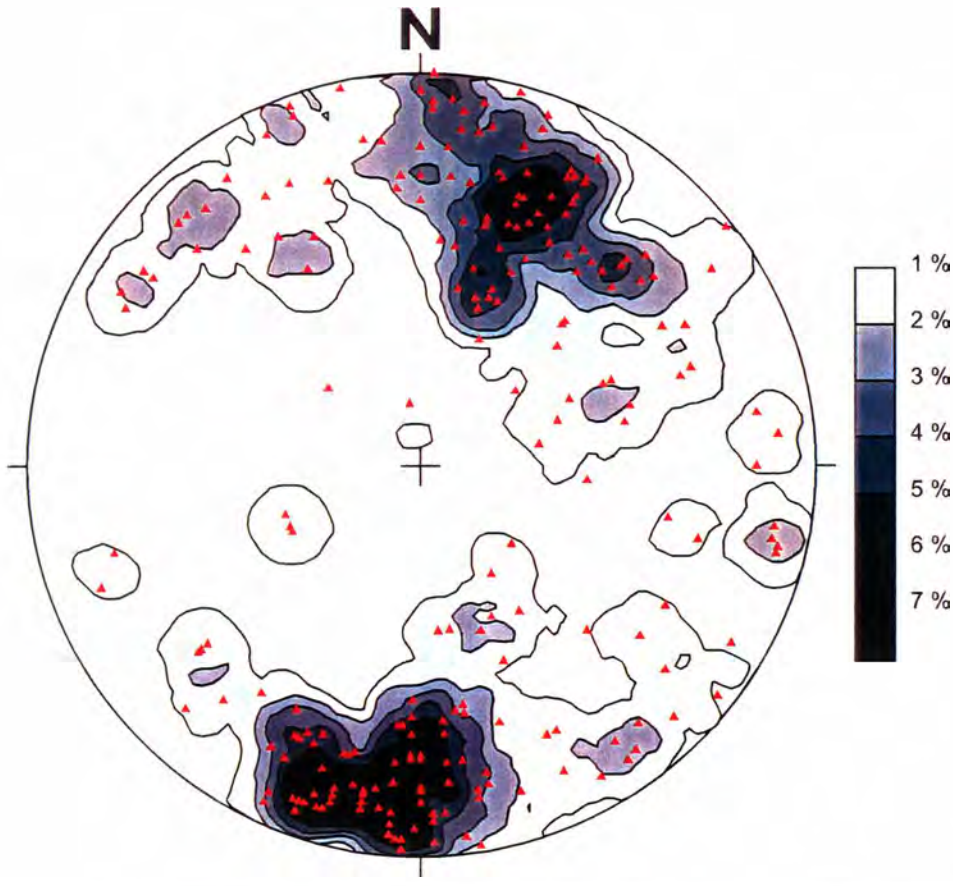

(B)

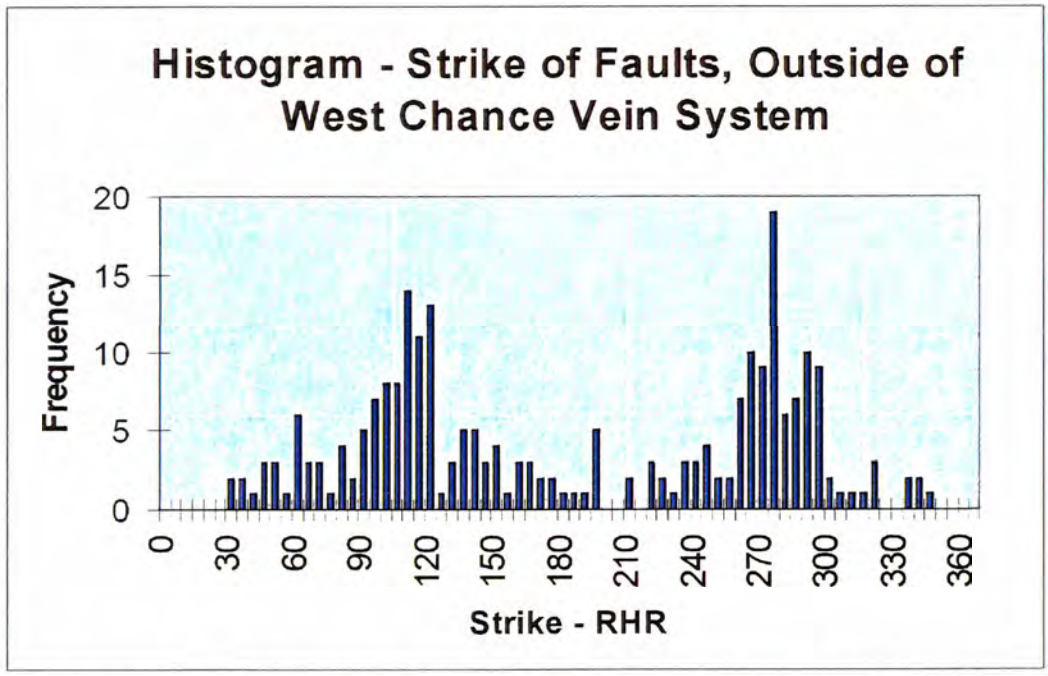

Figure 21. Characteristics of faults in surrounding area of the West Chance vein system. (A) equal area stereonet of poles to fault planes. N=250, search area=1.0%, peak=8.0. (B) Histogram of strike of faults outside of West Chance. All data compiled from drift and attack ramp maps.

fault movement are absent in this segment of the fault. Using stratigraphic controls from drill hole data and mapping, the marker bed can be projected into the Chance fault where the 2700 drift crosses the fault. The attitude of the bedding is different on either side of the structure - in the footwall, bedding is oriented 275, 84 NE, and in the hanging wall 254, 55NW. Differences in bedding attitudes in the two different structural blocks suggest that the Chance fault may have a rotational component; however, calculations based on these two bedding measurements show only 3-5 degrees can be explained by rotation about the pole to the fault. Strike separation of the marker bed is 28.9 meters (95 feet), and dip separation is 20.11 meters (66 feet). Although additional information, such as an intersecting feature with this ash layer, is needed to determine a piercing point and therefore net slip, the orientations of bedding and the Chance fault along the 2700 drift suggests that there is very little separation. The amount of slip has very little exploration significance especially since mineralization is located generally parallel to the Chance fault, rather than displaced by it.

Petrofabric Analysis and Ore Microscopy

Fifty-five oriented samples were collected from the West Chance vein system for microstructural analysis. These samples represent rocks within the fault zone as well as wall rocks adjacent to the fault zone. Thin sections were made from approximately 50% of the oriented samples collected. In samples that contained lineations, thin sections were cut perpendicular to the fault surface and parallel to the lineations. However some samples collected from within the fault zone did not contain lineations. In these samples, other indicators present in the face such as drag folds, Riedel shears, or vein offset, were used to aid thin section preparation. When movement indicators were not present, two

orthogonal directions were cut – one assuming dip-slip motion, the other assuming strike-slip motion.

Both brittle and ductile features were observed in thin section. Ductile features included folding, quartz deformation (undulatory extinction, subgrain boundary formation, and recrystallization), sulfide foliation, and mylonitic fabric in siderite-quartz veins. These features were observed throughout the fault zone. Brittle features included offset veinlets, fractured and displaced quartz, siderite, and tetrahedrite grains, and brecciation. Figure 22a-d are photomicrographs of the typical textures found along the West Chance. These observed features along with other kinematic fault indicators such as rotated pyrite and quartz grains, stretched clasts, and sericite lineations, interpreted to have formed during fault movement, were used to evaluate the deformational history of faulting.

Observations of kinematic indicators were made on opaque minerals in 5.08 x 7.65 cm (2 x 3 inches) thin sections from rocks within the West Chance fault zone. Although ore minerals were present in these samples, the sulfide material in the fault zone was typically fine grained and provided little insight into kinematic history. Rotated pyrite grains were an exception to this observation. Figure 23a-d is a series of photomicrographs showing common kinematic indicators from samples collected in the West Chance. Fault motion detected from kinematic indicators was recorded on data sheets and a slip vector was determined from the most commonly occurring motion. Figure 24 shows a data sheet from sample SS-9A, 4200 West Chance cross-cut. The majority of kinematic indicators show down plunge lineation which suggests normal

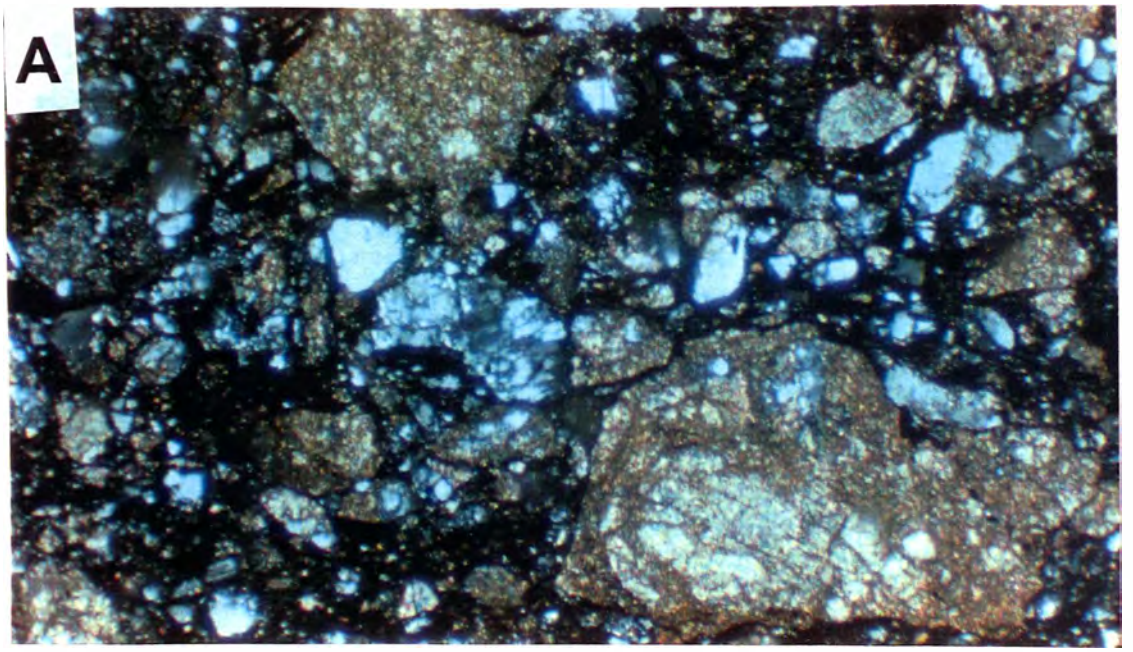

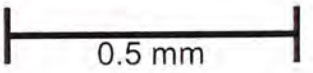

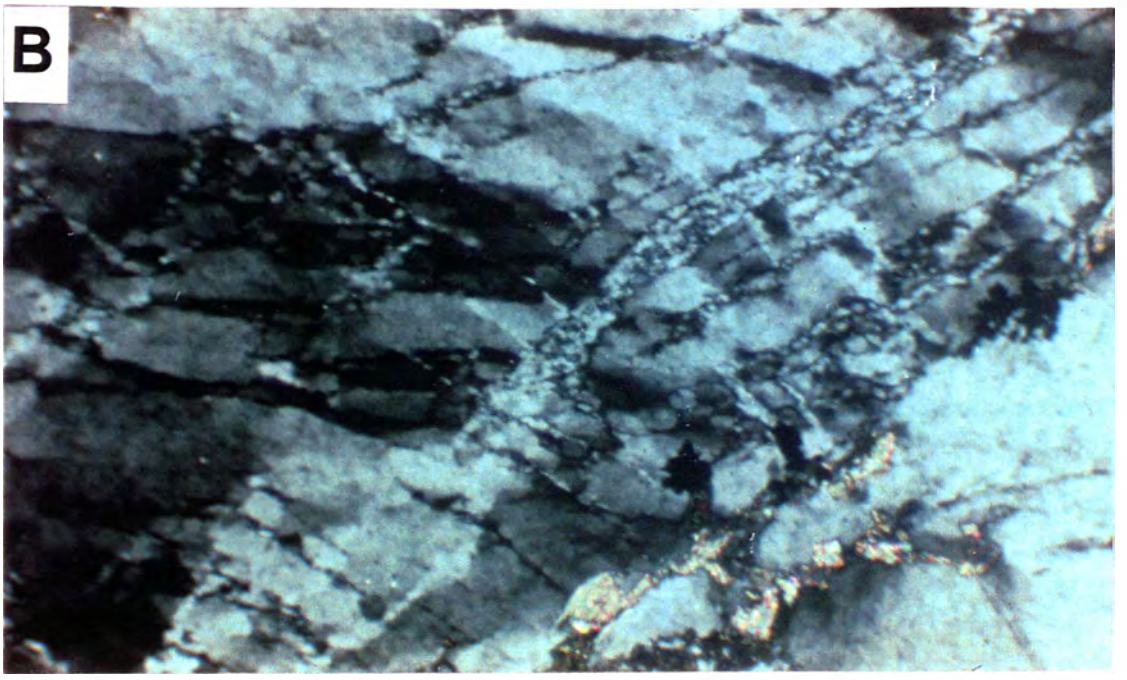

Figure 22a and b. Photomicrographs of common textures found in the West Chance vein system. (A) shows sharp, angular brecciated clasts in a fine grained sulfide matrix; sample SS-5 4200 WC X-cut (B) shows fracturing, undulatory extinction, and recrystallization in quartz grain.
Sample SS-9A 4200 WC X-cut

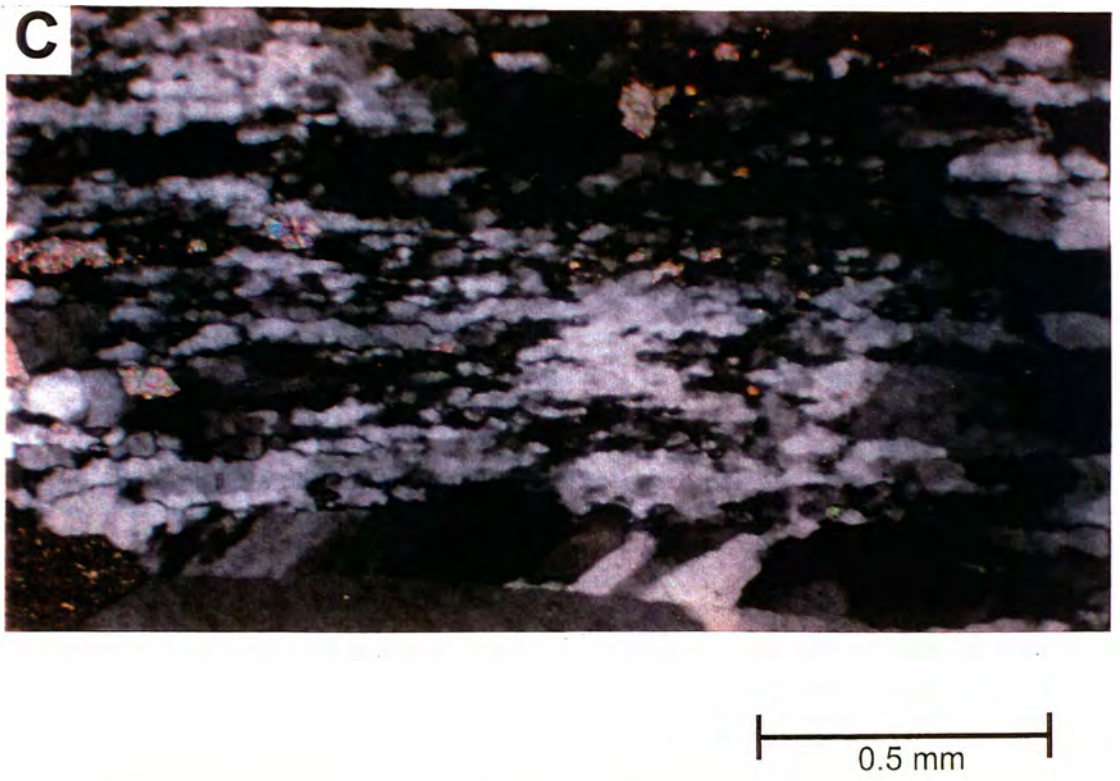

Figure 22c and d. Photomicrographs of common textures found in the West Chance vein system. (C) mylonitic texture in quartz grains;sample from wallrock SS-24A; 2700 WC drift.(D) sulfide foliation - sample SS-1; 3100 E9E.

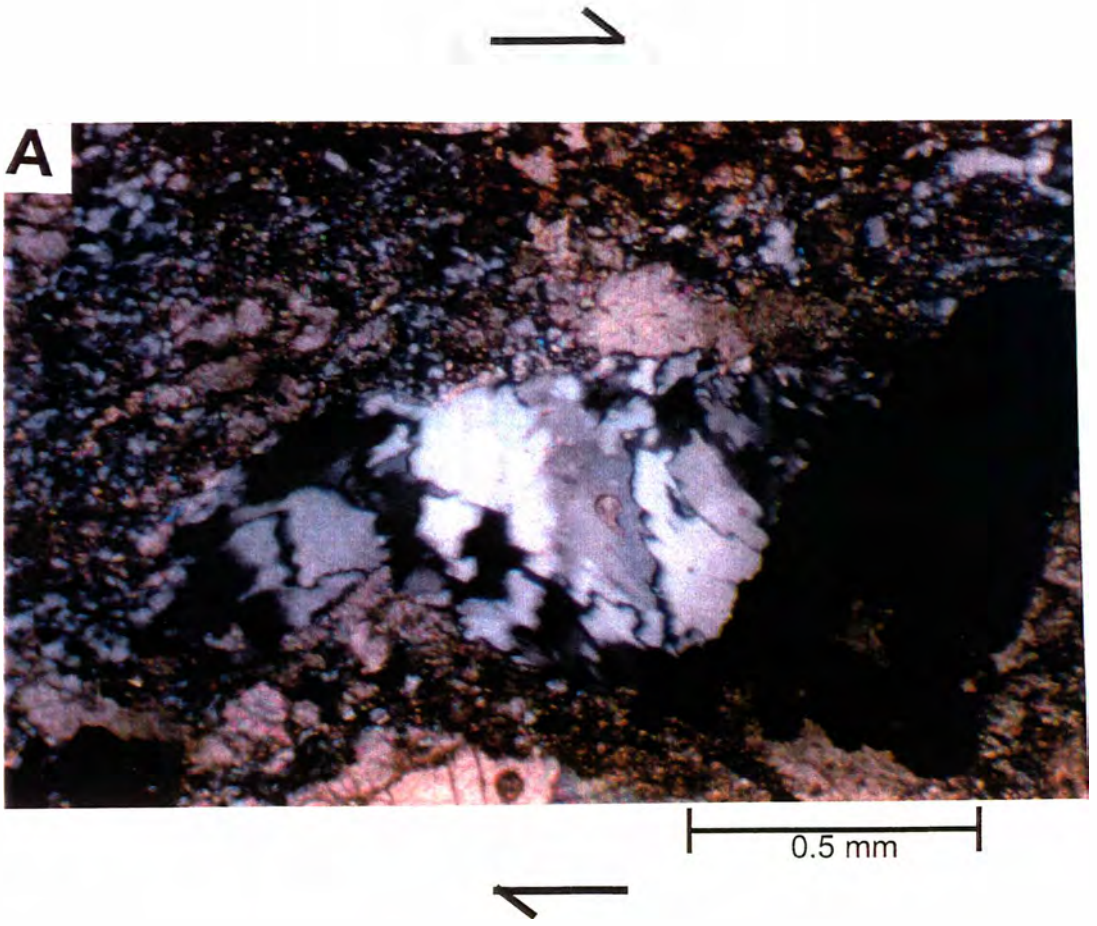

Figure 23a. Photomicrograph of common kinematic indicators from the West Chance fault-vein system. (A) Rotated pyrite grain with recrystallized quartz tail indicating reverse motion. Fault attitude = 105, 65SW; lineation = 70, 205; SS-22; 2700 WC drift.

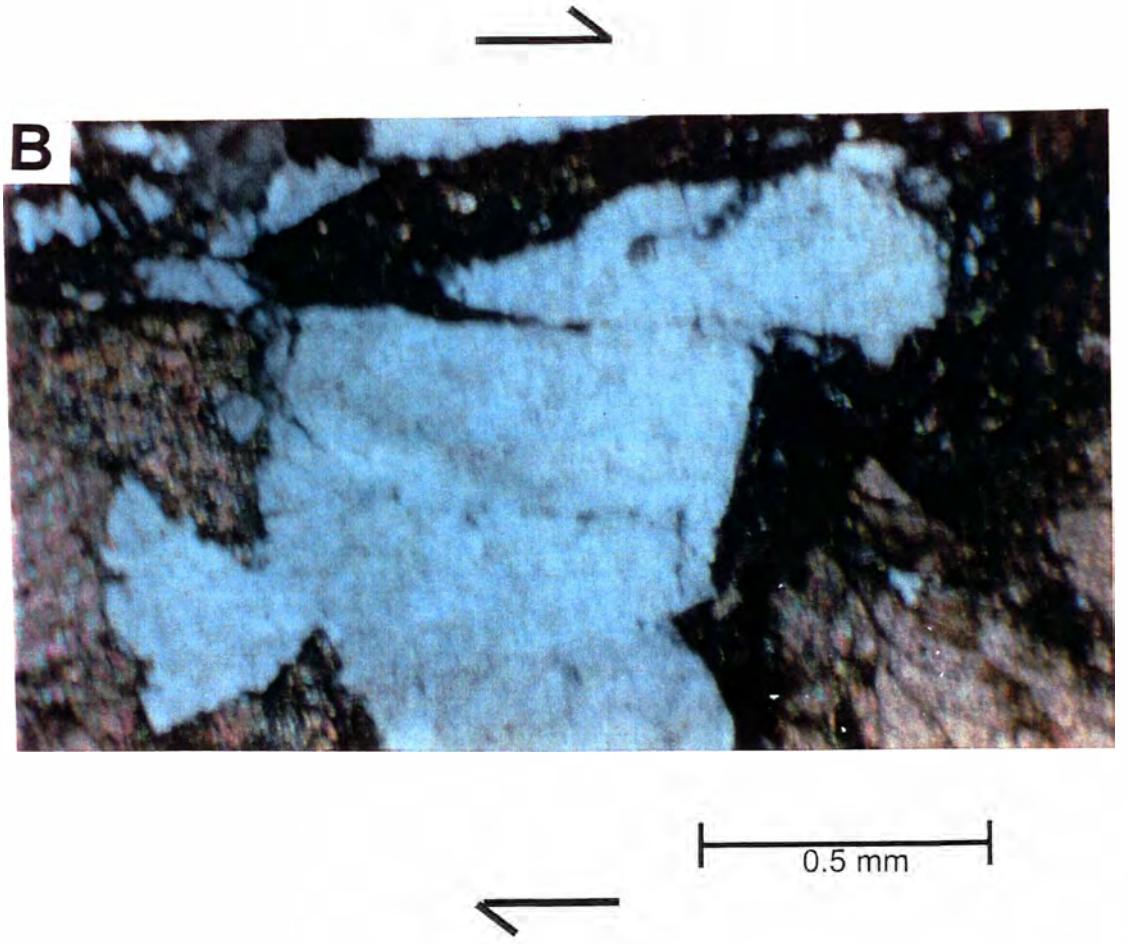

Figure 23b. Photomicrograph of common kinematic indicators from the West Chance vein system. (B) offset fractured quartz grain; top to right; thin section mounted upside down; sample indicates left-lateral motion; SS-5; 4200 WC X-cut.

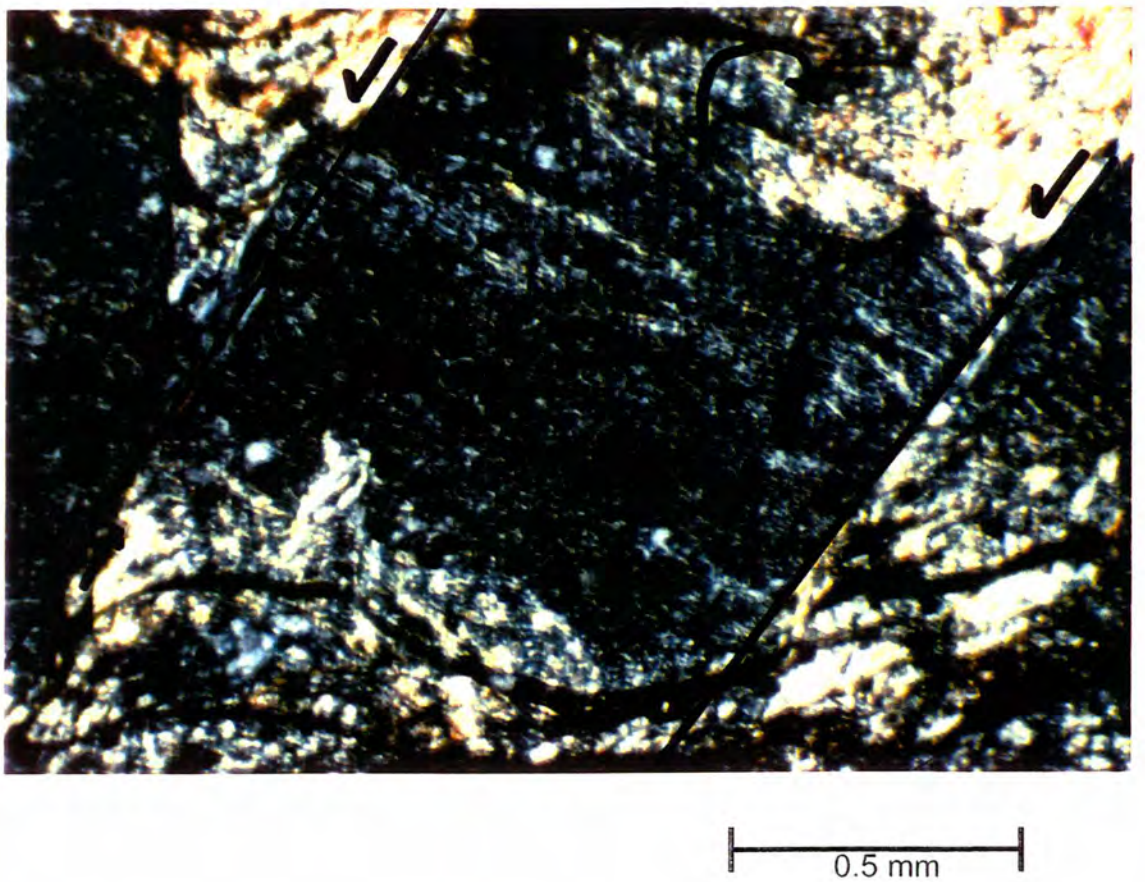

Figure 23c. Photomicrograph of common kinematic indicators from the West Chance vein system. (c) offset and rotated grains showing left lateral motion; fault attitude = 090, 60S; lineation = 35, 260; SS-20; WC West end of drift

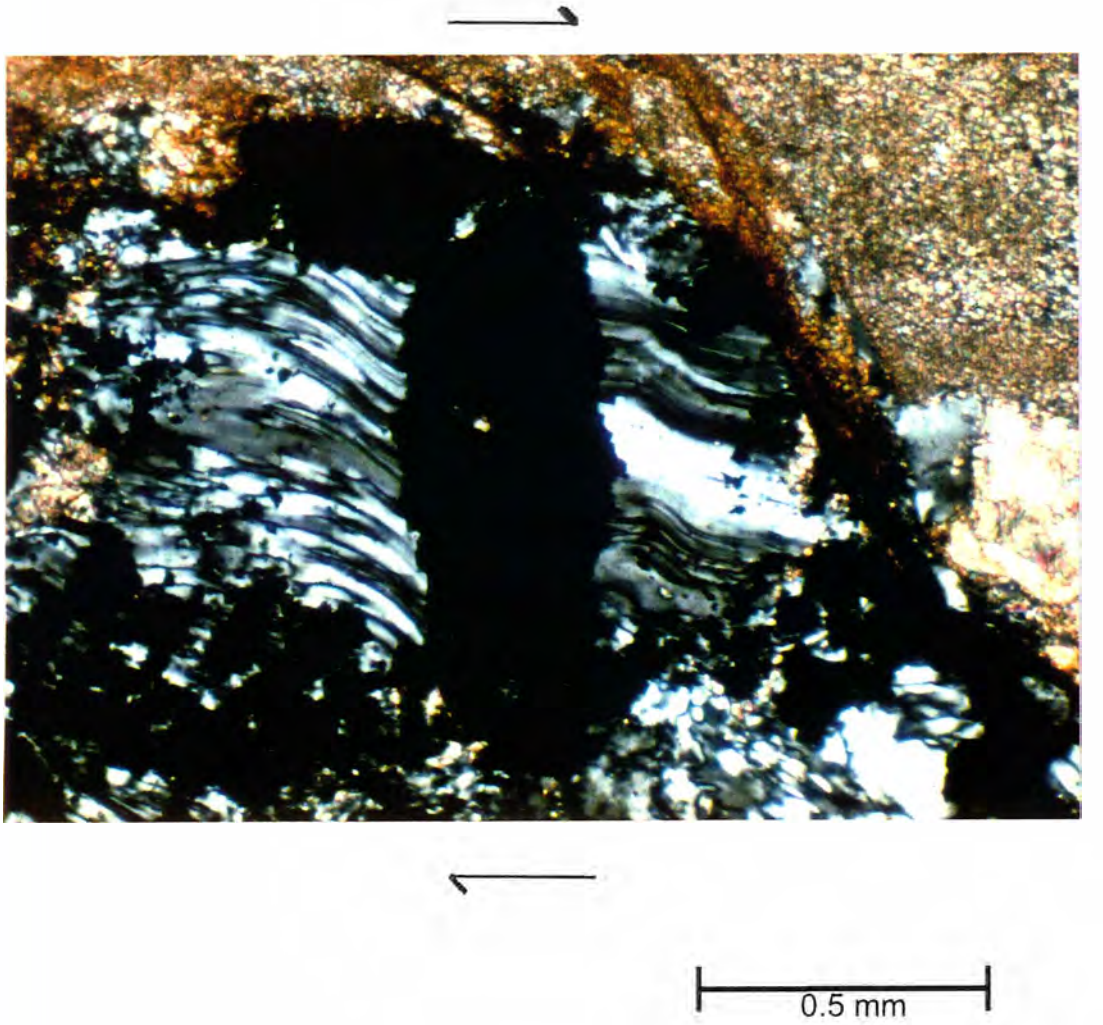

Figure 23d. Photomicrographs of common kinematic indicators from the West Chance fault-vein system. (D) rotated pyrite grain showing normal then reverse motion. Overall sense is reverse as shown in figure 34;
fault attitude = 093,65S; lineation = 65, 205; SS-9a 4200 WC X-cut

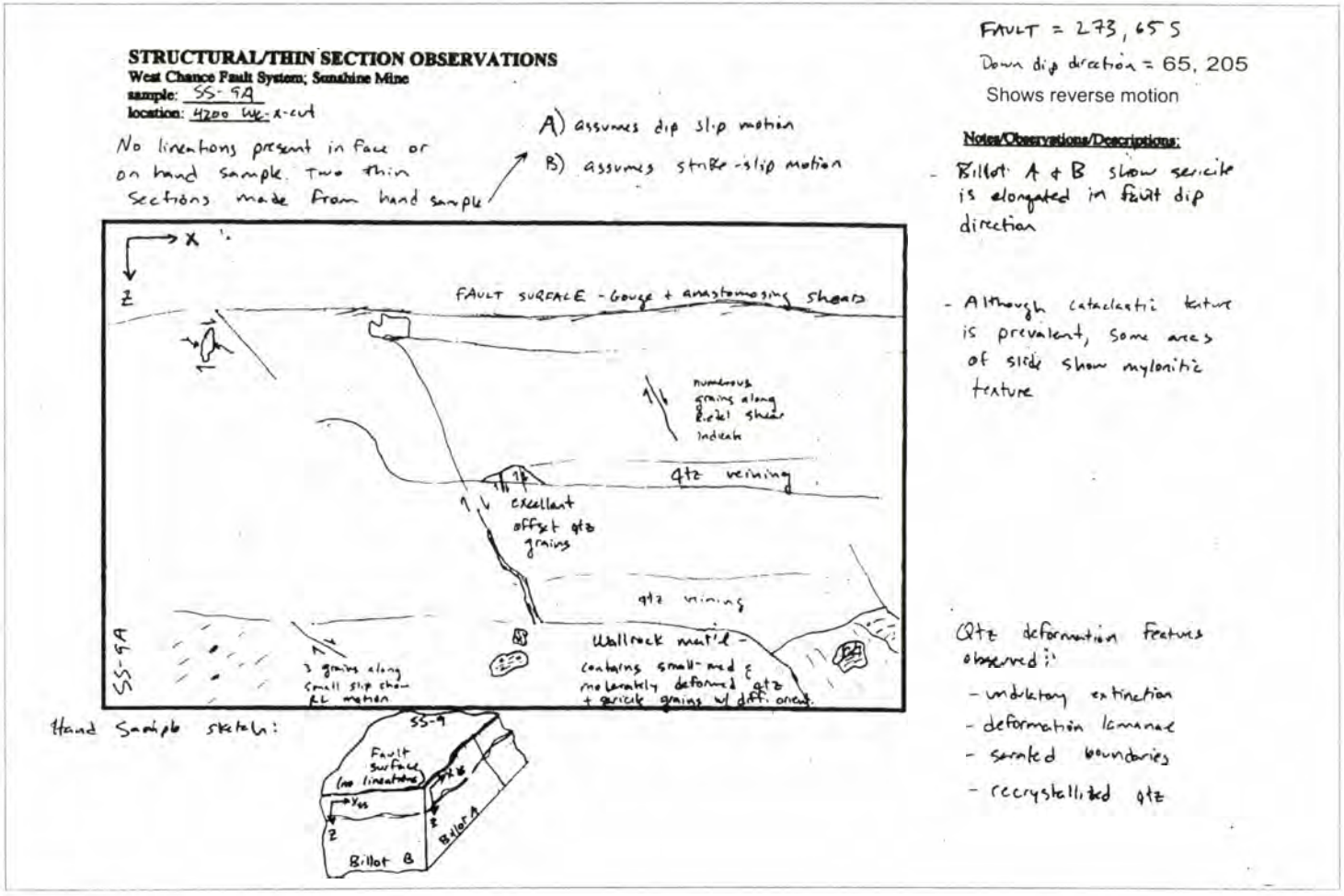

Figure 24. Example of kinematic data sheet. Many kinematic indicators show reverse motion.

motion. Figure 25 is a slip linear plot of slip vectors determined from all thin sections. The arrows in this diagram indicate the motion of the footwall relative to hanging wall. This figure shows several directions of movement – normal (4X), right-lateral (3X), left-lateral (3X), reverse (3X), and strike slip – (right or left lateral unknown) (1X). Mineral lineations, weakly defined by sericite, were observed in several samples. This lineation showed dip-slip motion in some samples and strike-slip in others.

A shear foliation defined by deformed galena was observed in most of the oriented hand samples from Pb-rich veins collected throughout the West Chance. Small, rotated quartz grains within the softer foliated sulfide matrix suggest this foliation was a result of reverse motion. The shear foliation was observed to wrap around and sometimes cross-cut clasts contained in the galena vein. The composition of the clasts include tetrahedrite, quartz, and siderite. Clasts tend to be elongated in the direction of the lineation, which was typically the dip direction of the fault plane. Clasts also exhibit a distinctive fracture pattern. The shear foliation, clasts, and fracture patterns are shown in the hand sample of figure 26 and the composite sketch of figure 27. Fractures are filled with different material depending on clast composition. Siderite clasts are filled with tetrahedrite; tetrahedrite clasts are filled with very fine-grained sulfides (the fine-grained texture prevented identification of the sulfide) and quartz; quartz clasts are filled with sulfide material. Several important characteristics of this fracture pattern include the observation that fractures usually terminate at the clast boundary, and typically are found to occur in the same orientation from clast to clast, irrespective of clast or fracture fill composition.

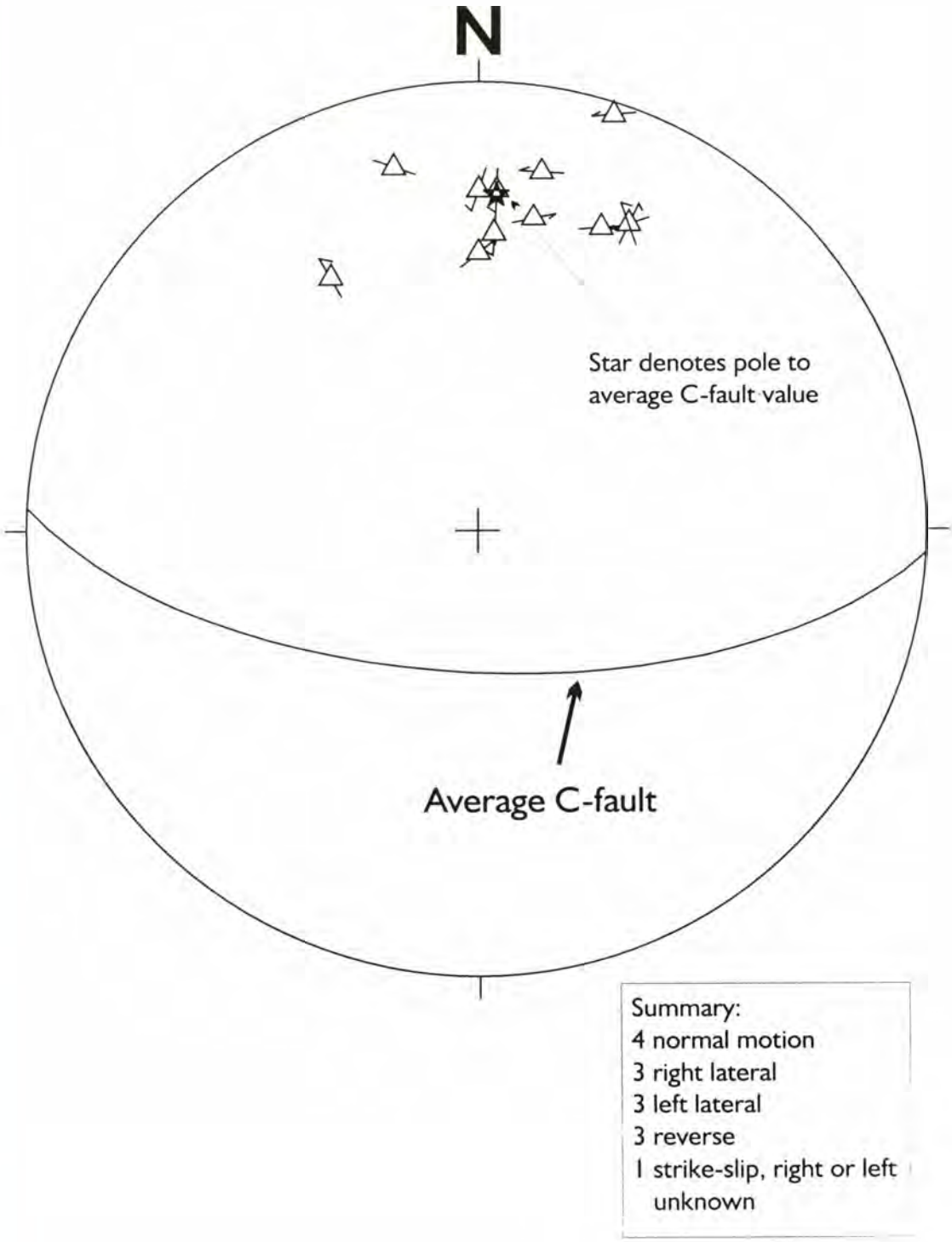

Figure 25. Equal area slip linear plot of slip vectors obtained from thin section observations from vein material. Arrows indicate FW relative motion in a fixed HW reference frame. (Right arrow=right lateral; left arrow=left lateral; up arrow=normal motion; down arrow=reverse motion)

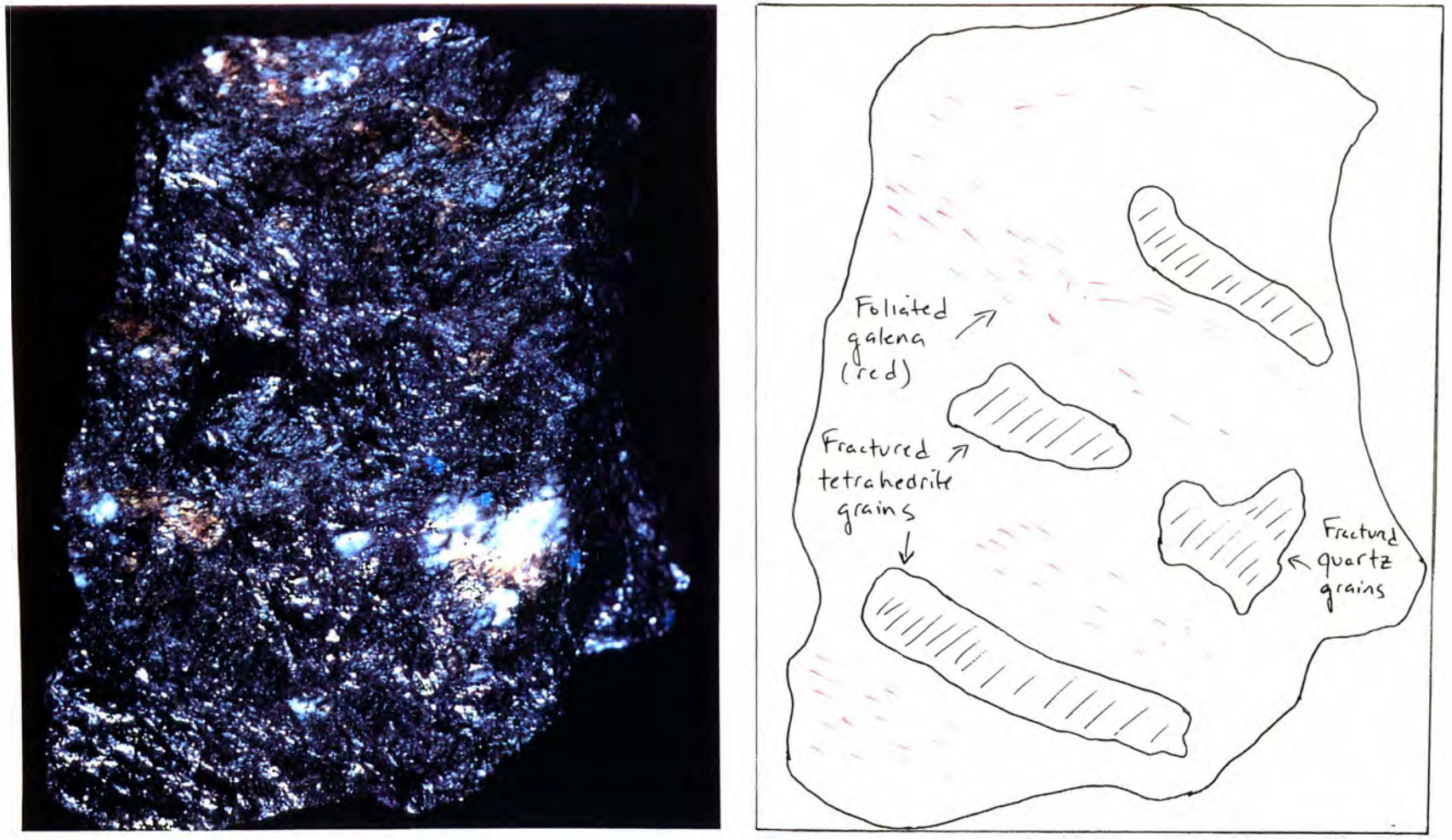

Figure 26. Photograph of hand sample of tetrahedrite and quartz clasts in foliated Pb vein.

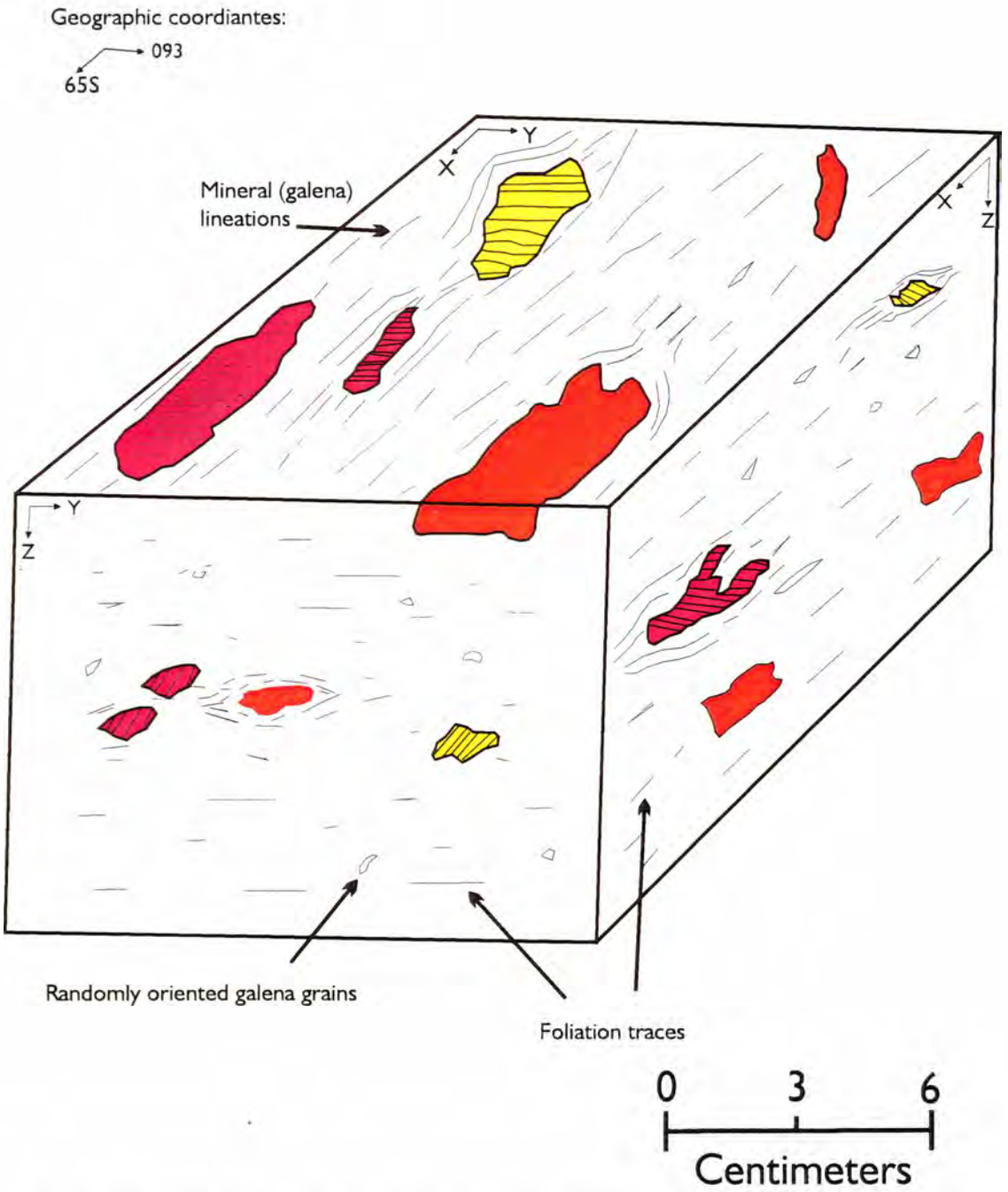

Figure 27. Schematic block diagram showing orientation of siderite (orange), tetrahedrite (red), and quartz (yellow) clasts and fractures in clasts in foliated galena sample. Quartz and tetrahedrite fractures are filled with fine-grained sulfide material; siderite fractures are filled with tetrahedrite. Compiled from samples SS-1 (WC-9), SS-2 (WC-10), SS-25 (WC-25). Angle between lineation in XY plane and fractures in clasts is approximately 50°. Foliation was observed to locally cut tetrahedrite clasts XYZ represents maximum, intermediate, and least axis of strain ellipsoid. X-direction corresponds to stretching direction of strain ellipsoid.

Similar clasts have been previously observed at other mines in the Coeur d'Alene district. Waldschmidt (1925) observed flow structures in galena, from the Bunker Hill mine, that contained clast fragments of other harder minerals that were frequently rolled and transported. At the Hecla East mine, galena in the ore body acted as a "putty-like mass" in which suspended broken fragments of pyrite, tetrahedrite, sphalerite and pyrrhotite, all showed a stringing out and definite arrangement parallel to the flowage of the galena (Vokes, 1969). It is important to note that the sequence of mineralization reflected in the clast and fracture composition represents the same paragenetic sequence found in the vein systems of the mine. This would suggest that the clasts are a result of the brecciation of pre-existing mineralized veins (i.e. mineralization occurred before the formation of the shear foliation), or that brecciation and mineralization were broadly synchronous.

Ambiguity exists when trying to classify the filled fractures as shear or extensional. In general, fracture infilling texture and the angle between fracture and the associated shear, or between sets of fractures, are often used as the defining criteria for extension veins. Displacement or pinnate fractures along the main fracture are good identifying criteria for shear fractures. However, one must also take into account that the fracture might have originated as an extension fracture and then been subsequently sheared. In clasts such as those shown in figure 27, fractures locally follow cleavage in siderite clasts. Small pinnate fractures are found along larger fractures; however, displacement, even on the microscopic scale, is rarely observed. The angle between fractures and foliation is generally 30°-40°.

Although the scope of this project did not include a detailed description of ore microscopy, textures of ore forming minerals were observed in conjunction with petrofabrics. It was observed that siderite and quartz were deposited first, followed by tetrahedrite, with galena representing the last stage of mineralization. Pyrite was observed to be deposited in two different episodes, with the first one following quartz, and the second following lead deposition. Early pyrite was often highly fractured, and commonly filled with quartz.

Two explanations are offered to explain the origin of the fractures in the breccia clasts. Fractures could have formed in the same stress regime that formed the shear foliation. This would require the clasts to be brecciated, fractured, and filled with the same paragenetic sequence as that observed in existing veins suggesting a prolonged period of faulting and mineralization. This scenario best explains fracture orientations. A second explanation would be that the fractures formed in a different stress regime than the shear foliation and the shear foliation represents the disruption of veins. The consistent orientation of fractures is then coincidental and represents an earlier faulting event overprinted by a reverse faulting event. The author favors the second explanation since this scenario better explains the observed mineralization sequence.

Bedding and Cleavage

The West Chance vein system is located on the overturned limb of the Big Creek anticline. An abundance of parasitic folds on the overturned portion of the anticline have been previously identified by mine geologists and are schematically shown in figure 4. Bedding measurements compiled from drift and stope maps of the West Chance were used to examine the variation of bedding within the West Chance. Figure 28 shows poles

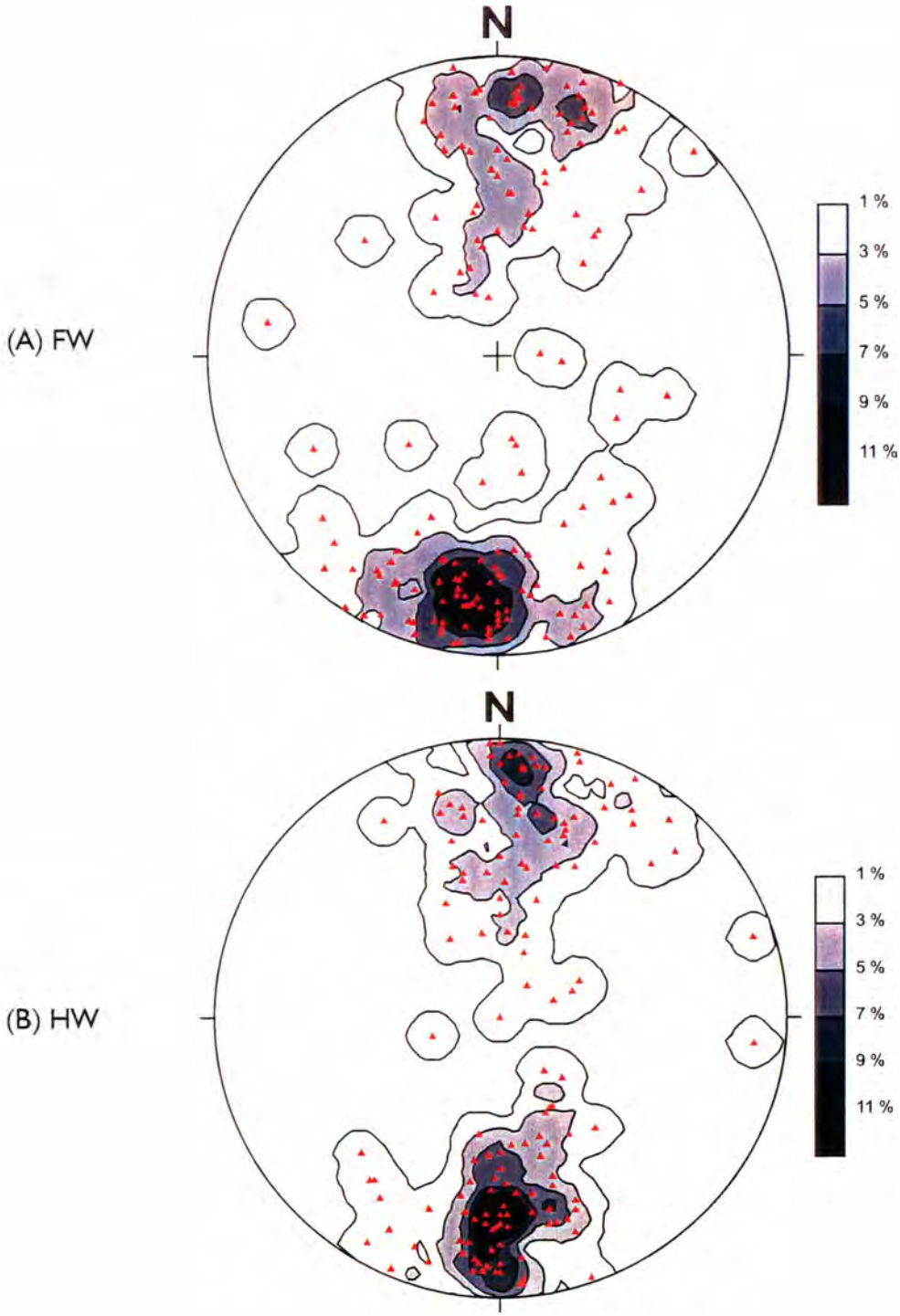

Figure 28. Contoured equal area lower hemisphere stereographic plot of poles to bedding planes. Contour intervals indicate 1-3-5-7-9-11% per 1% area, with a maximum of 13%. (A) shows poles to footwall bedding, n=150. (B) shows poles to hanging wall bedding, n=154.

to bedding in the footwall and hanging wall of the West Chance fault. The general attitude of bedding is west striking and steeply dipping north or south. Local variations do exist, probably due to parasitic folds. A comparison of footwall and hanging wall bedding plane poles shows there is only a small difference in attitudes of these two data sets (figure 28). Due to the variation in bedding and the anastomosing nature of the fault zone, mineralized veins have been observed to both cut and parallel bedding.

Attitudes of a penetrative cleavage were also compiled from drift and stope mapping. Cleavage is best developed in the softer, more argillaceous units. Poles to these cleavage planes are shown in figure 29. Also shown in this figure are the attitudes of the axial plane of the Big Creek anticline. Surface mapping by Gale 1936 and mine geologists in 1990's have shown that the axial plane of the Big Creek anticline changes orientation from east to west. East of Big Creek the attitude of the axial plane is 062, 89 SE; west of Big Creek the attitude is 091, 76 SW. The majority of the West Chance ore body lies to the west of Big Creek. The alignment of the penetrative cleavage with the axial plane of the Big Creek anticline west of Big Creek suggests this cleavage is an axial plane cleavage. This relationship is examined further in the discussion section.

Folding

Drag folding is present in many of the stopes of the West Chance vein system. Most drag folds are small scale, open folds, generally less than 0.91 meters (3 feet) in wavelength, and occur within 3.04 meters (10 feet) of the Chance fault. The degree of drag folding varied from small open folds to small amplitude, tight folds. Drag folds were observed in different orientations and are present in the back of stopes and drifts as well as stope faces. Different orientations of drag folding suggest different episodes of

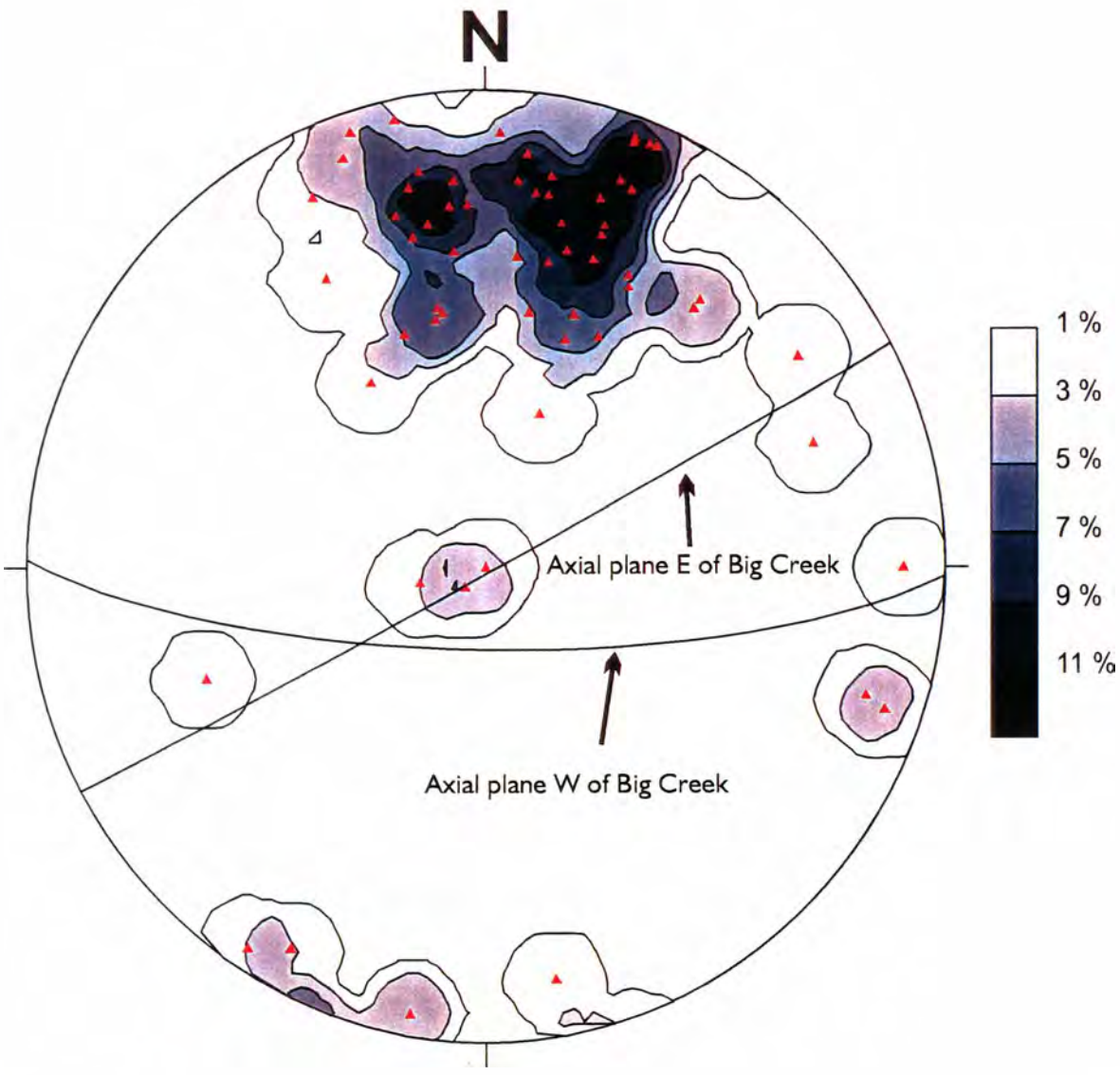

Figure 29. Contoured equal area lower hemisphere stereographic plot of poles to cleavage planes. Contour intervals indicate 1-3-5-7-9-11% per 1%area, with a maximum of 13%. Axial plane for the Big Creek anticline, east and west of Big Creek is also plotted.

deformation and/or directions of fault movement. Drag folding of the wallrock fabric, individual siderite, quartz, or sulfide veins, or a combination of all of the above were observed routinely. Drag folding was also observed to predate mineralization and postdate mineralization (31 ER4 – wallrocks, siderite-quartz, and sulfide material are all folded) – figure 30. Drag folds were also present on the 2700, 3100 and 3700 West Chance attack ramps adjacent to the Chance fault.

Another style of folding is found on several levels within the West Chance vein system. These folds differ from drag folds described above due to their location, size and type of material being folded. These folds occur 9.1 to 15.2 meters (30-100 feet) into the hanging wall of the West Chance fault, have axial traces that extend for approximately 304 meters (1000 feet), and fold siliciclastic rocks of the St. Regis and Revett formations. An example of this style of folding is found on the 4200 level where an anticline-syncline pair, with a fold axis shallowly plunging to the west, extends over 300 meters (~1000 feet). Folds with similar characteristics of the 4200 level are found on 2700 and 3100 levels. It was not determined if these two folds are associated with fault movement along the West Chance fault or part of the folding event that produced the Big Creek anticline or both. However, these folds change orientation from NW to EW similar to the Chance fault. This suggests that the folds and fault are coeval.

Veining and Faulting

Veining along the West Chance vein system is discontinuous and atypical with respect to most ore bodies in the mine, and displays unique relationships to faulting. A

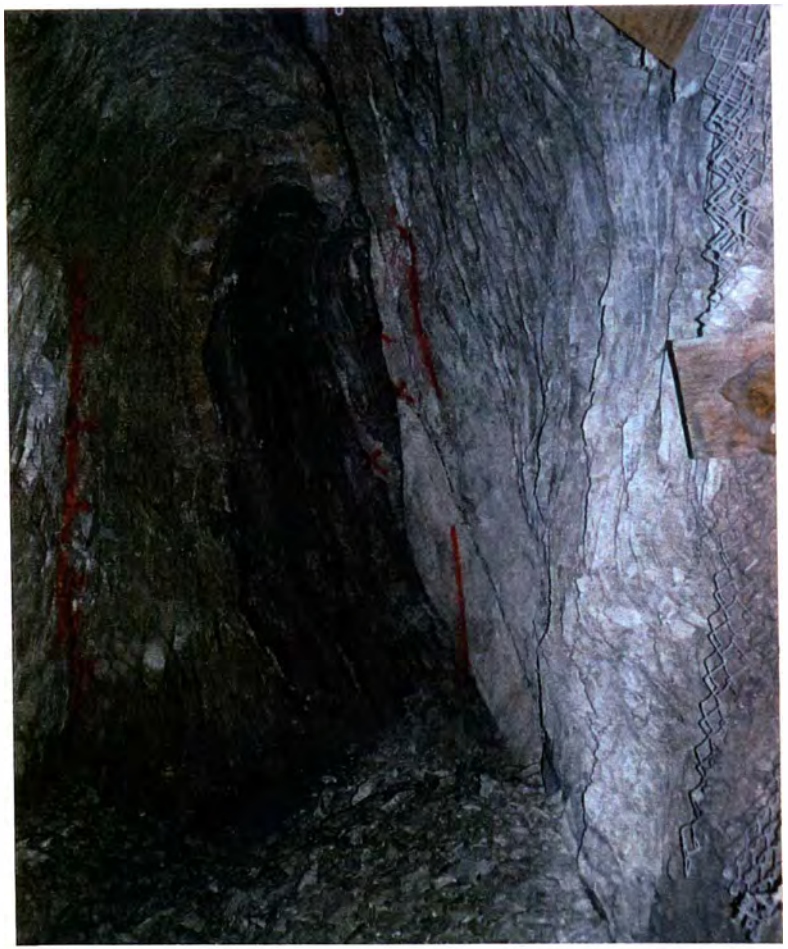

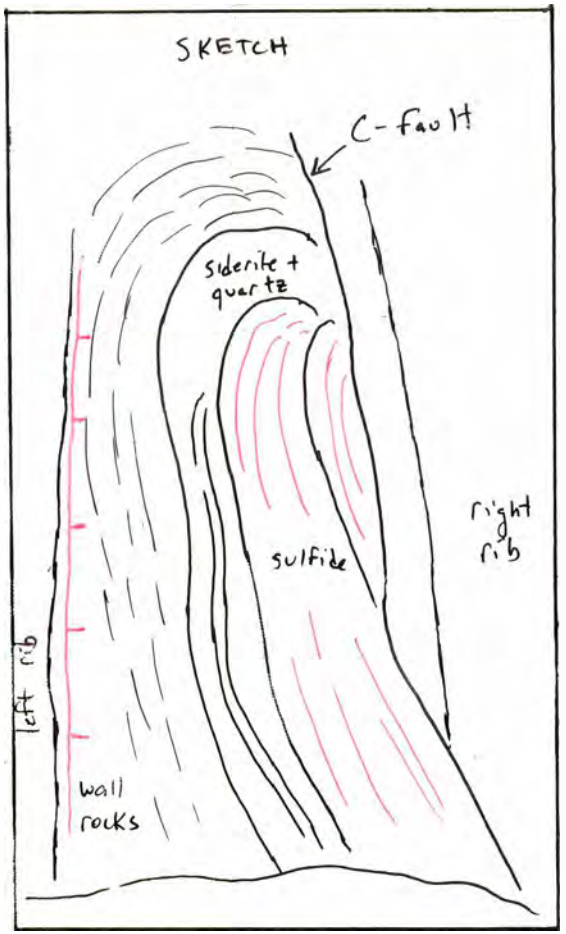

Figure 30. Cross-sectional view of a West Chance stope face illustrating post-ore drag folding of wall rocks and mineralized veins adjacent to the Chance fault. This fold could be interpretated as normal drag or compression folding cut by faulting. Red paint on left indicates scale with 0.305 m.(1.0 foot) increments. 3100 ER4 A East - 5/7/98

composite drawing of the common components of the West Chance vein system is shown in figure 31. This figure was compiled from face sketches and observations taken on daily visits to mine workings. Photographs of some of the isolated features that make up the composite drawing are shown in 32a-f.

As shown in the figures 31, 32a, and 9a, siderite and quartz can occur as discrete, variable width veins, which parallel C-fault, or as isolated fault lozenges produced during shearing. Siderite-quartz veins generally trend west and dip steeply to the south; however they can locally deviate from the east-west orientation and trend in a north-south direction. The amount of sulfide mineralization in siderite-quartz veins is highly variable. Sulfide veins (both tetrahedrite and galena) in the West Chance can be equally discontinuous. These veins are generally parallel to the general trend of the West Chance fault, but can locally vary from this orientation. Tetrahedrite is found to fill cleavage fractures in siderite-quartz veins, as small veinlets, or disseminated in the fault zone. Lead veins can occur as coarse grained foliated veins in the hangingwall or footwall, or as fine grained recrystallized material next to C-fault.

The relationships between veining and faulting are also shown in figure 32. Veins are typically bounded by faults, and sometimes siderite-quartz veins are in fault contact with lead veins (figure 32b). Riedel shears and drag folding in the wall rocks indicate both strike-slip (figure 32c) and reverse motion. Often folding which indicates reverse motion can be observed in the same face with offset veins indicating normal motion (figures 32d and e), which can suggest a strike-slip component. In the West Chance vein system, veins can be observed to cut faults and faults can be observed to cut veins. This mutual

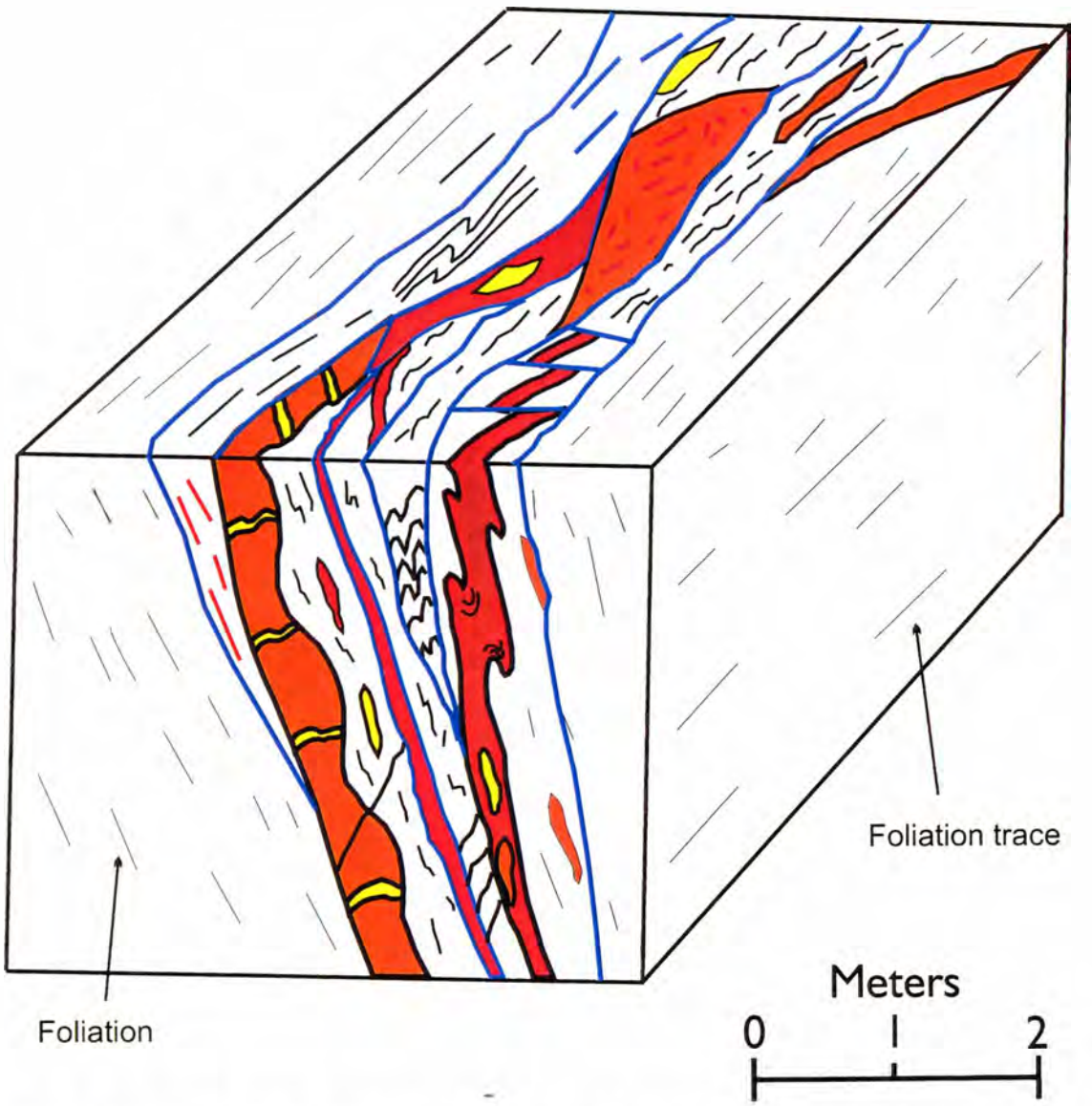

Figure 31. Block diagram, compiled from face sketches, showing the various features of veining and the relationship to faults in the West Chance vein system. Vein features include variable width siderite-quartz veins, multiple phases of veining, extension (ladder) veins which cut siderite veins and are cut by later sulfide veins. Veins are typically bounded by faults; Riedel shears and drag folding indicate both strike-slip and dip-slip motion has occurred; veins are cut by faults, and faults are subsequently cut by veins indicating faulting was ongoing during mineralization. Orange=siderite; red=sulfide mineralization; yellow=quartz; blue thick line=faults; black solid lines = Riedel shears;dashed black lines=wall rock fabric.

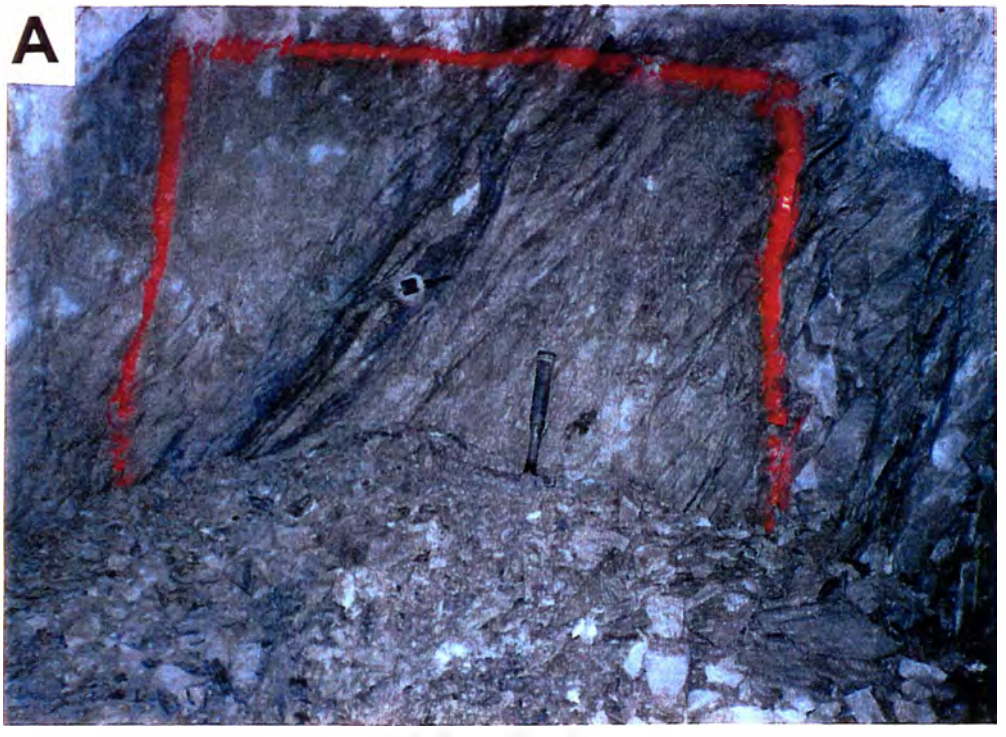

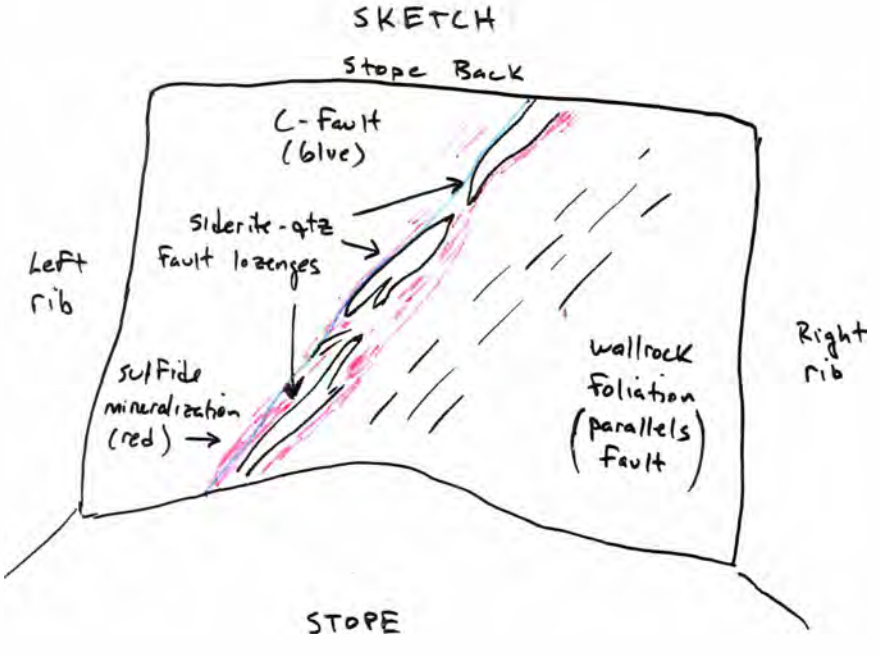

Figure 32a.. Photograph showing various elements in the vein-fault composite diagram (figure 31). (A) siderite-quartz fault lozenges in sulfide matrix. In this photo, wall rock fabric parallels fault and vein. 3100 West Chance.

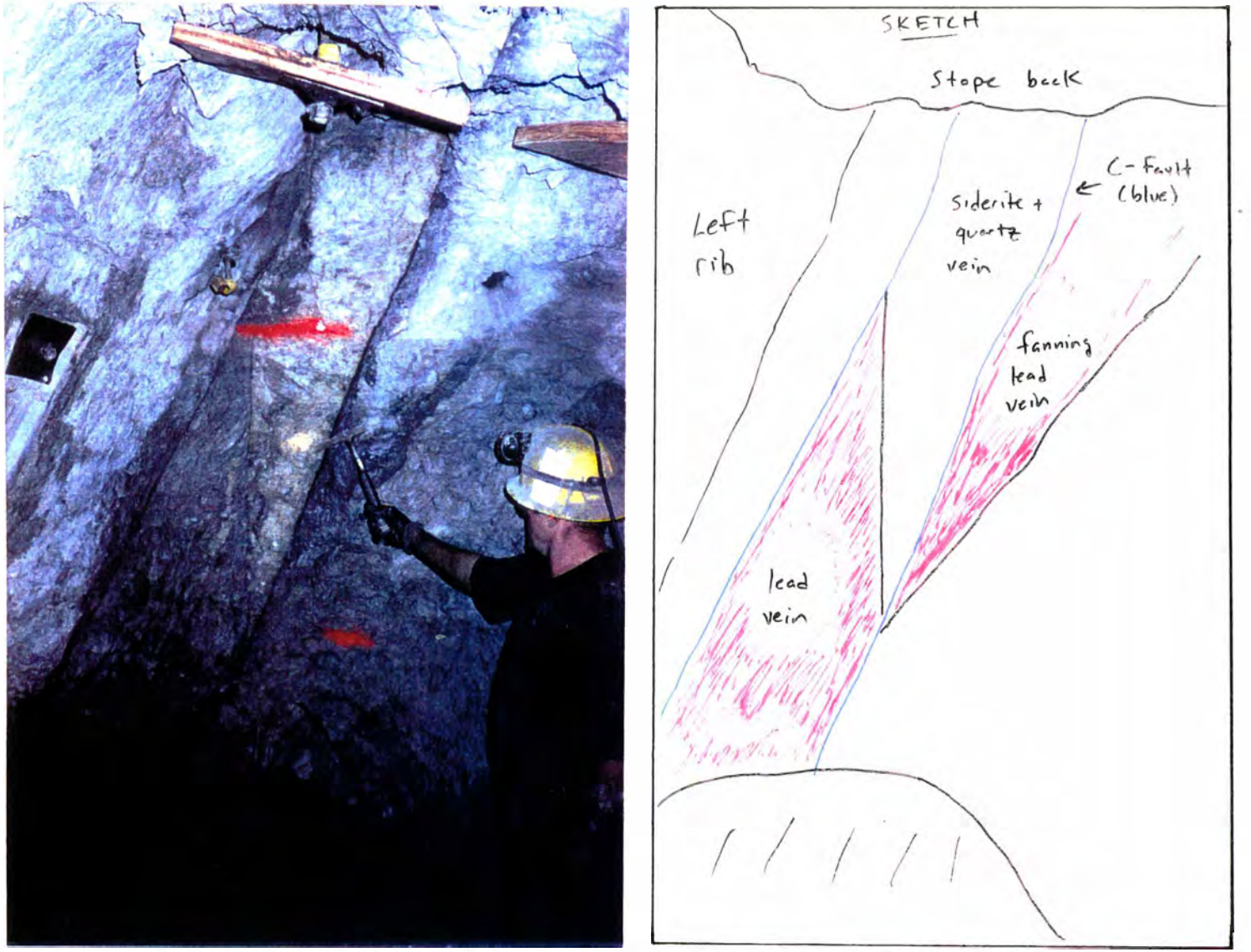

Figure 32b. Photograph showing various elements in the vein-fault composite diagram (figure 31). (b) Siderite-quartz vein in fault contact with lead vein. Veining is also fault bounded on both sides. Notice fanning lead vein on right side of photo.

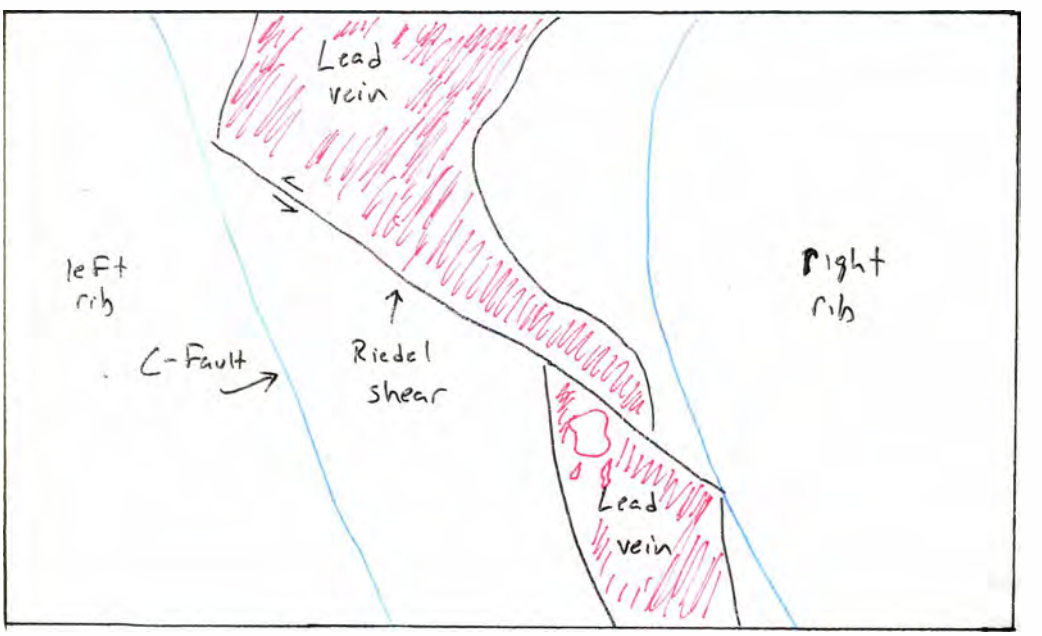

Figure 32c . Photographs showing various elements in the vein-fault composite diagram (figure 31). (C) Looking up at a Riedel shear in back offsetting lead vein; indicates strike slip motion. 3100 E10E, Floor 8; 8/27/96.

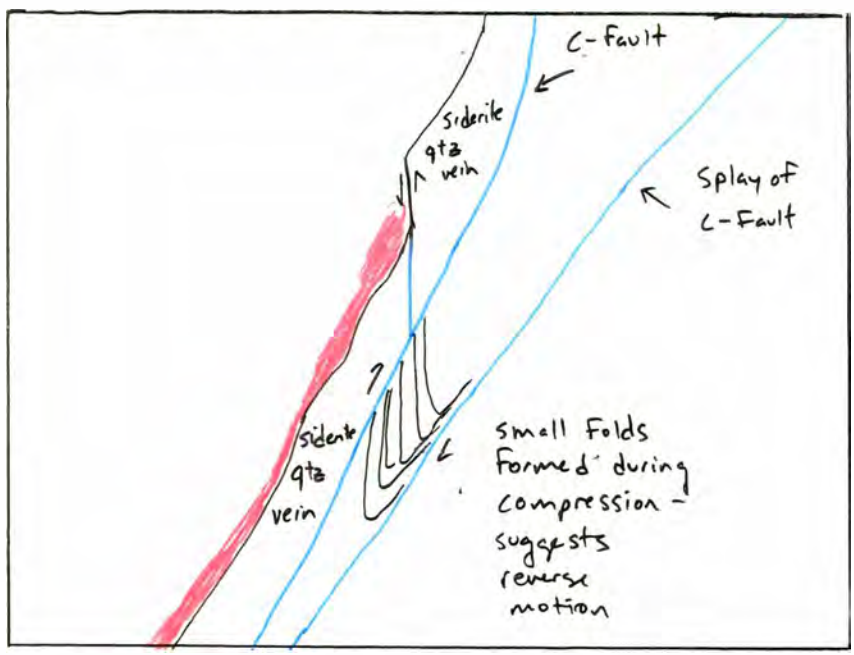

Figure 32d. Photographs showing various elements in the vein-fault composite diagram (figure 31). (D) Photo showing folding which indicates reverse motion and vein offset which indicates normal motion; 3700 West Chance.

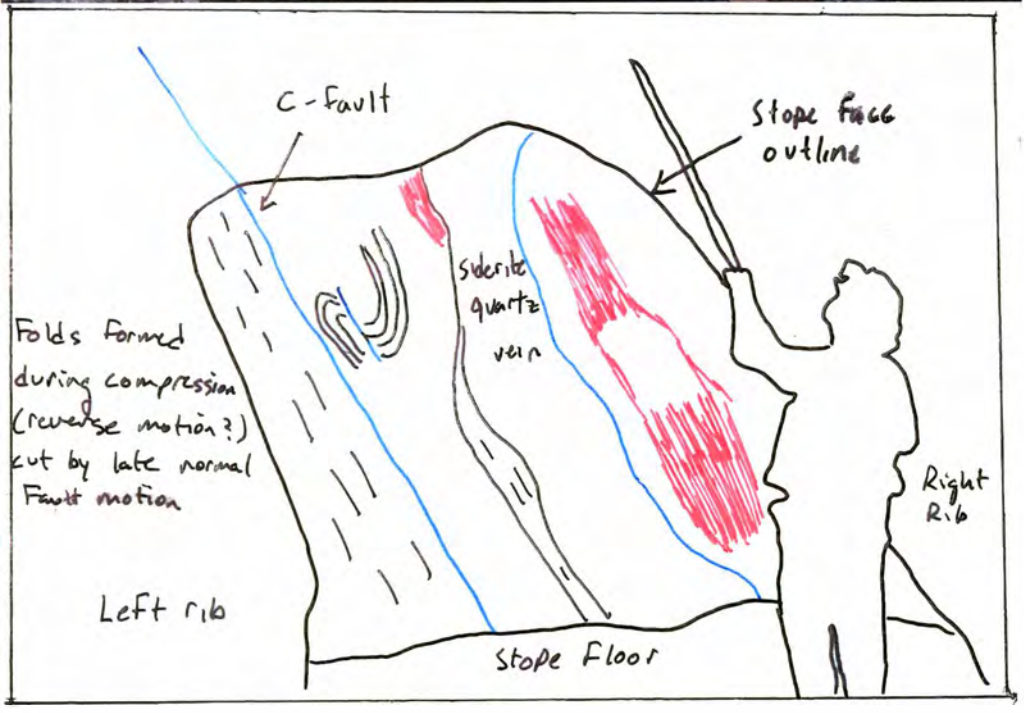

Figure 32e. Photographs showing various elements in the vein-fault composite diagram (figure 31). (E) Photo showing drag folding which indicates reverse motion and vein offset which indicates normal motion. Also notice irregular nature of siderite-quartz and lead vein and folding of wall rock fabric.

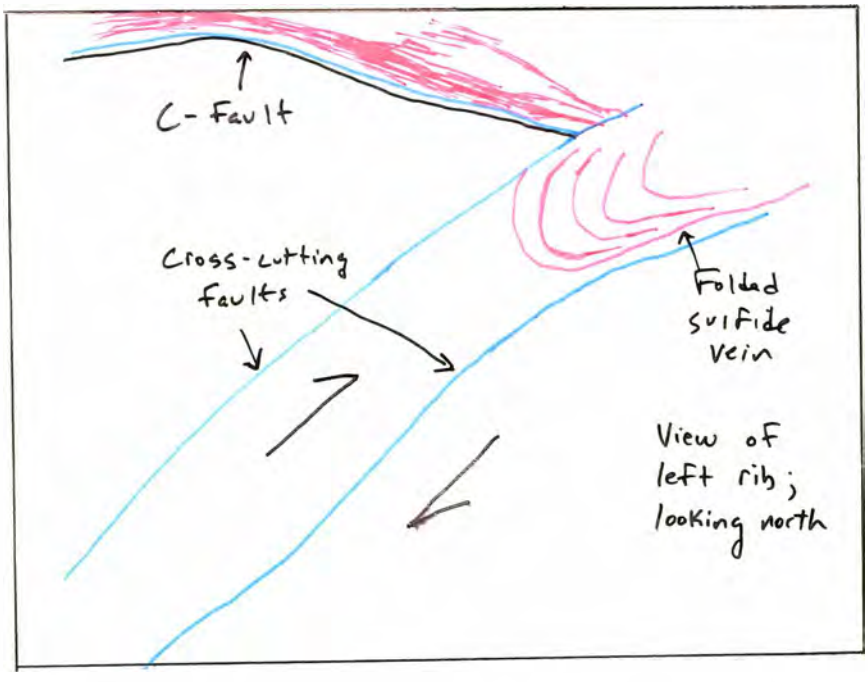

Figure 32f. Photographs showing various elements in the vein-fault composite diagram (figure 31). (F) Folding of sulfide vein along reverse fault. Shown fault cuts and offsets C-fault. Both photos are from 2700 ER2D -E 11/19/98.

crosscutting relationship suggests faulting was ongoing during mineralization. Faulting is also observed to cut late stage lead veining which suggests post-ore movement has taken place. It was noted that most vein types in the West Chance vein system are fault bounded. Most veins in the West Chance, except ladder veins and barren quartz veins, are highly sheared and do not exhibit fracture filling texture as observed in other ore bodies, e.g., in the Chester Hook area (Husman, 1989). Since the West Chance vein system occurs along a major fault system, it is suggested that the original depositional texture has not been preserved due to the multiple episodes of deformation.

Stress Fields

The relationship between extension veins and associated faults can give theoretical orientations of stress fields. This section compiles new and existing data on extension veins and associated faults in the Sunshine mine while attempting to determine the prevailing stress field during mineralization. The theoretical stress field will be used as a tool in the interpretation of the type of faulting, strike-slip or dip-slip, which accompanied mineralization.

Three different types of extension veins were used for the purposes of calculating stress fields: – ladder veins, barren quartz veins (both measured in the West Chance), and mineralized veins from the Chester Hook area. Both the ladder veins and the barren quartz veins were identified as extension veins based on their fracture filling texture. This fracture-filling texture is shown in figure 33. Ladder veins were used for fluid inclusion analysis and have been described in chapter 2. Barren quartz veins were found in the footwall and hanging wall of the Chance fault, were 2.54-5.08 cm (1-2 inches)

Figure 33. Photomicrograph showing fracture filling texture of quartz ladder vein.
3700 ER2B-E

wide and occurred in a variety of orientations. These two vein sets are referred to as small quartz veins of the West Chance in the discussion section. Husman (1989) described the mineralized veins of the Chester Hook as exhibiting a fracture-filling texture. These veins were 1.5 to 3.0 meters (5-10 feet) in width and constituted the economic ore in that area. Ladder and barren quartz veins were typically found in contact with the West Chance fault, and are interpreted to be a result of motion along this fault. As mentioned in chapter 2, ladder veins were formed after the deposition of siderite, but before sulfide (tetrahedrite or galena) mineralization. Cross-cutting relationships show that the barren quartz veins were either pre-, syn-, or post- mineralization. Although the author did not have a chance to observe the Chester Hook area, veins from this part of the mine are interpreted to be associated with movement along the Syndicate fault due to the close proximity of the two features. The veins from the Chester Hook area represent all stages of mineralization. A stress field was also calculated using the general orientation of the West Chance vein system and the attitude of the WNW trending Chance fault. Using the whole West Chance system in this way assumes the vein system formed as an extension vein and was subsequently sheared.

To determine the principal stress directions, the attitudes of the extension vein and the fault interpreted to be associated with the extension vein were plotted on a stereonet. The technique to determine the principal stress directions was outlined in Reid (1993). The orientation of σ_3 was interpreted to be the pole to the extension vein; σ_2 was interpreted to be the intersection of the fault and extension vein, and σ_1 was interpreted to be 90 degrees from σ_2 in the plane of the extension vein. Theoretical slip lines were interpreted to be 90 degrees from σ_2 in the plane of the fault. Calculated stress fields and

slip lines are shown on the equal area stereographic projections in figure 34. Barren quartz, ladder, and the Chester vein as well as the overall West Chance vein system are denoted by different symbols in the figure. Overall, figure 34 shows variation in the theoretical principal stress directions. Points representing σ_1 are mostly clustered in the northeast quadrant of the steroenet. Intersections of extension veins and faults, represented by the σ_2 plot, lie mostly in the southern half of the stereonet, and vary from trending west with a shallow plunge (ladder veins and some small barren quartz veins in the West Chance) to trending south with a steep plunge (Chester and West Chance vein systems and some small barren quartz veins). Extension directions, represented by the σ_3 plot, show shallow north directed extension directions for the Chester and West Chance vein systems, and shallow northeast to steep southeast extension directions for small quartz veins of the West Chance. Closer examination of the clustering of σ_1, and orientation of σ_2 and σ_3 suggests left-lateral motion along the WNW Chance and Chester faults during mineralized vein formation and oblique left-lateral to reverse motion along the West Chance fault during barren quartz vein formation. The plot of slip lines suggests that fault motion varied from strike-slip to dip-slip. Although the stress fields appear complicated, most data shows left-lateral and reverse motion on faults parallel to the West Chance fault.

Several explanations are offered to explain this variation. First, a varying stress field could have produced the distribution of principal stresses seen in figure 34. Given the prolonged deformational history of the Sunshine mine, and the tectonic history of the Coeur d'Alene district, a varying stress field is certainly possible. With the assumption

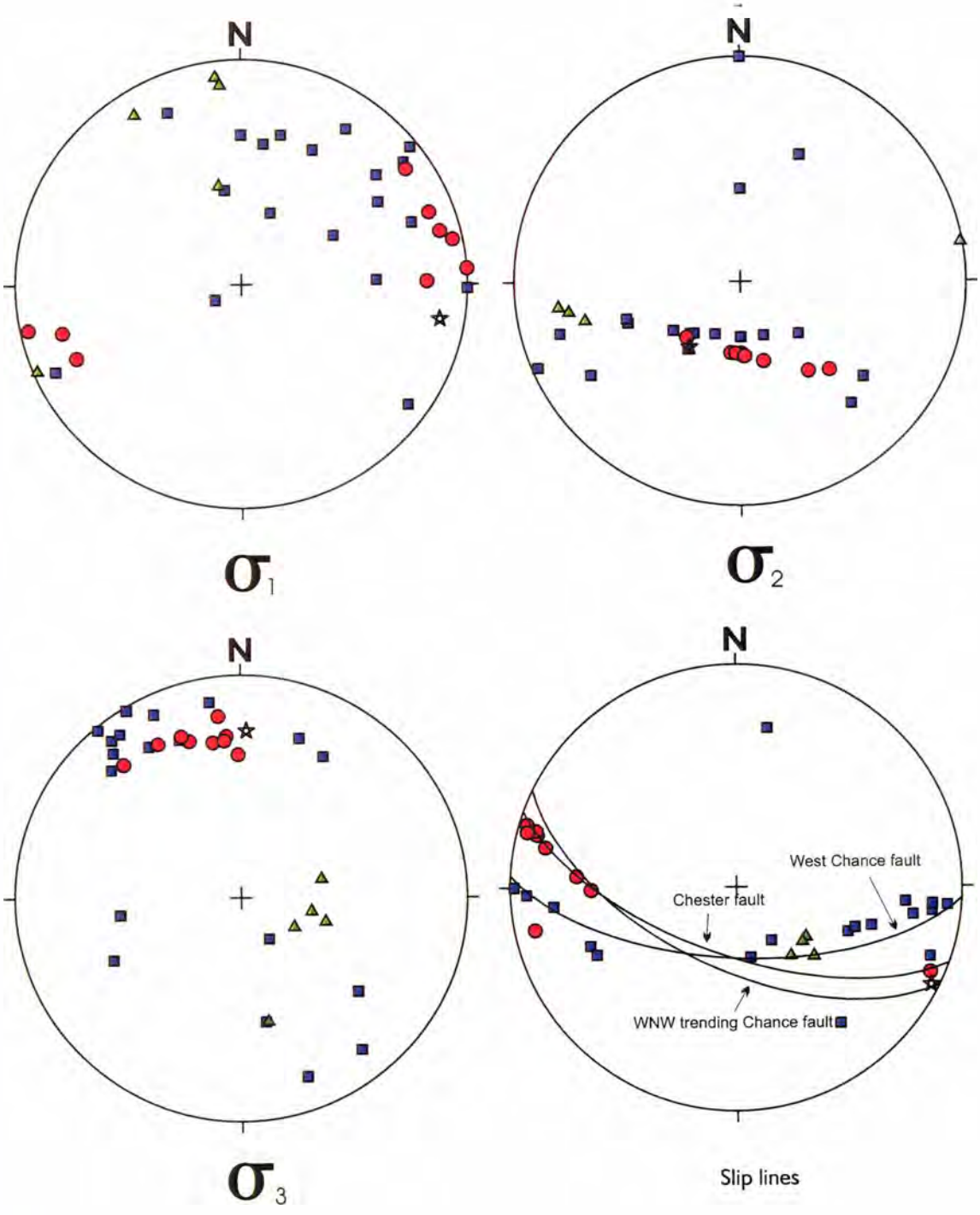

Figure 34. Stereographic plot of sigma$_1$, sigma$_2$, sigma$_3$, and slip line for vein sets in the Sunshine Mine. Red circles = Chester veins; green triangles = West Chance ladder quartz extension veins; blue squares = West Chance non-mineralized quartz extension veins; yellow star = West Chance mineralized vein system. See text for explanation.

that the distribution of stresses reflects a varying stress field, the stereographic plots of figure 34 can be interpreted to show various episodes of fault movement – reverse, left-lateral, and oblique left-lateral. Based on the variation observed in the theoretical stress fields, it is suggested that reverse and left-lateral motion represent the end members of fault motion. The array of motions which occurs between these end members would then show a record of the stress field as it was moving from one end member stress regime to another. The distribution of principal stresses could also be the result of rotating blocks. Different sections of rock between faults could have acted as individual blocks. The variation in the calculated stress fields would then be a result of rotation of these blocks. A third explanation for the scattered array of principal stresses is transpression, with regional σ_1 in the NE quadrant and local movement on the West Chance fault which varied with time or alternated between left-lateral and reverse motion. A fourth explanation for the scattered array is that the formation of these veins were not associated with the Chance fault or any subsidiary faults.

Structural Control of Ore Shoots

In order to evaluate the potential correlation between the distribution of ore and its relationship to strike and/or dip, silver grades, obtained from the daily assay database, were plotted as a function of strike and dip. Figure 35 shows an XY plot of grade versus dip for approximately 380 measurements from the West Chance vein system. The figure shows no statistical correlation between grade and dip of the fault, within the limited range of fault dip (45-70°). This would suggest that fault dip variation is not the dominant structural control on ore location or ore grade. Figure 36 shows an XY plot of strike versus grade for approximately 161 measurements from the West Chance. Strike is

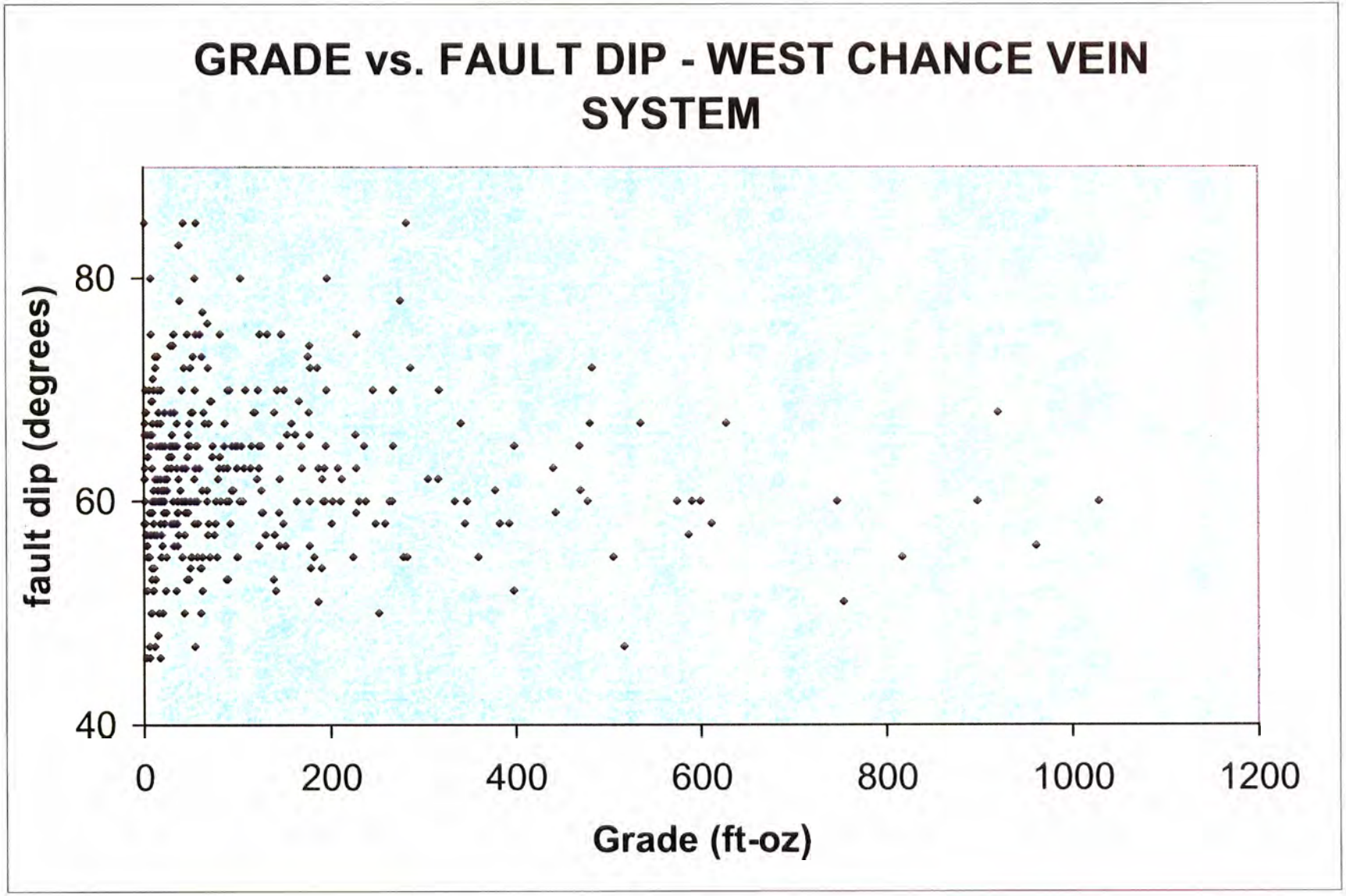

Figure 35. Ag Grade vs. Fault Dip plot for sample assays (n=380) in the West Chance Vein System

not always measured on routine sampling due to the potential of metallic objects in stopes yielding erroneous measurements. Figure 36 that within the limited strike (065-120) range of the ore body, no significant correlation exists between strike and Ag-grade.

Although the graphs indicate there is not a correlation between strike and dip and ore grade, mapping in the West Chance vein system shows a correlation may exist in some areas. On a large scale, mineralization is present where the WNW-trending Chance fault turns westerly (figure 5), suggesting that strike is a structural control. Figure 37 is a plan view map of the 2700 ER6 1B East stope. Starting in the west, mine grade mineralization ($\geq$ 15 opt) follows the E trending C-fault for 25 feet. At this point, a NW-trending fault truncates C-fault. C-fault changes orientation, splays into the hanging wall and loses mine grade mineralization. C-fault then turns back to the E and ore grade increases. Figure 37 thus exemplifies a correlation between strike and mineralization. In this particular case, ore is found where C-fault trends east and not found where C-fault trends northeast. This relationship between strike and grade can be observed in several other stopes in the West Chance. However, this correlation does not always hold true and in other places, examples can be found where strike does not control ore location or grade. Figure 38, a plan map of 31 E9E Fl.8, exemplifies an instance where the change in strike does not correlate to a change in ore grade. Ore grade is consistent although a change in strike is observed. Yet another example is shown in figure 39, a plan map of 2700 ER6-2D-W Fl.2. Here ore grade is highly variable along the length of the stope where there is no variation in strike. These examples of mapping in the West Chance vein system indicates small scale changes in strike are not the dominant structural control of ore grade or thickness, but can be a local contributing factor.

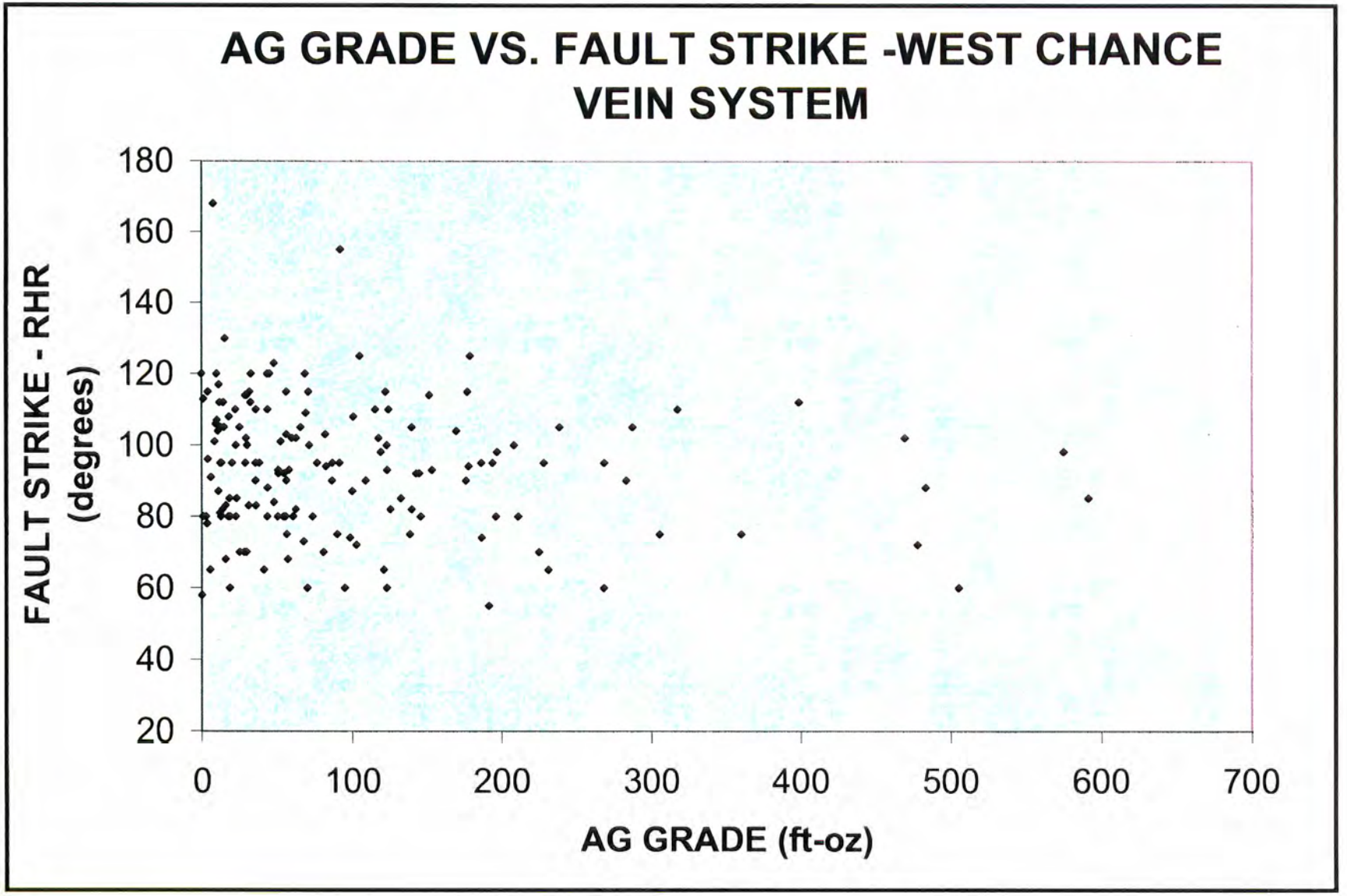

Figure 36. Ag grade vs. fault Strike plot for sample assays (n=161) in the West Chance Vein System

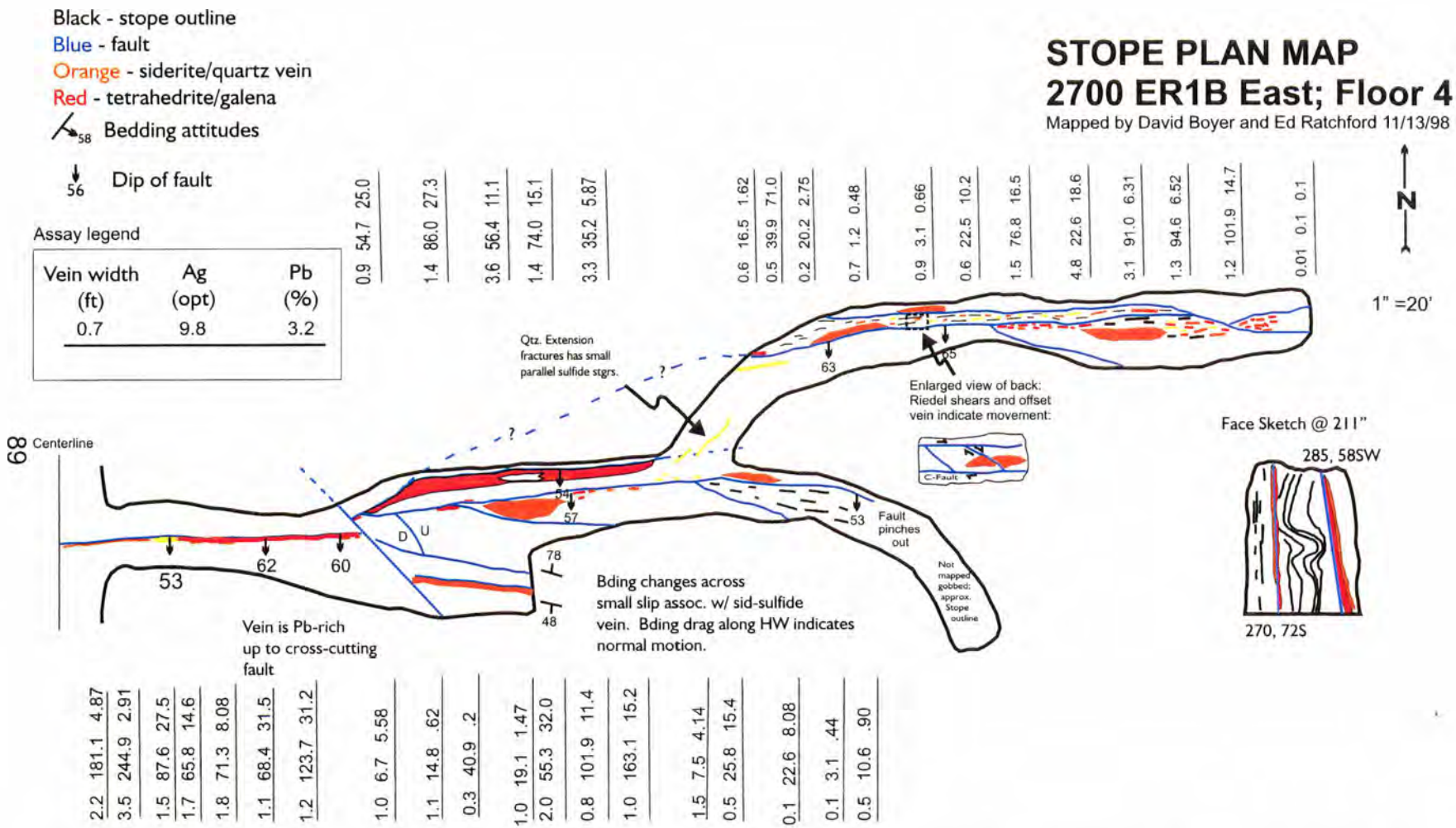

Figure 37. Stope map of 2700 ER 1B East, showing a change in mineralization is associated with a change in the orientation of strike.

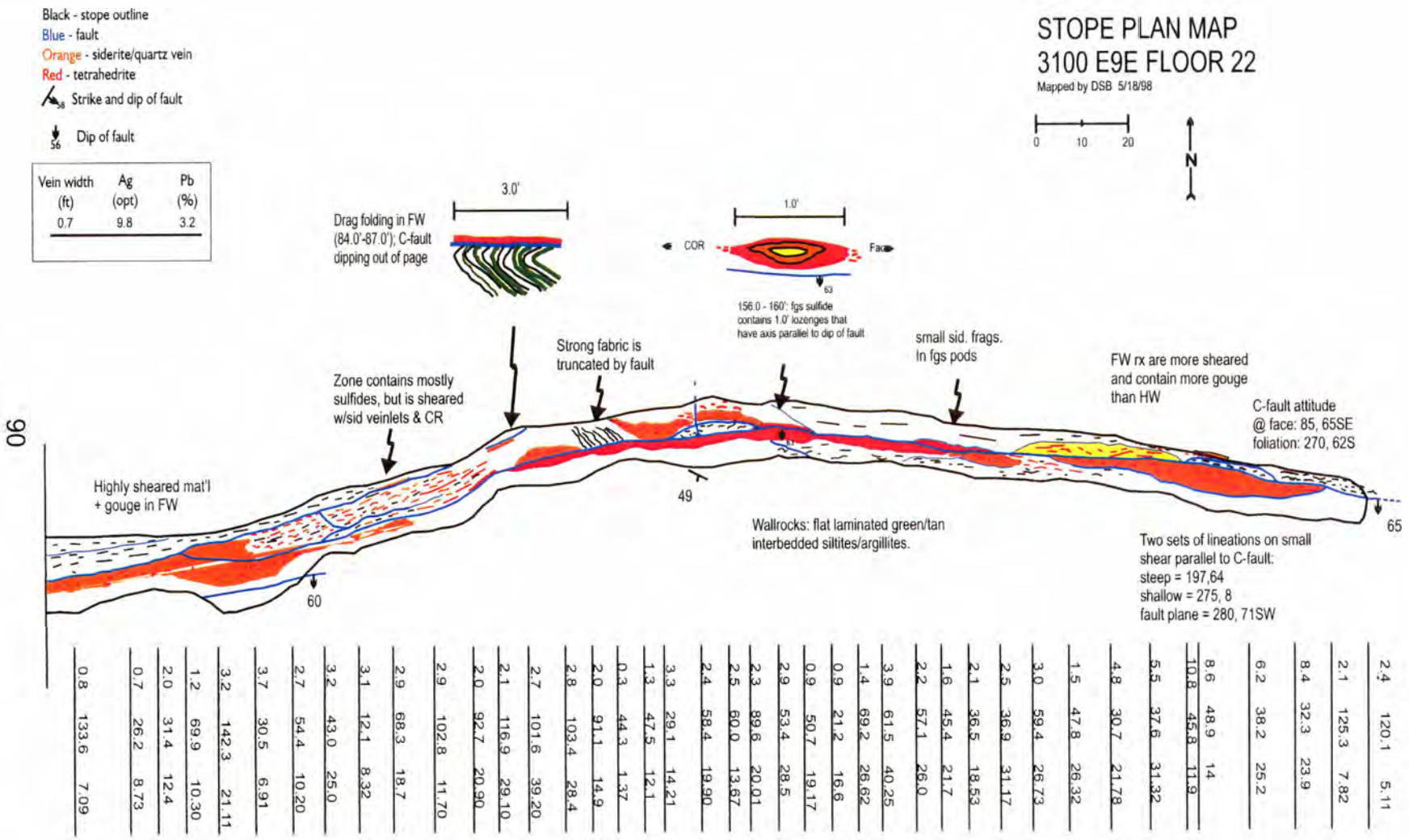

Figure 38. Stope plan map of 3100 E9E Floor 22, showing variation in ore grade asociated with variation in orientation of strike.

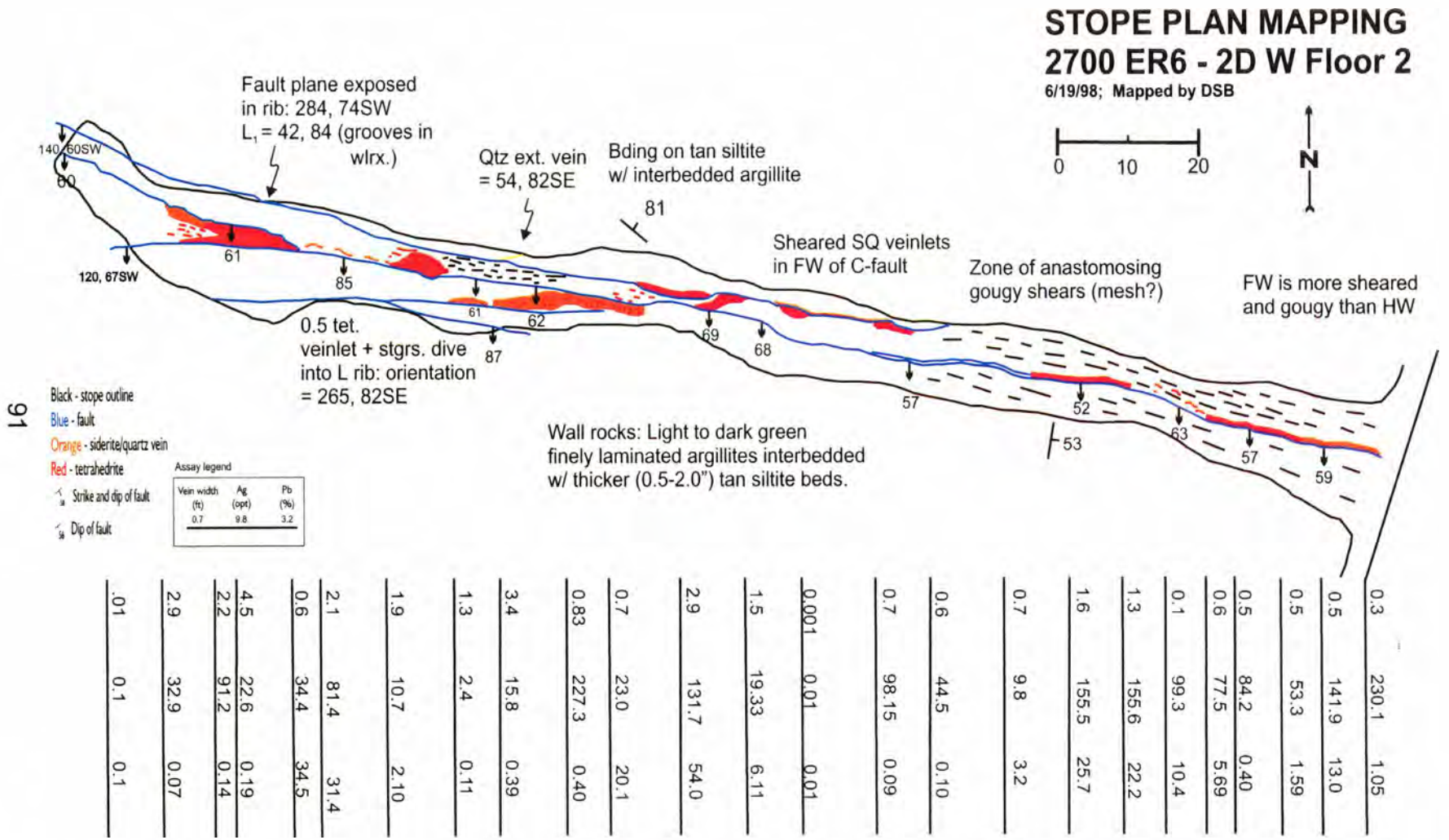

Figure 39. Stope map showing variable mineralization associated with little variation in the orientation of C-fault.

Orientations of ore shoots can yield clues into the structural control of the ore body and/or fluid flow. A longitudinal section of the West Chance ore body, with contoured Ag grades is shown on plate A. Over 8000 assay values of Ag were converted to foot-oz/ton by multiplying the assay value by the vein width. These values were then assigned an XY coordinate within the ore body. The Quicksurf™ computer program generated surfaces from which contours were calculated and drawn based on the statistical distribution of the data. As shown in Plate A, a generally steep, 60-80°W rake of the ore shoots can be seen. This trend of the ore shoots is better defined in the lower and eastern portion of the ore body. The same procedure was used to show Pb values (in foot-weight %) within the ore body, and is shown in Plate B. The Pb values show a similar rake in the ore body as Ag values, although not as pronounced. The most notable characteristic in plate B is that Pb values increase along the eastern flank of the West Chance vein system. Lead values also slightly increase toward the top of the ore body, especially above the 3100 level. The geometric orientation of ore shoots are suggested to be a result of fluid flow during fault movement. If reverse motion was synchronous with mineralization, the ore shoots would represent the slip line or slip parallel fluid flow. If strike-slip motion was synchronous with mineralization, the ore shoots would represent the σ_2 direction and indicate the flow of mineralizing solutions during deposition. The zonation of Pb observed in the West Chance vein system is also suggested to be related to fluid flow. Sunshine mine geologists and the author have noted that the eastern portion of the West Chance fault is highly fractured and contains many splays due to the change in trend (WNW to W) of the Chance fault. This author suggests that the lead utilized this fracture/splay system during deposition. It is also suggested that the lead was

remobilized. Galena has a lower melting temperature and would explain why only the Pb was remobilized. Conversely, a set of late fractures may have developed after Ag deposition, but before or during Pb deposition which concentrated the Pb mineralization along the east side of the West Chance ore body.

Discussion

Results of the structural analysis in this study are summarized as follows: 1) the West Chance fault-vein system is a west-trending zone of anastomosing shears, fractures and veins; 2) kinematic evidence from wall rocks, Pb-veins, and thin section observations shows evidence for reverse, normal, and strike-slip movement during the kinematic history of the West Chance fault-vein system; 3) cleavage in the West Chance roughly parallels the axial plane of the Big Creek anticline; 4) mutual cross-cutting relationships between faults and veins suggest faulting was ongoing during mineralization; 5) theoretical stress fields, based on extension vein orientations, show principal stresses varied between left-lateral and reverse faulting during the structural history of the West Chance; 6) smaller scale variation in fault strike and dip do not appear to be the dominant structural control of ore grade or placement, but locally may be significant; and 7) ore shoots in the West Chance ore body have a 60-80^{o} westerly rake. Interpretations associated with these conclusions are discussed below.

Cleavage Formation

Cleavage formation in the Coeur d'Alene district has been related to one of two deformational events: deformation associated with large folds such as the Big Creek anticline (Hobbs et al., 1965) or shear related-metamorphic foliation (Reid et al., 1995). Measurements collected from the West Chance for this study indicate that cleavage is

approximately parallel to the axial plane of the Big Creek anticline within the West Chance vein system. This simple relationship would suggest that cleavage formation was synchronous with the formation of the Big Creek anticline. However, this model is challenged by other studies. The penetrative foliation has been related to high angle reverse motion over a broad shear zone (Reid et al., 1995, White, 1989, Wavra et al., 1994). This interpretation is based on observations that cleavage crosses fold axial planes at small to moderate angles and contains dip parallel lineations defined by elongate minerals, rock fragments (mesoscale) and aligned prismatic and flaky minerals (microscale). The same authors argue that shearing responsible for cleavage formation is synchronous with mineralization since ore veins parallel foliation.

There seems to be no unequivocal answer to the process of cleavage formation. In the author's opinion, supporters of shear formed foliation overlook the fact that lineations may simply be related to shear reactivation of an earlier axial plane cleavage associated with the Big Creek anticline. It was also observed in the West Chance that mineralization both cut and paralleled foliation. Also cleavage is sheared, drag folded, and faulted. Based on observations in the West Chance, the author favors a model where cleavage formation is synchronous with fold formation and predates faulting. However this model does not explain the areas where cleavage was observed to cut fold axial planes.

Strike Slip vs. Dip –Slip Movement and its Association with Mineralization

Debate over the relative timing and kinematics of deformation and mineralization has been a part of the Coeur d'Alene mining district since its initial discovery. Until recently (1990's) it was generally accepted that mineralization was associated with strike-

slip motion along the Osburn fault and other west-northwest-trending faults. This hypothesis is based on the geometric relationship between the major faults and veins – with veining occurring as west-trending link veins between west-northwest-trending faults (figure 5). This strike-slip model represents classic Andersonian fault mechanics (Anderson, 1951) where the maximum principal stress is directed EW and the minimum principal stress directed NS. This stress regime would yield left-lateral motion along WNW faults and the link veins would represent extension veins, opening in the σ_3 direction. Ore shoots, which were later found to rake 70°W, would represent the σ_2 direction.

Evidence from this study supporting left-lateral motion includes: 1) theoretical stress fields that indicate extension vein formation is congruent with left-lateral movement, 2) geometric relationship of the west-trending West Chance vein system relative to the WNW-trending unmineralized segment of the Chance fault, and 3) a small population of kinematic indicators from petrographic analysis shows left-lateral movement on the West Chance fault. A small population of wall rock lineations and a larger population of Pb-vein lineations indicate either left-lateral or right-lateral motion, since directional indicators were not present on these lineations.

Evidence for right-lateral motion comes from mapping in the 2700 ER6-2D stope, shown in figure 40. In this stope discontinuous mineralization occurred along the eastern 30m (~100 feet) of a west-trending fault. At this point, a north to northeast-trending, high grade, siderite-quartz vein was found linking the west-trending fault with another west-trending fault 30 feet to the south. A vertical high grade ore shoot is bounded between the two faults and low grade mineralization is present east and west of this ore

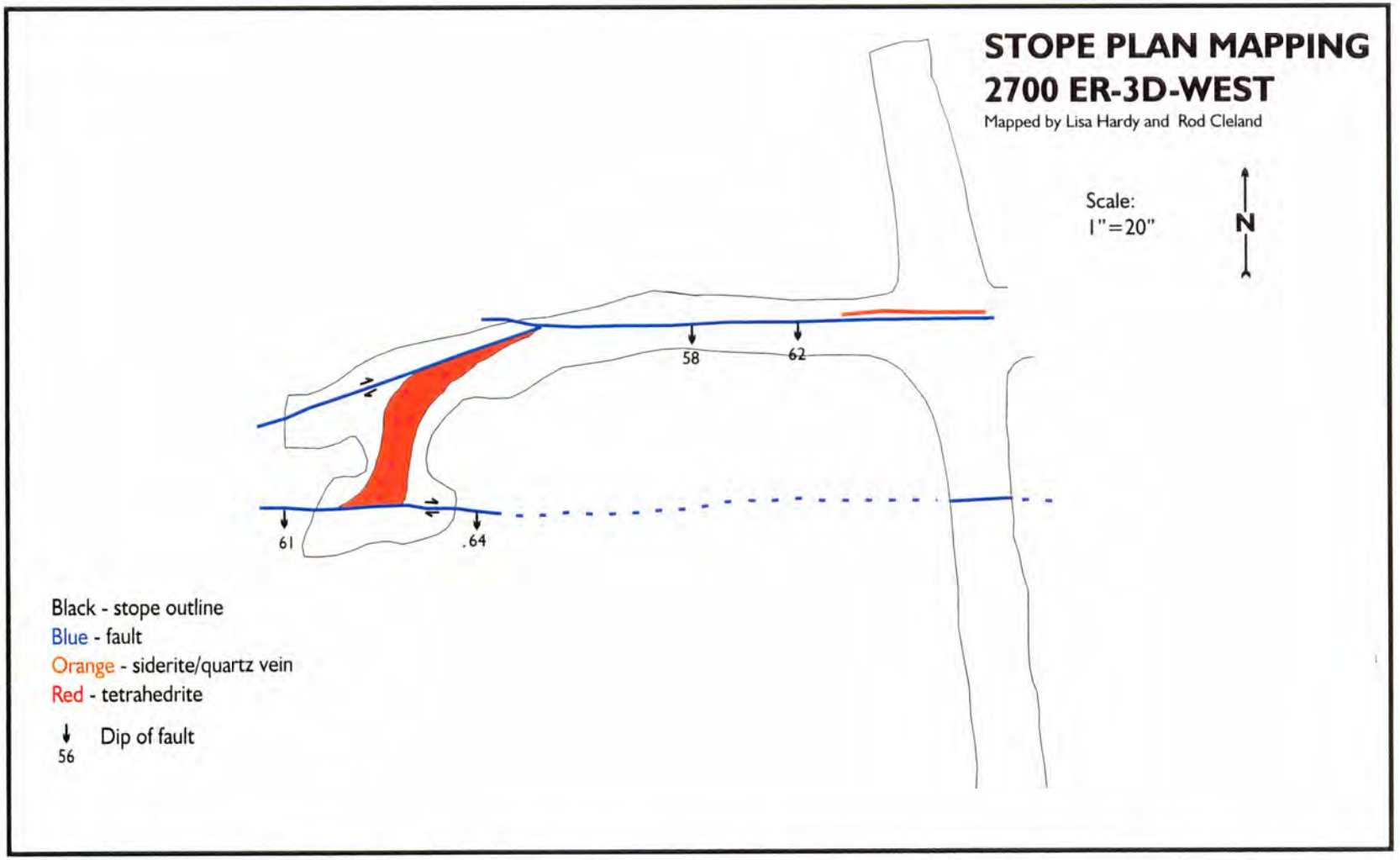

Figure 40. Simplified stope plan map of 2700 ER6-3D West showing north-trending high grade siderite-tetrahedrite-quartz vein. Vein geometry is interpreted by this author to be a result of either right-lateral motion during syn- or post-ore deposition or left-lateral motion during syn-ore deposition.

shoot. Drag folding on both ends of the vein indicates right-lateral motion. A second interpretation of figure 40 would suggest that the vein is sigmoidal and formed during left-lateral motion. Similar structures exist between ER6-1D-West and ER5D-West, resulting in a vertical ore shoot of high-grade ore which extends for approximately 30m (100 feet). The fault-vein-ore shoot orientation shown in figure 40 and described in the text above, suggests right-lateral syn- or post-ore motion or left-lateral syn-ore motion. Other evidence suggesting strike slip motion, which may or may not be associated with mineralization, includes observations from stopes shown schematically in the vein-fault composite diagram (figure 31).

A sample collected from 3100 E9E, floor 7 shows evidence for the association of strike-slip motion and mineralization. Oriented sample SS-25 was collected from a quartz extension vein and associated late stage Pb-vein and shows several important crosscutting relationships. The sample was located approximately 0.6m (2.0 feet) from the identified C-fault. The Pb-vein was found to fill the center portion of the quartz vein and both the quartz vein and the Pb vein cross-cut the penetrative fracture cleavage. The orientation of the features found in this sample are shown on a stereographic plot in figure 41. The quartz vein was identified as an extension vein based on infilling texture found in the vein and had an orientation of 250, 88 NW. Small slickensided surfaces indicates that the extension vein was subsequently sheared. Filling this extension vein was a lead vein which has a shear foliation. The orientation of the shear foliation is 060, 55SE and is sub-parallel to C-fault. This foliation is similar to the shear foliation shown in the block diagram of figure 27. Rotated quartz clasts and lineation direction indicate the shear foliation in the sulfide vein was formed during reverse motion. This shear

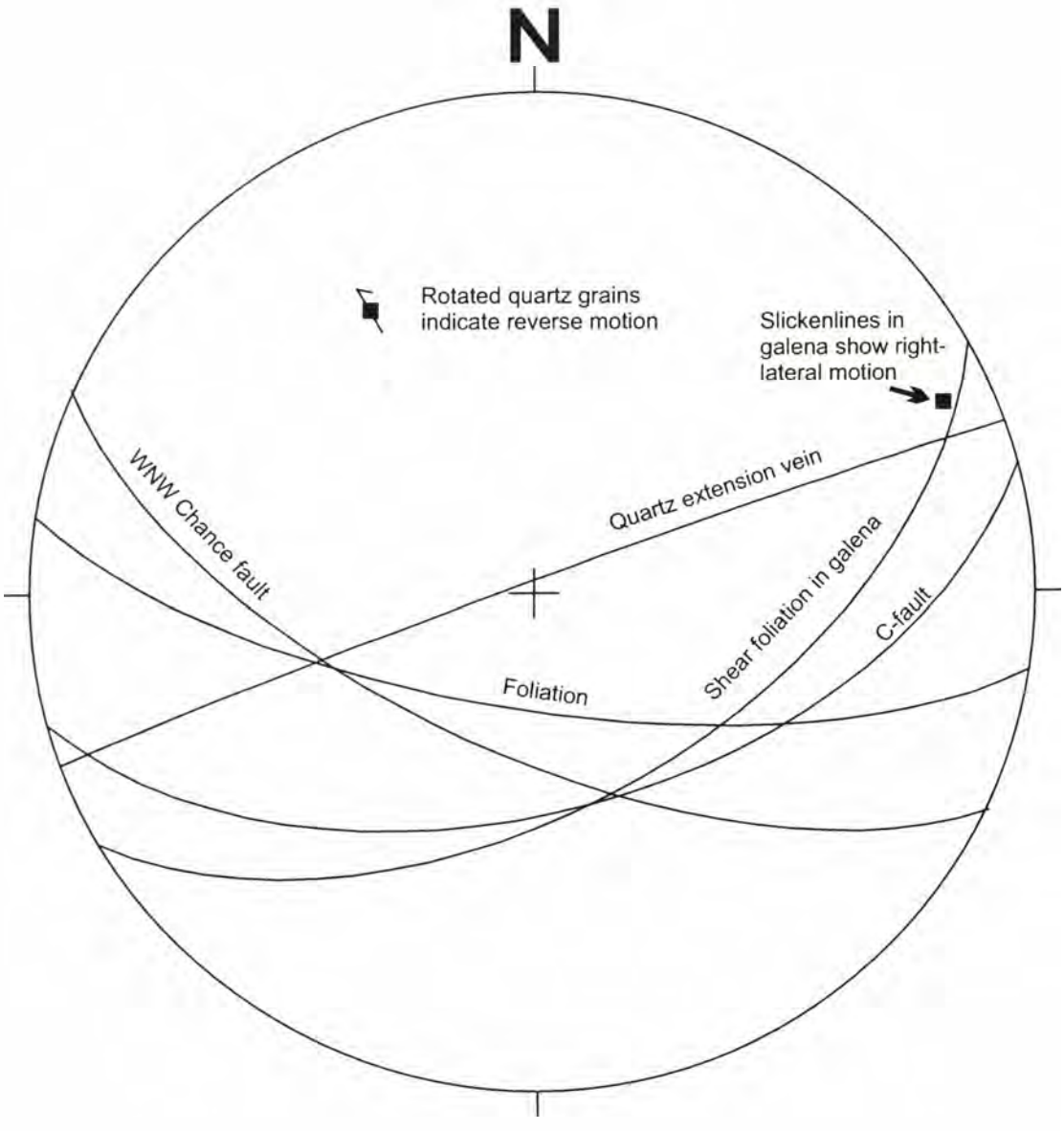

Figure 41. Stereographic projection of sample SS-25, showing relationships between wallrock foliation, C-fault, quartz extension vein, shear foliation in galena, and kinematic indicators associated with some of these features.

foliation cross-cuts and wraps around clasts of tetrahedrite and siderite, and these clasts have a distinctive fracture pattern as also shown in figure 27. Finally, a surface, with slickenlines indicating strike-slip motion, is found cross-cutting all of the previous features.

It is the interpretation of the author that SS-25 represents multiple episodes of fault movement. It is suggested that due to the orientation of the extension vein with respect to WNW-trending Chance fault, this vein represents an early left-lateral fault event. Since the lead vein fills the extension vein, it is suggested that lead deposition occurred in the same stress regime. The shear foliation was formed by reverse motion and is suggested to represent a later stress regime. Finally, it is suggested that the slickensided surface to represent late strike-slip motion. In summary, this rock represents an extension vein, filled with sulfide material, which formed under a stress field correlative to the hypothetical stress field suggested for Chester Hook vein formation. Deformation of the sulfide vein occurred during reverse motion and postdates an earlier fracture forming/lead deposition event. Lastly, strike-slip motion, represented by sub-horizontal slickenlines, overprints all of these features. Kinematics on these slickenlines (left vs. right) is unknown.

More recently, and primarily based on the work of Wavra et al (1994), it has been widely accepted that mineralization was contemporaneous with dip-slip motion at the Sunshine mine. In Wavra's et al (1994) study, important kinematic evidence in the veins and wall rocks were coupled with geometric relationships of structural features which led to new interpretations. In their study, a large body of evidence indicated reverse motion, along both west and west-northwest faults, during the structural evolution of the Sunshine

mine. Evidence showing reverse motion included 1) slickenlines, defined by stretched and recrystallized quartz and sericite, found on reverse shear-stepped bedding plane surfaces. This indicated that reverse motion was pre-ore since mineralized veins cut bedding planes; 2) slickenlines measured on the Chance, Silver Syndicate, and Chester fault plunge steeply to the SW and rake to the west in the plane of these structures. A second set of shallow-plunging slickenlines were observed to overprint these steep slickenlines; 3) mud clasts in the wall rocks locally were elongated and crudely foliated in the plane of the fault and plunge near the dip line; and 4) when representative siderite-quartz veins from the Sunshine mine were plotted on beta and S plane diagrams (Reid et al., 1995) they intersect on a line which plunges steeply to the south. Reverse motion on some WNW faults (Silver Syndicate, Big Creek, and Alahambra) has been identified by Hobbs et al. (1965). Similar dip-slip fabrics have been reported at the Bunker Hill mine (Juras, 1977a), and at the Galena and Gold Hunter mines (Wavra et al., 1994). Recognizing that these structural features parallel the orientation of ore shoots led Wavra et al. (1994) to make the interpretation that the mineralization was contemporaneous with reverse motion and that the ore shoots represent slip-parallel fluid flow.

This model suggests that non-Andersonian mechanics were operative in generating steep ore shoots and related structures during reverse motion. Space for ore deposition is created, in part, where the vein or fault dip flattens. Flattening is a result of refraction of the vein or fault as it passes through different lithologies. During reverse motion these flattened areas open, and space is created. This relationship was observed on a small segment of the Copper vein ore body (Wavra et al., 1994).

Evidence from the author's study which suggests that dip-slip motion may be associated with mineralization includes 1) the larger population of lineations in wall rocks and smaller population of Pb-vein lineations show dip-slip motion; 2) a small population of kinematic indicators from thin sections that indicated reverse motion; 3) observations from stopes which show faulting was ongoing during mineralization – some of this faulting shows reverse motion. Other evidence showing dip-slip motion, which may or may not be associated with ore deposition, is indicated by vein offset and drag folding as shown in figures 30 and 31.

However, the dip-slip model does not explain several important observations. Most importantly, the model doesn't address how space is created parallel to the fault. If space is partially created as suggested, by Wavra et al. (1994), then one would expect horizontal ore shoots, and a strong correlation between dip angle and grade. This study has shown that the ore shoots are steeply raking in the ore body and that there is no statistical correlation between dip and grade. The Wavra model also doesn't address the fault-vein geometry shown in figure 5. Wavra et al. (1994) do entertain the idea that the dip-slip fabrics found in their study may overprint the mineralized structures; however, they reject this idea since no obvious stretching fabric overprinting the ore shoots nor relict fabrics representing a earlier phase of faulting (in wall rocks or veins) were observed. In this study, elongated tetrahedrite clasts in shear foliated Pb-veins shown in figures 26 and 27, were observed and it is suggested that this may be evidence that there is indeed a stretching fabric parallel to fault dip and that the fractures in these clasts represent a relict fabric. It was also observed in this study that most of the deformation in the West Chance vein system was brittle in character. Consequently, a relict fabric may

not ever have been created under brittle conditions and any brittle structures could be easily overprinted.

It is important to look at other mining districts in the world where mineralization is synchronous with steep reverse faulting. Archean gold-quartz vein deposits are commonly hosted by high-angle reverse faults in the Val d'Or area, Abitibi Quebec (Boullier and Robert, 1992). At the Mouska mine in the Bousquet mining district, southern Abitibi greenstone belt, mineralization is also associated with high-angle reverse faults (Belkabir et al., 1995). In both of these areas, mineralization is both lithologically and structurally controlled, is associated with ductile and brittle-ductile shear zones, and has ore shoots that are steeply plunging within the ore body. Ore bodies are generally E trending. Ore deposition synchronous with reverse motion is well accepted. However, some important differences are present with respect to the Coeur d'Alene district. Overall, ore bodies in the Abitibi district are associated with ductile deformation. In the Bousquet District, host shears are superimposed on the regional foliation, and both appear to have formed from the same bulk strain field. This may or may not apply to the Coeur d'Alene district, and depends on which cleavage formation model is correct. If foliation is synchronous with shearing in the Couer d'Alene district then it more closely resembles the Abitibi district. Additionally, the large-scale vein geometry is markedly different. Map scale veins in the Abitibi show similar orientations for faults and veins, whereas different orientations of mineralized and unmineralized faults and veins are seen at the Sunshine mine (figure 5). Unmineralized extension veins in the Abitibi are flat, indicating vertical σ_3. This is rare in the Coeur d'Alene district. Vein formation in the Abitibi has been attributed to fluid over-pressuring as suggested by Sibson (1989), based

primarily on the observation of mutual cross-cutting relationships between extension veins and faulting. Although comparisons can be drawn, the Sunshine mine and the Coeur d'Alene district are not typical high-angle reverse shear vein deposits.

Fluid-Fault Interaction

The importance of fluids in deformation and faulting has long been recognized. During mineralization, fluid pressure (P_f) is a key parameter affecting faulting and may have played an important role in the structural evolution of the West Chance. Epithermal mineralization is commonly localized in fault-fracture systems developed in the brittle regions of the crust. Increased pore fluid pressure under certain conditions can facilitate fault movement. Models for fluid-fault interaction have been proposed for several mining districts (Sibson, 1987) and in many non-economically mineralized fault systems. To understand how and if fluid pressure played a critical role in the structural evolution of the West Chance, it is necessary to discuss current principles of fluid-fault models – namely the fluid pressure cycling models and fault reactivation models of Sibson et al. (1989).

In homogeneous isotropic rock under triaxial stress ($\sigma_1 > \sigma_2 > \sigma_3$), brittle faults appear to form in accordance with the Coulomb criterion for shear failure of intact material (Anderson, 1951). How readily a fault is reactivated is dependent on the orientation of the prevailing stress field. Faults that remain close to Andersonian attitudes, where the angle, (θ), between σ_1 and the slip line is ~ 30°, are favorably oriented for reactivation. If the reactivation angle, θ_r, departs from this optimal angle by > 15°, the faults become unfavorably oriented for reactivation, and new faults are formed. However, if elevated fluid pressures are present, the effective stress, ($\sigma_n - P_f$), approaches

zero, and reactivation of the existing fault may occur (Sibson, 1989). The fluid effectively counteracts the increased normal stress due to non-optimal orientation and facilitates fault movement.

Given these premises, active faults may be defined as favorably oriented for reactivation, unfavorably oriented, or severely misoriented, depending on their attitude in the prevailing stress field Sibson (1989). Elevated P_f is required to reactivate unfavorably oriented faults. If elevated P_f is not present, new faults will form in accordance with Andersonian mechanics. When faults are severely misoriented with respect to the prevailing stress field, and $P_f > \sigma_3$, extension veins are likely to develop in regions below the zone of impermeability. If left-lateral faulting occurred during mineralization, faults would be more or less favorably oriented (angle between EW extension veins (σ_1) and the Chance fault is approximately 30°). In this case fluids would facilitate fault slip, but are not required. If the reverse fault model is correct, and σ_1 is parallel to ladder veins, high P_f is required because the angle θ_r is ~90°.

The fault valve model suggested by Sibson (1989) incorporates the concept of fluids and faulting for unfavorably oriented faults such as steep reverse faults. In this model, fluid pressure is elevated by the presence of an impermeable layer or by the cementation of a hydrothermally choked fault system. When fluid pressure is elevated to a point where reactivation of the fault occurs, the impermeable layer is breached, and mineralized fluid is discharge along the fault. Under certain circumstances, fluid pressure will build high enough to form hydraulic extension veins. In essence, under certain P_f conditions, misoriented faults have the capability to be reactivated and act as valves that then allow the upward discharge of hydrothermal fluids.

Criteria for the fault valve model as delineated by Sibson (1981, 1991, and 1996) includes, 1) $P_f > \sigma_3$; 2) misoriented faults (with respect to Andersonian theory) and the absence of any through-going faults that are more favorably oriented for reactivation; 3) permeable-impermeable episodes; 4) faults crossing an impermeable zone – such as a lithologic contrast; and 4) mutual cross-cutting relationships between pre-failure extension veins lying in the σ_1/σ_2 plane and post-failure discharge veins lying parallel to the fault zones (however, less extreme forms, where $P_f < \sigma_3$, may occur without pre-failure hydraulic extension fractures). The ability of faults to become impermeable barriers during fluid pressure buildup and permeable conduits during episodes of fault movement is crucial to the fault-valve model. Evidence for fault-valve activity includes textural evidence of incremental deposition following episodes of fault slip (Sibson, 1981) and evidence from fluid inclusion studies of fault-hosted hydrothermal material that suggests fluid pressure was varying in a cyclic manner (Boullier et al., 1992).

This study suggests that several of these criteria are present in the West Chance, and that fluid pressure was a critical component in the evolution of the West Chance vein system. Lithologic zones that could pose as permeable-impermeable boundaries are numerous in the Belt rocks of the Sunshine mine. The Revett and St. Regis Formations host the West Chance vein system. In general, these units contain hard, impermeable, quartzite and siltite, with interbedded argillic layers. On a larger scale, the hard, impermeable, quartzite units of the Revett Formation overlay softer, permeable layers of the Burke Formation. Textural evidence from fault zone rocks shows fault breccia is hydrothermally sealed (figure 22a) with sulfide mineralization, which could act as an impermeable barrier. Extension veins are indeed present in the form of subhorizontal

ladder veins, suggesting at some point, elevated pressures were present. Where these ladder veins are present, there is a mutual cross-cutting relationship with longitudinal veins (figure 9a). The photograph illustrates siderite veins are cut by subhorizontal quartz ladder veins, which are then cut by longitudinal sulfide veins. The longitudinal sulfide veins are interpreted as discharge veins based on terminology of Sibson, 1989. This geometry implies reverse motion during mineralization. However, there are also steep veins that could represent fluid overpressure during strike-slip motion. Finally, it has been shown from veining in the West Chance vein system (figure 31) that hydrothermal mineralization is episodic, with pulses of fluid associated in time with increments of shear displacement on fracture systems.

In the author's opinion, components of the fault-valve model were integral in the evolution of the West Chance vein system. The presence of these components suggests fluids did facilitate fault movement, however, clearly the fault-valve model doesn't explain the complex structural history in the West Chance vein system and the Sunshine mine and must be integrated with evidence for changing stress fields.

Suggested Models

Evidence from this study suggests multiple phases of fault movement have occurred in the kinematic history of the West Chance fault-vein system. It is also noted that cross-cutting relationships between strike-slip and dip-slip kinematic indicators are elusive. This observation makes chronological interpretations difficult. Evidence also suggests multiple phases of fluid flow, and that fluids were important in faulting. Therefore several models are proposed to account for the observations and discussion presented in this study.

Three models are proposed to explain fault motions in the West Chance. The models are based on the premise that a change in the regional stress field is directly related to a change in fault motions. The changes in regional stress fields are attributed to a varied tectonic history. The models represent possible sequences of right-lateral, left-lateral, and reverse motion. It is suggested in all of these models that right-lateral motion is the last (or current) fault motion. This is supported by stress field determinations from recent earthquakes. A fault-plane solution for a August 1988 magnitude 4.1 tectonic earthquake that occurred 15 km northeast of Mullan, Idaho, shows together with previous *in situ* stress measurements, that the Coeur d'Alene mining district lies within a regional northeast-southwest extensional regime with the maximum compressive stress directed northwest-southeast (Sprenke, 1991). This orientation favors right-lateral slip on steeply dipping west northwest trending faults and bedding planes common in the district.

The first model suggests reverse, left-lateral, then right-lateral motion as the sequence of fault kinematics. The regional stress regime would change from northeast-southwest compression to east-west compression, followed by northwest-southeast compression, with σ_3 vertical. Evidence supporting this model includes the relative timing shown by differing lineation orientations in wall rock and Pb veins. As shown in figure 20, a larger population of lineations indicating dip-slip movement is found in the wall rocks adjacent to veins and a larger population of lineations indicating strike-slip motion is found in Pb-veins. One possible explanation for these observations is that the wall rocks better preserve the older linear fabric, while Pb veins preserve later stages of fault motion. This model is not favored by the author because it is supported by only a small number of observations from this study.

A second model suggests that dip-slip movement was present throughout most of the structural evolution of the district and that only two stress regimes were present in the history of the West Chance vein system – reverse and right lateral. Regional stress regimes associated with this model would be northeast-southwest compression followed by the present day stress regime of right-lateral motion. This is the model favored by Wavra et al. (1994), and arguments for and against this model are discussed above. The author does not favor this model, mainly because it fails to address the evidence which indicates left-lateral motion, as discussed above.

The third model suggests left-lateral, reverse, then right-lateral motion as the sequence of fault kinematics. In this model the regional stress regime would change from east-west compression to northeast-southwest compression to northwest-southeast compression, with σ_3 orientation changed from northeast to vertical to northwest. It is suggested in this model that a large amount of left-lateral evidence was not preserved in the veins or wall rocks due to later reverse motion. If ore was deposited in extension veins during left-lateral motion, then the shear foliation found in some Pb veins would suggest reverse motion followed left-lateral motion. Structural relationships from sample SS-25 also support reverse motion following left-lateral motion. It is the opinion of the author that most of the evidence from this study supports this model.

Other factors which are suggested to influence the West Chance vein system, and would require further analysis, are fluid pressure, transpression or rotation and changing intermediate and least principal stresses. Fluids, derived either from basin dewatering or magmatism must have been present during the geologic evolution of the West Chance. The extent to which these fluids interacted with faults during the kinematic history of the

West Chance is not completely shown by the work in this study; however, elements of the fault valve model are present as discussed above. Faults could have been "misoriented" with respect to the stress field yet fluid pressure would be high enough to facilitate fault motion. Elevated P_f together with changing stress fields is indicated by the presence of extension veins in several orientations. A change in the orientations of the intermediate and least principal stress could also be an explanation for varying fault motions. This is possible if σ_2 and σ_3 are close to or equal in magnitude. This change in σ_2 and σ_3 would cause a change in fault movement without a change in the regional stress fields and could explain part of the fault history in the West Chance vein system. For example, in a transpressive environment, with a constant northeast directed σ_1, changing σ_2 or σ_3 from vertical to horizontal would cause fault motion to change from left-lateral to reverse without large changes in principal stress directions. A final possibility is that the smooth variation of lineations (figure 20) and extension veins (figure 34) reflects rotation of rocks in a relatively constant stress field. Further analysis is needed to integrate the exact role of these processes.

BIBLIOGRAPHY

Anderson, A.L., 1949, Monzonite intrusion and mineralization in the Coeur d'Alene district, Idaho: Economic Geology, v.44, pp. 169-185.

Anderson, E.M. 1951, The dynamics of faulting, 2nd ed.: Edinburgh: Oliver and Boyd, 206p.

Bennett, E.H. and Venkatakrishan, R., 1982, A palinspastic reconstruction of the Coeur d'Alene mining district based on ore deposits and structural data: Economic Geology, v. 77, pp. 1851-1866.

Belkabir, Abdelhay, and Hubert, Claude, 1995, Geology and Structure of a Sulfide-rich Gold Deposit: An Example from the Mouska Mione, Bousquet District Canada, Economic Geology, vol. 100, pp. 1064-1079.

Bodnar, R.J., T.J. Reynolds and C.A. Kuehn, 1985, Fluid Inclusion systematics in epithermal systems. In: Society of Economic Geologists, Reviews in Economic Geology, 2, Geology and Geochemistry of Epithermal Systems, B.R. Berger and P.M. Bethke, eds., pp.73-98.

_____and Vityk, M.O., 1994, Interpretation of Microthermometric Data for H_2O-NaCl Fluid Incluisions, In: Fluid Inclusions in Minerals: Methods and Applications; Short Course of the Working Group (IMA) "Inclusions in Minerals" (Pontignano-Siena, 1-4 September 1994).

Bond, W.D., Wavra, C.S., Cleland, R.W, Reid, R.R., 1992, Nature and genesis of ore shoots at the Sunshine mine, Coeur d'Alene district, Idaho, Abstracts with Program, vol. 24, Geological Society of America, p.4.

Boullier, Anne-Marie, and Robert, Francois, 1992, Paleoseismic events recorded in

Archean gold-quartz vein networks, Val d'Or, Abitibi, Quebec, Canada, Journal of Structural Geology, Vol. 14, pp. 161-179.

Constantopolus, J.T., 1989, Oxygen and hydrogen isotope geochemisty of the Coeur d'Alene mining district, Idahp: Unpublished Ph.D dissertation, Moscow, Idaho, University of Idaho, 134p.

_____1994, Oxygen isotope geochemistry of the Coeur d'Alene mining district, Idaho: Economic Geology, vol.89, pp. 944-951.

Crawford, M.L., 1981, Fluid inclusions in metamorphic rocks-Low and medium grade, in Hollister, L.S., and Crawford, M.L., eds., Fluid Inclusions: Applications to petrology: Mineralogical Association of Canada Short Course Handbook, vol.6, pp. 157-181.

Crosby, G.M., 1984, Locations of Coeur d'Alene orebodies in belt stratigraphy, Montana Bureau of Mines and Geology Special Publication 90, 61p.

Eaton, G.F., Criss, R.E., Fleck, R.J., Bond, W.D., Cleland, R.W., Wavra, C.S., 1995, Oxygen, Carbon, and Strontium Isotope Geochemistry of the Sunshine Mine, Coeur d'Alene Mining District, Idaho, Economic Geology, vol. 90, pp. 2274-2286.

Fryklund, V.C., Jr., 1964, Ore deposits of the Coeur d'Alene district, Shoshone County, Idaho: U.S. Geological Survey Professional Paper 445, 103p.

Gale, H., 1936, unpublished geology consulting report.

Gott, G.B., and Cathrall, J.B., 1980, Geochemical-exploration studies in the Coeur d'Alene mining district, Idaho and Montanna: U.S. Geological Survey Professional Paper 1116, 63p.

Haas, J.L. Jr., 1976, Physical properties of the coexisting phases and thermochemical properties of the H_2O component in boiling NaCl solutions, U.S.G.S. Bulletin 1421-A.

Harrison, J.E., Griggs, A.B., Wells, J.D., 1974, Tectonic features of the Precambrian Belt Basin and their influence of post-Belt structures, U.S. Geological Survey Professional Paper 866, 15p.

Hedenquist, J.W., and Henley, R.W., 1985, The importance of CO2 on freezing point measurements of fluid inclusions: Evidence from active geothermal systems and implications for epithermal ore deposition: Economic Geology, vol. 80, pp. 1379-1406.

Hobbs, S.W., and Fryklund, V.C., 1968, The Coeur d'Alene district, Idaho, in Ore Deposits of the United States, v.2 (Graton-Sales Volume): American Institute of Mining Engineers, New York, pp. 1417-1435.

_____Griggs, A.B., Wallace, R.E., and Campbell, A.B., 1965, Geology of the Coeur d'Alene mining district, Shoshone County, Idaho: U.S. Geological Survey Professional Paper 478, 139p.

Husman, James Roger,1989, Structural geology of the Sunshine Mine with special emphasis on the formation of the "Hook area" veins , Coeur d'Alene mining district, Shoshone County, Idaho, 71p.

Juras, D.S., 1977a, Structure of the Bunker Hill mine, Kellogg, Idaho: U.S. Geological Survey Professional Paper 478, 139p.

_____1982, Structure of the Bunker Hill Mine, Kellogg, Idaho, in Society of Economic

Geologists Coeur d'Alene field conference, 1977: Idaho Bureau of Mines and Geology Bulletin 24.

Kerr, P.F., and Kulp, J.L., 1952, Precambrian uraninite, Sunshine mine, Idaho: Science, v.115, pp.86-88.

Kerr, P.F., and Robinson, R.F., 1953, Uranium mineralization in Sunshine mine, Idaho: Mining Geology, pp. 495-511.

Leach, D.L., Landis, G.P., and Hofstra, A.H., 1988, Metamorphic origin of the Coeur d'Alene base- and precious-metal veins in the Belt basin, Idaho and Montana: Geology, vol.16, pp. 122-125.

-1998, Hofstra, A.H., Church, S.E., Snee, L.W., Vaughn, R.B., and Zartman, R.E., Evidence for Proterozoic and late Cretaceous-early Tertiary ore-forming events in the Coeur d'Alene district, Idaho and Montanna, Economic Geology, vol. 93, pp. 347-359.

Marshak, S. and Mitra, G., 1988, Basic Methods of Structural Geology. Prentice Hall, New Jersey.

Potter, R.W. II, Brown, D.L., 1977, The Volumetric Properties of Aqueous Sodium Chloride Solutions from O° to 500 °C at Pressures up to 2000 Bars Based on a Regression of Available Data in the Literature, U.S.G.S. Bulletin 1421-C, Clynne, M.A., Brown, D.L., March-April 1978, Freezing Point Depression of Aqueous Sodium Chloride, Economic Geology, vol .73, pp. 284-285.

Ramalingaswamy, V.M., and Cheney, E.S., 1982, Stratiform mineralization and origin of some of the vein deposits, Bunker Hill mine, Coeur d'Alene district, Idaho, in R.R. Reid and G.A. Williams, editors, Society of Economic Geologists' Coeur

d'Alene Field Conference, Idaho—1977: Idaho Bureau of Mines and Geology Bulletin 24, pp. 35-43.

Ransome, F.L. and Calkins, F.C., 1908, The Geology and Ore Deposits of the Coeur d'Alene District, Idaho: U.S. Geological Survey Professional Paper 62, 203p.

Rasor, C.A., 1934, Silver mineralization in the Sunshine mine, Coeur d'Alene district, Idaho: Idaho University, Master's thesis.

Reid, R.R., Wavra, C.S., and Bond, W.B., 1995, Constriction Fracture flow: A Mechanism for Fault and Vein Formation in the Coeur d'Alene District, Idaho, Economic Geology, vol. 90, pp. 81-87.

Reid, R.R., 1993, Structure Short Course for Exploration Geologists – Notes -

Roedder, E., 1984, *Fluid Inclusions,* Mineralogical Society of America, Volume 12, 646p.

Sibson, R.H., 1981, Fluid flow accompanying faulting: field evidence and models, in Earthquake Prediction: An International Review, D.W. Simpson and P.G. Richards (Editors), American Geophysical Union Maurice Ewing Series 4, pp. 593-603.

_____1987, Earthquake rupturing as a mineralizing agent in hydrothermal systems, Geology, v.15, pp. 701-701.

Sibson, R.H., Robert, F. and Poulsen, K.H., 1989, High angle reverse faults, fluid-pressure cyling and mesothermal gold-quartz deposits. Geology vol. 16, pp.551-555.

Sibson, R.H., 1991, Implications of fault-valve behaviour for rupturing nucleation and recurrence,

_____1996, Structural permeability of fluid-driven fault-fracture meshes, Journal of Structural Geology, vol. 18, no. 8, pp. 1031-1042

Sorensen, A.H., 1968, Genesis, mode of origin, and age of the Coeur d'Alene ore deposits, Idaho: Private Publication, 89p.

Sprenke, K.F., Stickney, M.C.,Dodge, D.A., Hammond, W.R., August 1991, Seismicity and Tectonic Stress in the Couer D'Alene District, Bulletin of the Seismological Society of America, Vol. 81, no. 4, pp. 1145-1156.

Springer, D., 1993, Compilation of Coeur d'Alene mining district production figures: Wallace, Idaho, Wallace District Museum.

Trachte, C.B., 1993, Geochemical Study of the Copper Vein, Sunshine Mine, Kellogg, Idaho, Master Thesis, Washington State University, 102 p.

Umpleby, J.B., and Jones, E.L., Jr., 1923, Geology and ore deposits of Shoshone County, Idaho: U.S. Geological Survey Bulletin 723, 156p.

Vokes, F.M., 1969, A Review of the Metamorphism of Sulfide Deposits, Earth-Science Reviews, v. 5, pp. 99-143.

Waldschmidt, W.A., 1925, Deformation in ores, Coeur d'Alene district, Idaho, Economic Geology, vol. 20, pp. 573-586.

Wallace, C.A., D.J. Lidke, and R.G. Schmidt (1990). Faults of the Central Part of the Lewis and Clark Line and Fragmentation of the Late Cretaceous Foreland Basin in West-Central Montanna, Geological Society of America Bulletin., vol. 102, pp. 1021-1037.

Wavra, C.S., Bond, W.D., Reid, R.R., 1994, Evidence from the Sunshine Mine for Dip-

Slip Movement during Coeur d'Alene District Mineralization, Economic Geology, vol. 89, pp. 515-527.

White J.D.L., White, D.L., Vallier, T., Stanley, G.D., Ash, S.R., 1992, Middle Jurassic strata link Wallowa, Olds Ferry, and Izee terranes in the accreted Blue Mountains island arc, northeastern Oregon, Geology, vol. 20., pp. 729-732.

White, B.G., 1989, Superposed map-scale folds and subsequent veins unrealted to Osburn strike-slip fault, Coeur d'Alene Mining District, Shoshone County, Idaho: Geological Society of America, Rocky Mountain-Cordilleran Sections, Abstracts with Program, vol. 21, pp.158.

_____1998, New tricks for and old elephant: revising concepts of Coeur d'Alene geology, Society for Mining, Metallurgy, and Exploration, Inc., Preprint for presentation at SME annual meeting, 12p.

Winston, D.W., 1986, Middle Proterozoic tectonics of the Belt Basin, Western Montana and northern Idaho: in Belt Supergroup, S.M. Roberts (ed.): Montana Bureau of Mines and Geology Special Publication 94, pp. 237-244.

Yardley, B.W.D., 1993, An Introduction to Metamorphic Petrology, Longman Scientific and Technical, 248p.

Yates, M.G., and Ripley, E.M., 1985, Fluid inclusion and isotopic studies of the Galena mine, Coeur d'Alene mining district, Idaho [abs.]: Geological Society of America Abstracts with Programs, vol.17, pp. 756.

Zartman, R. E., and Stacey, J.S., 1971, Lead isotopes and mineralization ages in Belt Supergroup rocks, northwestern Montanna and northern Idaho, Economic Geology, vol. 66, pp. 849-860.

APPENDIX A: FLUID INCLUSION ANALYSIS

The following description of experimental methods is taken from Hass (1976), Potter (1977), and Brooks (1986). Changes have been made only where the procedures in this study differ from those of Brooks (1986).

Sample preparation consisted of polishing the sample chips on both sides with 1-micron diamond grit. The sample chips were mounted on microscope slides with superglue and removed for analysis with acetone. The sample chips were approximately 0.03 to 0.09 millimeters thick.

The sample chips were first examined on a petrographic microscope to determine the character of the inclusions (i.e. primary, pseudosecondary, secondary) and to map suitable inclusions for analysis. The chips were then transferred to the heating/cooling stage for microthermometric measurement.

Fluid inclusions were analyzed microthermometrically with a fluid inclusion gas flow heating and cooling stage at Western Washington University. Heating was done with air heated by electric filament and forced through the sample chamber. Temperatures were recorded and compiled. Ice melting temperatures were obtained by first freezing the sample with nitrogen gas, cooled by passing through liquid nitrogen, and forced through the sample chamber. Due to the small size of the inclusions, the nucleation of a solid ("crunch") in the fluid inclusions, or lack thereof, could be definitively determined during only a portion of the freezing runs. The degree of precision for the measurement of final melting temperatures depended on the temperatures at which these definitive determinations could be made, and is estimated to be +/- 0.5 ^{o}C.

Calibration of the fluid inclusion stage was done using synthetic fluid inclusions of pure H_2O and H_2O of known salinity. This assured accuracy throughout the temperature range investigated in this study. Temperatures were measured by means of a thermocouple in contact with the sample chip.

During heating runs, inclusions were repeatedly homogenized to determine the homogenization temperature and, in most instances, the measurements were reproducible. Homogenization data are listed in table 2.

Final melting temperatures of ice from Type I inclusions were measured, and the salinities of the fluid were determined using this temperature and the equations of Potter et al (1978):

Wt. % NaCl equivalent = $0.00 + 1.76958Y - 4.2384 \times 10^{-2}Y^2 + 5.2778 \times 10^{-4}Y^3$ +/- 0.028, where Y equals freezing point depression in degrees Celsius. Freezing data are listed in Table (2).